International Atomic Energy Agency

INDC(CCP)-336
Distr.: L

INDC INTERNATIONAL NUCLEAR DATA COMMITTEE

TRANSLATION OF SELECTED PAPERS
PUBLISHED IN YADERNYE KONSTANTY (NUCLEAR CONSTANTS 4, 1985)

(Original Report in Russian was distributed
as INDC(CCP)-255/G)

Translated by A. Lorenz
for the
International Atomic Energy Agency

August 1991

IAEA NUCLEAR DATA SECTION, WAGRAMERSTRASSE 5, A-1400 VIENNA

INDC(CCP)-336
Distr.: L

TRANSLATION OF SELECTED PAPERS

PUBLISHED IN YADERNYE KONSTANTY (NUCLEAR CONSTANTS 4, 1985)

(Original Report in Russian was distributed
as INDC(CCP)-255/G)

Translated by A. Lorenz
for the
International Atomic Energy Agency

August 1991

Reproduced by the IAEA in Austria
August 1991

91-03165

CONTENTS

EVALUATION OF THE FAST NEUTRON TOTAL CROSS-SECTION OF ^{238}U

G.V. Anikin, A.G. Dovbenko, I.I. Kotukhov,
V.P. Lunev, N.N. Titarenko

Abstract

Some comments on the evaluation of the total ^{238}U cross-section in the energy range from 0.01 to 20 MeV are presented. Although the coupled channel optical model is not entirely adequate, recommendations are given for the use of certain optical potential parameters.

Although most experimentalists estimate the accuracy of the total cross-section to be 1-2 %, the differences in the data measured by different authors is such that the actual uncertainty of this quantity is close to 5% or more. In addition, it appears that there is a general tendency for the average values of the total cross-sections to increase with the improvement of instrumental methods. This tendency seems to be real, inasmuch as a large number of factors which affect measurement results (e.g. the background, the inadequacy of the geometry, multiple scattering, and in particular resonance self-shielding) lead to a decrease in observed cross-section values. All of these factors must be taken into account in the evaluation of the total cross-section. The most probable value of the evaluated quantity should, as a rule, lie closer to the upper boundary of the region of uncertainty of the experimental values.

The evaluation of the total ^{238}U cross-section in the energy range of 0.04 to 1.5 MeV described in reference [1] (which is shown as curve 1 in the Figure below) can be considered as authoritative and in agreement with current experimental data [2,3]. In the region of partially resolved resonances (2-40 keV), the most realistic average values of the total cross-section are obtained in the work described in reference [4] (see insert in the Figure below) which is the result of a rigorous statistical procedure to

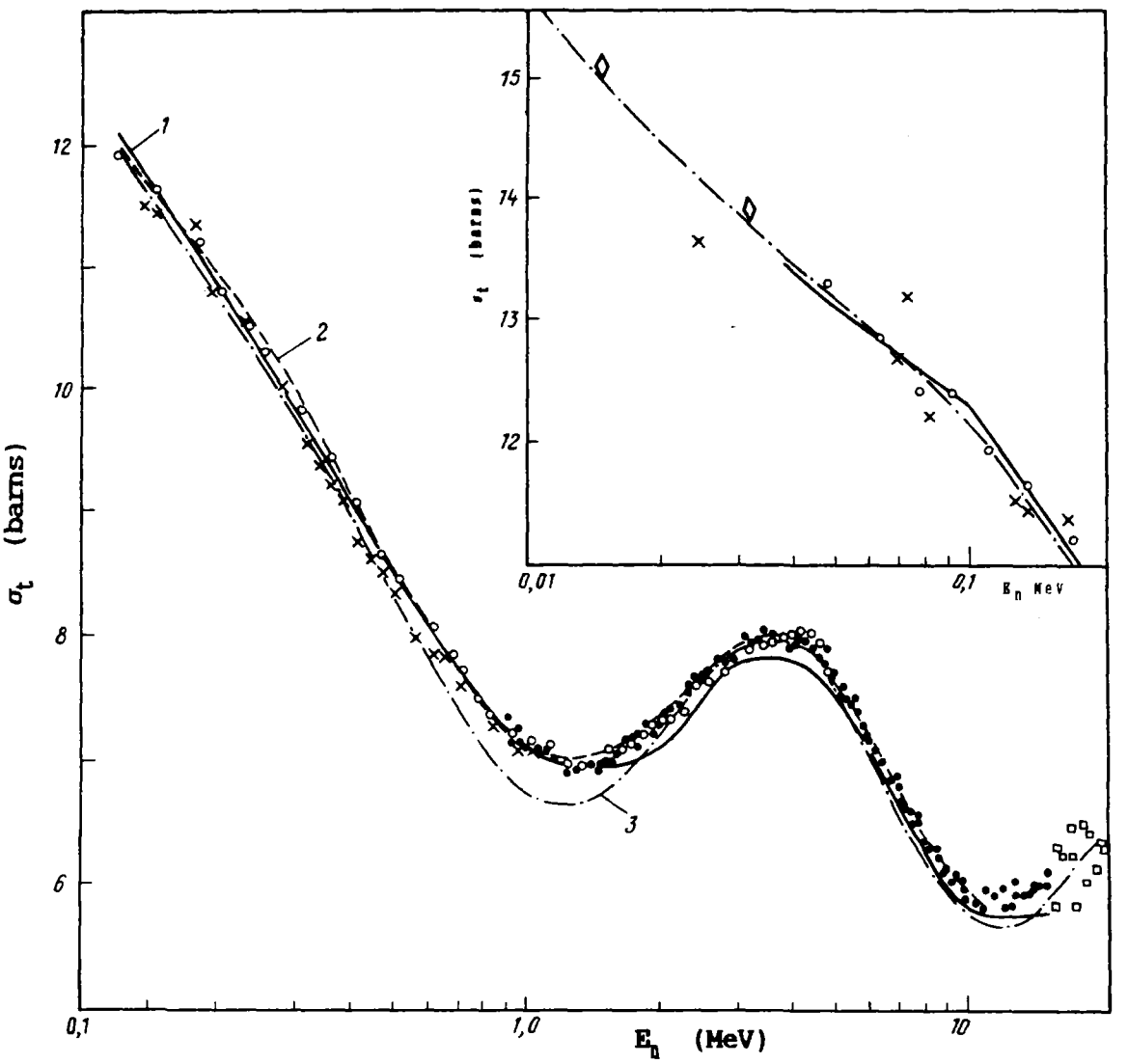

Total cross-section for the interaction of fast neutrons with ^{238}U Nuclei.

Experimental data: ∘ *- reference [2]*
x - reference [3]
◇ *- reference [4]*
• *- reference [5]*
□ *- reference [6]*

approximate experimental neutron transmission curves taking into account the variations in the average resonance parameters.

In addition to reference [2] data, the data reported in reference [5], which are in very good agreement with reference [2] data in the energy range of 1-4 MeV as well as with the total cross-section data given in reference [6], can be taken as the basis of the evaluated data in the energy range of 1.5-20 MeV.
Experimental data reported in reference [2] and [5] show that the

overall level of the cross-section evaluated in the energy range of 1.5 to 15 MeV in reference [1], must be raised by 2-3%. It can also be said that the level of the total cross-section reported in reference [7] is too high; however, the authors of this evaluation [7], after comparing their data with those reported in the ENDF/B-V library, consider that the ENDF/B-V data are too high by 0.3-1.5 %.

Taking the above commentary into consideration, it must be recognized that the ENDF/B-V evaluation of the ^{238}U total reaction cross-section is the most realistic.

The following additional remarks, regarding the application of the optical model to the evaluation of neutron data must be made. At the present time, this theoretical model is the only computational tool that is accessible to a broad number of users, which gives the possibility to perform a coordinated evaluation of most of the experimental data on the interaction of neutrons with nuclei.

In the last few years, there has been a concerted effort in the development of procedures for the calculation of cross-sections which take the strong coupling of channels into account [8]. As an example, reference [9] lists optical potential parameters which give an excellent description of total cross-sections in a broad energy range (see curve 2 shown in the Figure below), and gives a good description of angular distributions of scattered 4-15 MeV neutrons. However, in a subsequent publication by the same authors [10], the optical potential parameters were somewhat changed in order to have a better description of the angular distributions of elastically and inelastically scattered neutrons in the 0.7-3.4 MeV range, which at the same time significantly worsened the values of total cross-sections (see curve 3 in the Figure below).

This situation points to a general inadequacy of this computational procedure since one of the most important utility criterion of this procedure is the non-dependence of optical potential parameters on the data type. Thus, there is a lot of

work to be done in the perfection of optical model calculations and in the improvement of optical potential form-factors.

Although they yield cross-section values that are too low in the 0.1-1 MeV energy range, the optical potential parameters which can be recommended for the evaluation of cross-sections are those given in references [9] or [11].

REFERENCES

[1] NIKOLAEV, M.N., BAZAZYANTS, N.O., GORBACHEVA, L.V., Neutron data for uranium-238, Part 2, Obninsk, FEI (1979) (in Russian).

[2] POENITZ, W.P., WHALEN, I.F., Total neutron cross-sections of heavy nuclei, Nucl. Sci. and Eng. 78 (1981) 333.

[3] TSUBONE, I., KANDA, Y., NAKAJIMA, Y., FURUTA, Y., "Neutron total cross-section measurements of ^{238}U at the Fe-filtered neutron energy bands in keV region", (Proc. Int. Conf. on Nuclear Data for Science and Technology, Antwerp, 1982), (1983).

[4] VAN'KOV, A.A., GOSTEVA, L.S., UKRAINTSEV, V.F., Analysis of ^{238}U transmission experiments in the unresolved resonance region, Problems of Atomic Science and Technology, Ser. Nuclear Constants 3(52) (1983) 27-33 (in Russian).

[5] HAYES, S.H., STOLER, P., CLEMENT, J.N., GOULDING, C.A., The total neutron cross-section of ^{238}U from 0.8-30 MeV, Nucl. Sci. and Eng. 50 (1973) 243.

[6] BOWEN, P.H., SCANLON, J.P., STAFFORD, G.H., et al., Neutron cross-sections in the energy range 15 to 120 MeV, Nucl. Phys. 22 (1961) 640-662.

[7] SMITH, A., POENITZ, W.P., HOWERTON, R., Evaluation of the ^{238}U neutron total cross-section, Rep. ANL/NDM-74 (1974).

[8] TANURA, T., Computer program JUPITER-1 for coupled channel calculation, Rev. Mod. Phys. 37 (1965) 679.

[9] LAGRANGE, CH., "Evaluation of neutron-nuclear cross-sections in heavy nuclei with a coupled channel model in the range of energy from 10 keV to 20 MeV" (Proc. EANDC topical discussion on "Critique of nuclear models and their validity in the evaluation of nuclear data", Tokyo, 1975), Rep. JAERI-M-5984, Tokyo (1975).

[10] HAOUAT, G., LACHKAR, J., LAGRANGE, CH., et al., Neutron scattering cross-sections for ^{232}Th, ^{233}U, ^{235}U, ^{238}U, ^{239}Pu, ^{242}Pu between o.6 and 3.4 MeV, Nucl. Sci. and Eng. 81 (1982) 491-511.

[11] KLEPATSKIJ, A.B., KONSHIN, V.A., SUKHOVITSKIJ, E.SH., The coupled channel method and the evaluation of neutron data of fissile nuclei, Izv. Akad. Nauk BSSR, Ser. Fiz. Ehnerg. 2 (1984) 21 (in Russian).

POSSIBILITIES OF UPDATING THE ^{238}U EVALUATED NUCLEAR DATA FILE

A.B. Klepatskij, V.A. Konshin,
V.M. Masslov, E.Sh. Sukhovitskij

Abstract

A proposal to modify the angular distributions of elastically and inelastically scattered neutrons, the total cross-section and the (n,3n) reaction cross-section of the ^{238}U evaluated nuclear data file is presented. The coupled channel method and the statistical model are used for the analysis of the neutron scattering process.

An examination of the evaluated ^{238}U nuclear data file [1] shows that the incorporation of certain changes in this file could improve the agreement between the evaluated and experimental data. These changes would affect the following quantities:

The angular distribution of elastically and inelastically scattered neutrons.

As shown in the work described in reference [2], the experimental information on the optical cross-section of ^{238}U can be calculated to an accuracy which would fall within the limits of the experimental uncertainty using the coupled channel method with the following optical potential parameters:

$$\begin{aligned} V_R &= (45.87-0.3E)\ \text{MeV},\ r_R = 1.256\ \text{fm}^*,\ a_R = 0.626\ \text{fm}, \\ W_D &= \begin{cases} (2.95+0.4E)\ \text{MeV},\ E \le 10\ \text{MeV},\ r_D = 1.260\ \text{fm}, \\ (6.95\ \text{MeV},\ E > 10\text{MeV},\ a_D = (0.555+0.0045E)\ \text{fm} \end{cases} \\ V_{s0} &= 7.5\ \text{MeV},\ \beta_2 = 0.216,\ \beta_4 = 0.080. \end{aligned} \qquad (1)$$

A comparison of the differential cross-sections for elastic and inelastic neutron scattering as calculated by the authors using the generalized optical model and the parameters given above (1), with the existing experimental data is shown in Figures 1-5. The

* fm = 10^{-15} m

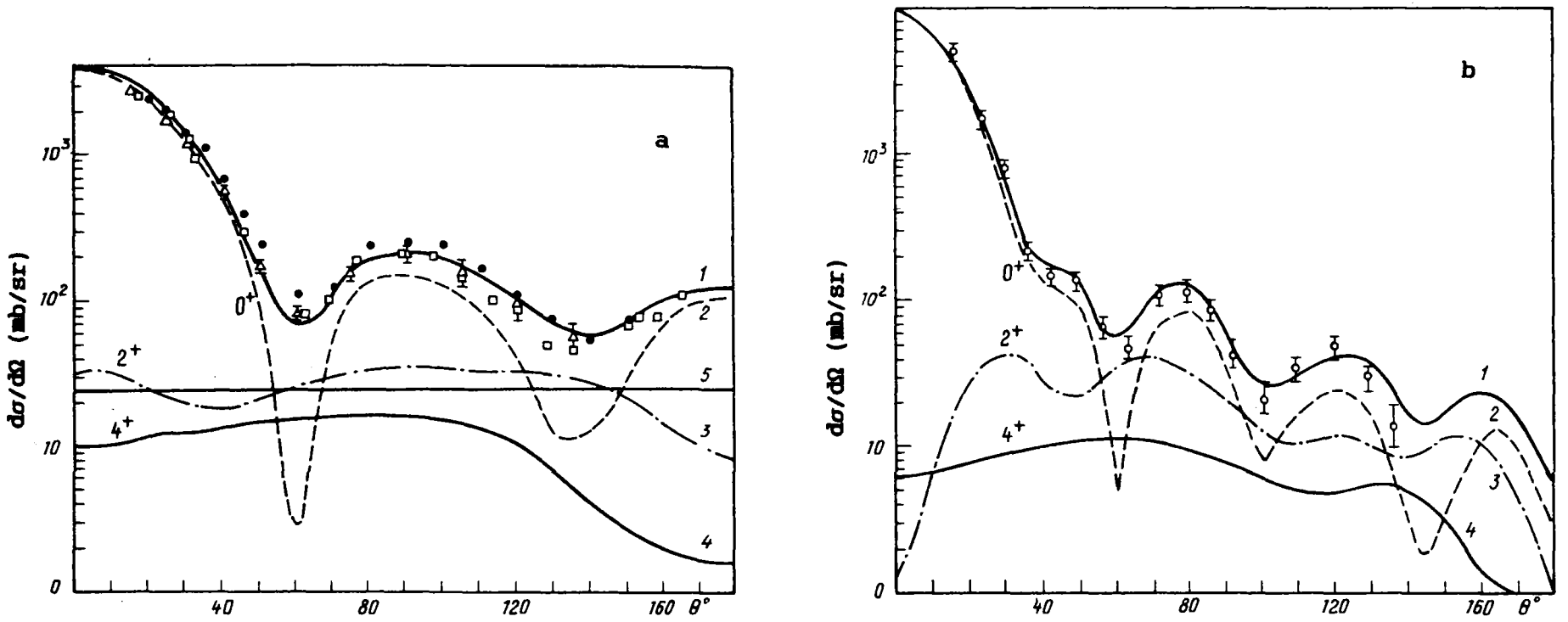

FIG. 1. Comparison of experimental and theoretical angular distributions of elastically scattered neutrons on (a) ^{238}U levels, and (b) on 0^+, 2^+, 4^+ levels, for 2 and 7.54 MeV incident neutron energies. Results of these calculations: 1 - sum of three levels, 2 - direct elastic scattering, 3,4 - direct excitation of levels 2^+ and 4^+ respectively, 5 - sum of compound contribution of three levels. Experimental data: (•, □, △) taken from reference [1].

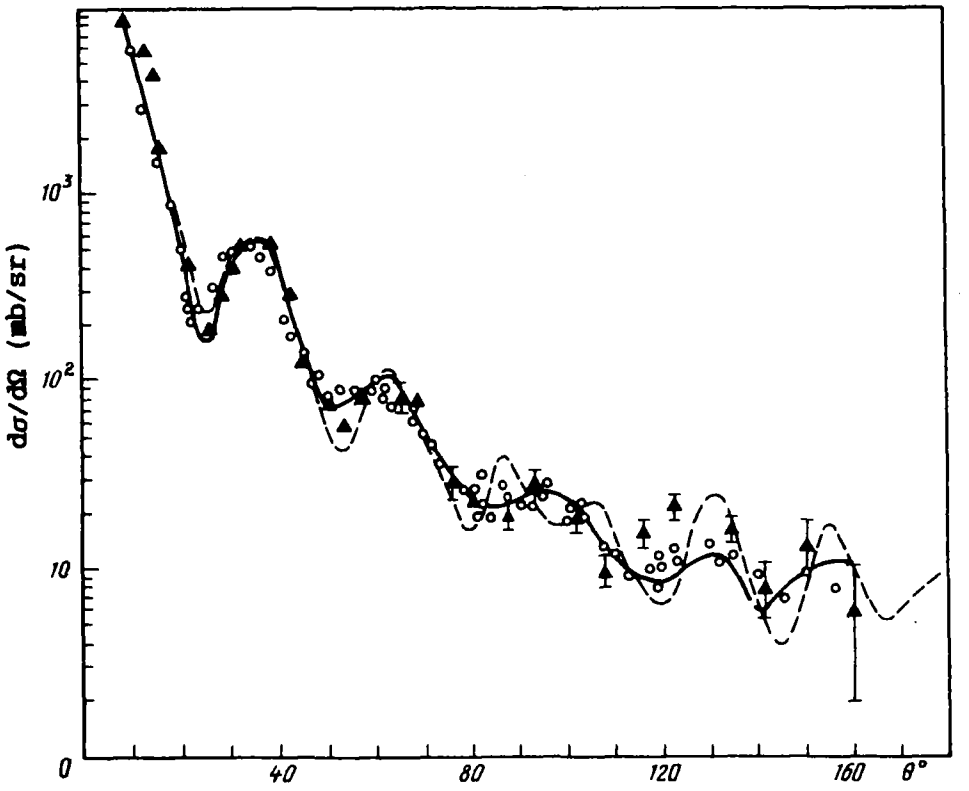

FIG. 2. Comparison of experimental data (taken from ref.[1]) with evaluated data on angular distribution of elastically scattered 15.2 MeV neutrons on ^{238}U: —— ref.[1] evaluation, – – – results of this evaluation (this curve represents the sum of theoretical data for the 0^+, 2^+, 4^+ levels shown in Fig.3).

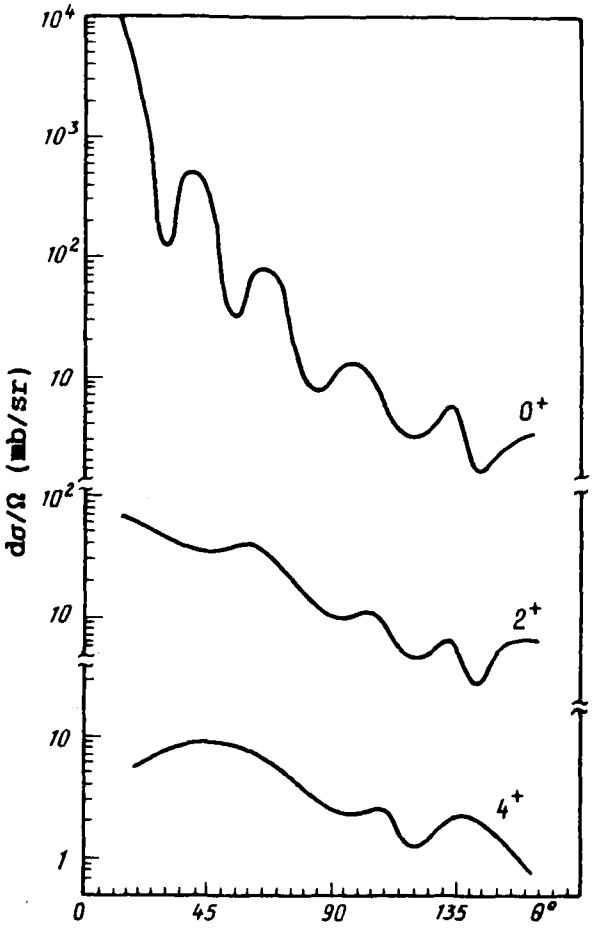

FIG. 3. Theoretical differential scattering cross-section for 15 MeV neutrons on the 0^+, 2^+, 4^+ levels.

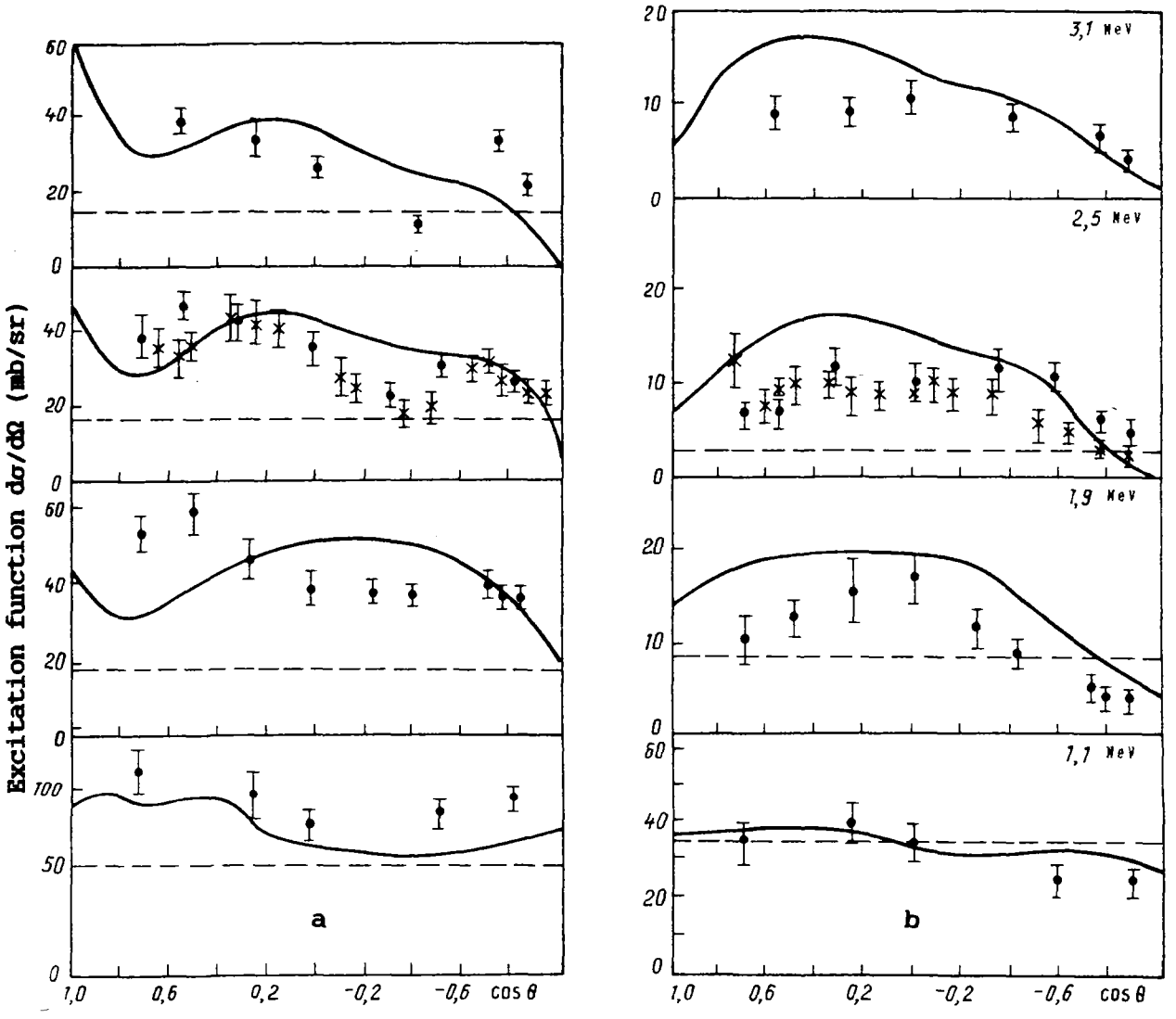

FIG. 4. Angular distributions of inelastically scattered neutrons on the (a) first(2^+ 45 keV) and (b) second (4^+ 148 keV) levels of ^{238}U for neutron incident energies of 3.1, 2.5, 1.9, and 1.1 MeV. Experimental data: ● - ref.[3], x - ref.[4].

calculated cross-sections include the compound nucleus contribution which is essential for neutron energies below 4 MeV.

Figures 1-3 show that the old experimental data on elastic scattering angular distribution can be interpreted correctly only if one takes the inelastic scattering contribution, at least for the first two excited states, into consideration; consequently, the evaluated data of reference [1], which were derived from older experiments, significantly underestimates the anisotropy of elastic scattering.

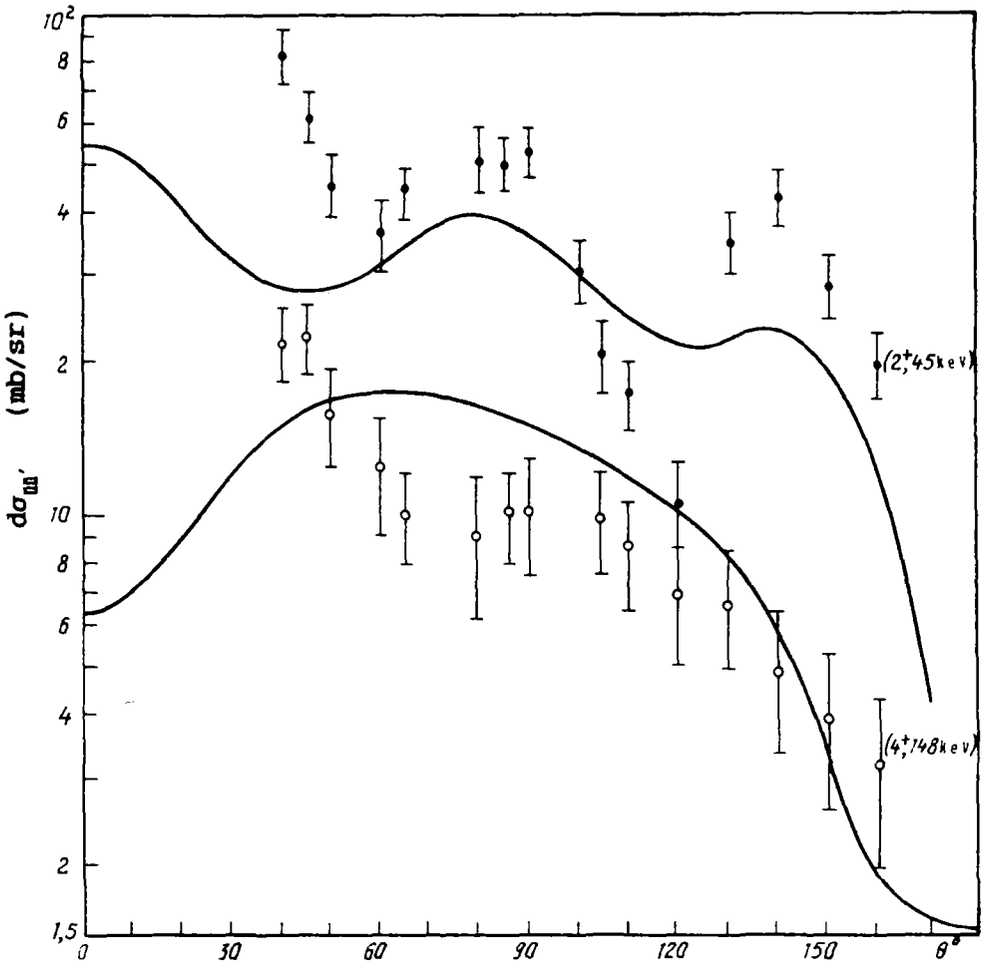

FIG. 5. Angular distributions of inelastically scattered 3.4 MeV neutrons on the first (2^+ 45 keV) and second (4^+ 148 keV) levels. Experimental data from ref.[5]: ● - 45 keV level, o - 148 keV level.

In the evaluated file described in reference [1], the angular distribution of the inelastically scattered neutrons is assumed to be isotropic. However, new experimental data on the angular distribution of inelastically scattered neutrons for the first two excited levels of ^{238}U have been published lately, namely, in reference [3] for the neutron energy range of 0.9 to 3.1 MeV, and in references [4] and [5] for the range of 2.5 MeV and 3.4 MeV. These experimental data, which are plotted in Figures 4 and 5, show the anisotropy of the inelastic scattering angular distributions for incident neutron energies of 1.1 to 3.4 MeV for the 45 and 148 keV levels. Our analysis of these data, performed with the aid of the coupled channel method and the statistical model, are represented in these Figures by continuous curves; the dashed curves represent the data from reference [1] which also

coincide with those from the ENDF/B-IV file. The overall picture given by the theoretical calculations illustrates the angular distributions of inelastically scattered neutrons for discrete levels. The poor agreement between the experimental and calculated data for the 4^+ level can be explained by the fact that the coupling used in the coupled channel analysis was for three levels, namely $0^+ + 2^+ + 4^+$, rather than for four, which should have included the 6^+ level, in order to obtain a satisfactory description of the inelastic scattering on the 4^+ level.

The suggestion is made in reference [1] to represent the angular distribution of neutrons scattered on the first three levels by using the results of this work, tabulated in Tables 1-3 in the form of Legendre polynomial coefficients:

$$\frac{d\sigma_{E_q}}{d\Omega} = \frac{\sigma_{E_q}}{4\pi\left[1 + \sum_{l=1}^{l_{max}} (2l+1)\, A_l P_l (\cos\theta)\right]} \qquad (2)$$

The total interaction cross-section in the energy region above 1 MeV

The most reliable total ^{238}U cross-section data are the experimental data published in references [7] and [9]. These data can be described theoretically up to 15 MeV within the limits of the experimental uncertainty with the application of the coupled channel method using the quoted optical potential parameters. The calculated and experimental data of the cross-section above 1 MeV are plotted in Figure 6. The comparison of these data show that results obtained using the coupled channel calculations (dashed curve) are in good agreement with the experimental data given in references [7-9] and lie somewhat higher than the evaluated data published in reference [1]. It is therefore suggested that the data published in references [7-9] and the results of this analysis be taken as the basis for the evaluation of this cross-section. A comparison of this evaluation with that published in reference [1] is shown in Figure 4; the difference between the two is approximately 1-3%.

TABLE 1. LEGENDRE POLYNOMIAL COEFFICIENTS A_I FOR THE ANGULAR DISTRIBUTION OF ELASTICALLY SCATTERED NEUTRONS

Coeff.	Neutron energy				
	0.025 MeV	0.050 MeV	0.10 MeV	0.25 MeV	0.50 MeV
A_1	$2,02275 \cdot 10^{-2}$	$4,29932 \cdot 10^{-2}$	$8,77427 \cdot 10^{-2}$	$2,41786 \cdot 10^{-1}$	$2,94366 \cdot 10^{-1}$
A_2	$3,42611 \cdot 10^{-4}$	$1,88161 \cdot 10^{-3}$	$7,90078 \cdot 10^{-3}$	$5,00859 \cdot 10^{-2}$	$1,06917 \cdot 10^{-1}$
A_3	$2,79668 \cdot 10^{-6}$	$3,85989 \cdot 10^{-5}$	$3,59507 \cdot 10^{-4}$	$6,64512 \cdot 10^{-3}$	$3,29144 \cdot 10^{-2}$
A_4	-	$6,17454 \cdot 10^{-7}$	$1,19948 \cdot 10^{-5}$	$4,18219 \cdot 10^{-4}$	$5,83009 \cdot 10^{-3}$
A_5	-	-	-	$8,79192 \cdot 10^{-7}$	$1,00325 \cdot 10^{-4}$
A_6	-	-	-	$2,69799 \cdot 10^{-7}$	$1,82843 \cdot 10^{-5}$
A_7	-	-	-	-	$3,50909 \cdot 10^{-7}$
	0.75 MeV	1.0 MeV	2.0 MeV	3.0 MeV	4.0 MeV
A_1	$3,58349 \cdot 10^{-1}$	$4,22629 \cdot 10^{-1}$	$6,79559 \cdot 10^{-1}$	$7,95906 \cdot 10^{-1}$	$8,41674 \cdot 10^{-1}$
A_2	$1,67666 \cdot 10^{-1}$	$2,32892 \cdot 10^{-1}$	$5,12150 \cdot 10^{-1}$	$6,31011 \cdot 10^{-1}$	$6,93552 \cdot 10^{-1}$
A_3	$8,79189 \cdot 10^{-2}$	$1,65679 \cdot 10^{-1}$	$4,06739 \cdot 10^{-1}$	$4,87819 \cdot 10^{-1}$	$5,55067 \cdot 10^{-1}$
A_4	$2,39989 \cdot 10^{-2}$	$6,21111 6 \cdot 10^{-2}$	$2,98223 \cdot 10^{-1}$	$3,83587 \cdot 10^{-1}$	$4,32966 \cdot 10^{-1}$
A_5	$1,03467 \cdot 10^{-3}$	$6,17977 \cdot 10^{-3}$	$1,28376 \cdot 10^{-1}$	$2,37214 \cdot 10^{-1}$	$2,97409 \cdot 10^{-1}$
A_6	$2,85300 \cdot 10^{-4}$	$1,66448 \cdot 10^{-3}$	$4,54960 \cdot 10^{-2}$	$1,12168 \cdot 10^{-1}$	$1,65517 \cdot 10^{-1}$
A_7	$2,07634 \cdot 10^{-5}$	$1,41514 \cdot 10^{-4}$	$9,95963 \cdot 10^{-3}$	$3,99396 \cdot 10^{-2}$	$7,89582 \cdot 10^{-2}$
A_8	$8,61443 \cdot 10^{-7}$	$7,97442 \cdot 10^{-6}$	$1,77177 \cdot 10^{-3}$	$1,18296 \cdot 10^{-2}$	$3,43112 \cdot 10^{-2}$
A_9	-	$2,12917 \cdot 10^{-7}$	$2,07142 2 \cdot 10^{-4}$	$2,66452 \cdot 10^{-3}$	$1,12132 \cdot 10^{-2}$
A_{10}	-	-	$1,58947 \cdot 10^{-5}$	$3,71202 \cdot 10^{-4}$	$2,45190 \cdot 10^{-3}$
A_{11}	-	-	$4,44297 \cdot 10^{-7}$	$5,57285 \cdot 10^{-5}$	$5,55441 \cdot 10^{-4}$
A_{12}	-	-	-	$5,16320 \cdot 10^{-6}$	$8,98714 \cdot 10^{-5}$
A_{13}	-	-	-	$1,01504 \cdot 10^{-7}$	$1,10808 \cdot 10^{-5}$
A_{14}	-	-	-	-	$1,56056 \cdot 10^{-6}$
A_{15}	-	-	-	-	-
A_{16}	-	-	-	-	-
A_{17}	-	-	-	-	-
	5 MeV	6 MeV	7 MeV	8 MeV	9 MeV
A_1	$8,60110 \cdot 10^{-1}$	$8,66590 \cdot 10^{-1}$	$8,66958 \cdot 10^{-1}$	$8,65408 \cdot 10^{-1}$	$8,65175 \cdot 10^{-1}$
A_2	$7,30311 \cdot 10^{-1}$	$7,48656 \cdot 10^{-1}$	$7,52616 \cdot 10^{-1}$	$7,47381 \cdot 10^{-1}$	$7,39663 \cdot 10^{-1}$
A_3	$6,06427 \cdot 10^{-1}$	$6,39385 \cdot 10^{-1}$	$6,53791 \cdot 10^{-1}$	$6,51947 \cdot 10^{-1}$	$6,42934 \cdot 10^{-1}$
A_4	$4,78475 \cdot 10^{-1}$	$5,18191 \cdot 10^{-1}$	$5,45820 \cdot 10^{-1}$	$5,58739 \cdot 10^{-1}$	$5,60608 \cdot 10^{-1}$
A_5	$3,47913 \cdot 10^{-1}$	$3,93284 \cdot 10^{-1}$	$4,30536 \cdot 10^{-1}$	$4,57556 \cdot 10^{-1}$	$4,72913 \cdot 10^{-1}$
A_6	$2,15248 \cdot 10^{-1}$	$2,66161 \cdot 10^{-1}$	$3,14076 \cdot 10^{-1}$	$3,54615 \cdot 10^{-1}$	$3,84594 \cdot 10^{-1}$
A_7	$1,21448 \cdot 10^{-1}$	$1,65828 \cdot 10^{-1}$	$2,12177 \cdot 10^{-1}$	$2,59102 \cdot 10^{-1}$	$3,00297 \cdot 10^{-1}$
A_8	$6,80606 \cdot 10^{-2}$	$1,07982 \cdot 10^{-1}$	$1,49830 \cdot 10^{-1}$	$1,93315 \cdot 10^{-1}$	$2,34954 \cdot 10^{-1}$
A_9	$3,00402 \cdot 10^{-2}$	$6,07231 \cdot 10^{-2}$	$1,00616 \cdot 10^{-1}$	$1,45726 \cdot 10^{-1}$	$1,88668 \cdot 10^{-1}$
A_{10}	$9,38149 \cdot 10^{-3}$	$2,53919 \cdot 10^{-2}$	$5,34064 \cdot 10^{-2}$	$9,31865 \cdot 10^{-2}$	$1,36382 \cdot 10^{-1}$
A_{11}	$2,69661 \cdot 10^{-3}$	$8,97903 \cdot 10^{-3}$	$2,27939 \cdot 10^{-2}$	$4,71801 \cdot 10^{-2}$	$7,89262 \cdot 10^{-2}$
A_{12}	$5,47216 \cdot 10^{-4}$	$2,21348 \cdot 10^{-3}$	$6,76122 \cdot 10^{-3}$	$1,70554 \cdot 10^{-2}$	$3,38890 \cdot 10^{-2}$
A_{13}	$8,82282 \cdot 10^{-5}$	$4,28156 \cdot 10^{-4}$	$1,58056 \cdot 10^{-3}$	$5,16330 \cdot 10^{-3}$	$1,21530 \cdot 10^{-2}$

TABLE 1. Continued.

Coeff.	Neutron energy				
	5 MeV	6 MeV	7 MeV	8 MeV	9 MeV
A_{I4}	$1,36867 \cdot 10^{-5}$	$7,42247 \cdot 10^{-5}$	$3,2II80 \cdot 10^{-4}$	$1,39I96 \cdot 10^{-3}$	$3,74994 \cdot 10^{-3}$
A_{I5}	$5,47II2 \cdot 10^{-7}$	$3,85383 \cdot 10^{-6}$	$2,27650 \cdot 10^{-5}$	$2,80096 \cdot 10^{-4}$	$8,84839 \cdot 10^{-4}$
A_{I6}	-	-	-	$4,80595 \cdot 10^{-5}$	$1,70872 \cdot 10^{-4}$
A_{I7}	-	-	-	$4,52374 \cdot 10^{-6}$	$1,82457 \cdot 10^{-5}$

	10 MeV	11 MeV	12 MeV	14 MeV	16 MeV
A_I	$8,69428 \cdot 10^{-1}$	$8,733I3 \cdot 10^{-1}$	$8,82558 \cdot 10^{-1}$	$9,05073 \cdot 10^{-1}$	$9,25222 \cdot 10^{-1}$
A_2	$7,38675 \cdot 10^{-1}$	$7,389I3 \cdot 10^{-1}$	$7,5I749 \cdot 10^{-1}$	$7,880I5 \cdot 10^{-1}$	$8,272I7 \cdot 10^{-1}$
A_3	$6,38455 \cdot 10^{-1}$	$6,34I30 \cdot 10^{-1}$	$6,44270 \cdot 10^{-1}$	$6,79885 \cdot 10^{-1}$	$7,304I9 \cdot 10^{-1}$
A_4	$5,6066I \cdot 10^{-1}$	$5,5646I \cdot 10^{-1}$	$5,63530 \cdot 10^{-1}$	$5,92409 \cdot 10^{-1}$	$6,43236 \cdot 10^{-1}$
A_5	$4,83099 \cdot 10^{-1}$	$4,85940 \cdot 10^{-1}$	$4,95849 \cdot 10^{-1}$	$5,2I62I \cdot 10^{-1}$	$5,6800I \cdot 10^{-1}$
A_6	$4,08I67 \cdot 10^{-1}$	$4,2I909 \cdot 10^{-1}$	$4,37720 \cdot 10^{-1}$	$4,639I4 \cdot 10^{-1}$	$5,03806 \cdot 10^{-1}$
A_7	$3,35367 \cdot 10^{-1}$	$3,595I4 \cdot 10^{-1}$	$3,826I3 \cdot 10^{-1}$	$4,I3324 \cdot 10^{-1}$	$4,48784 \cdot 10^{-1}$
A_8	$2,74026 \cdot 10^{-1}$	$3,04600 \cdot 10^{-1}$	$3,33I08 \cdot 10^{-1}$	$3,67338 \cdot 10^{-1}$	$3,98963 \cdot 10^{-1}$
A_9	$2,27579 \cdot 10^{-1}$	$2,59II8 \cdot 10^{-1}$	$2,883I3 \cdot 10^{-1}$	$3,23I78 \cdot 10^{-1}$	$3,5I655 \cdot 10^{-1}$
A_{I0}	$1,775I7 \cdot 10^{-1}$	$2,II785 \cdot 10^{-1}$	$2,42589 \cdot 10^{-1}$	$2,77872 \cdot 10^{-1}$	$3,03600 \cdot 10^{-1}$
A_{II}	$1,I4846 \cdot 10^{-1}$	$1,49249 \cdot 10^{-1}$	$1,82383 \cdot 10^{-1}$	$2,23568 \cdot 10^{-1}$	$2,5I028 \cdot 10^{-1}$
A_{I2}	$5,75473 \cdot 10^{-2}$	$8,44I33 \cdot 10^{-2}$	$1,I48I2 \cdot 10^{-1}$	$1,59209 \cdot 10^{-1}$	$1,9II37 \cdot 10^{-1}$
A_{I3}	$2,39385 \cdot 10^{-2}$	$3,96II3 \cdot 10^{-2}$	$6,I3838 \cdot 10^{-2}$	$9,85504 \cdot 10^{-2}$	$1,30602 \cdot 10^{-1}$
A_{I4}	$8,308II \cdot 10^{-3}$	$1,529I5 \cdot 10^{-2}$	$2,79482 \cdot 10^{-2}$	$5,2667I \cdot 10^{-2}$	$8,02244 \cdot 10^{-2}$
A_{I5}	$2,24265 \cdot 10^{-3}$	$4,652I2 \cdot 10^{-3}$	$1,05476 \cdot 10^{-2}$	$2,36646 \cdot 10^{-2}$	$4,4022I \cdot 10^{-2}$
A_{I6}	$4,8I982 \cdot 10^{-4}$	$1,I2278 \cdot 10^{-3}$	$3,40793 \cdot 10^{-3}$	$9,I0327 \cdot 10^{-3}$	$2,I5225 \cdot 10^{-2}$
A_{I7}	$5,80I42 \cdot 10^{-5}$	$1,52760 \cdot 10^{-4}$	$9,05688 \cdot 10^{-4}$	$2,94I03 \cdot 10^{-3}$	$9,I027I \cdot 10^{-3}$
A_{I8}	-	-	$1,85049 \cdot 10^{-4}$	$7,287I7 \cdot 10^{-4}$	$3,333I3 \cdot 10^{-3}$
A_{I9}	-	-	$2,02478 \cdot 10^{-5}$	$9,393I6 \cdot 10^{-5}$	$1,06862 \cdot 10^{-3}$
A_{20}	-	-	-	-	$2,36029 \cdot 10^{-4}$
A_{2I}	-	-	-	-	$3,48308 \cdot 10^{-5}$

Coeff.	Neutron energy		Coeff.	Neutron energy	
	18 MeV	20 MeV		18 MeV	20 MeV
A_1	$9,395I2 \cdot 10^{-1}$	$9,48694 \cdot 10^{-1}$	A_9	$3,76890 \cdot 10^{-1}$	$4,03I07 \cdot 10^{-1}$
A_2	$8,57709 \cdot 10^{-1}$	$8,79363 \cdot 10^{-1}$	A_{I0}	$3,2470I \cdot 10^{-1}$	$3,46462 \cdot 10^{-1}$
A_3	$7,74024 \cdot 10^{-1}$	$8,076I9 \cdot 10^{-1}$	A_{II}	$2,707I0 \cdot 10^{-1}$	$2,89864 \cdot 10^{-1}$
A_4	$6,92689 \cdot 10^{-1}$	$7,34039 \cdot 10^{-1}$	A_{I2}	$2,I3I3I \cdot 10^{-1}$	$2,32468 \cdot 10^{-1}$
A_5	$6,I6289 \cdot 10^{-1}$	$6,60126 \cdot 10^{-1}$	A_{I3}	$1,54434 \cdot 10^{-1}$	$1,75I8I \cdot 10^{-1}$
A_6	$5,47288 \cdot 10^{-1}$	$5,89302 \cdot 10^{-1}$	A_{I4}	$1,02952 \cdot 10^{-1}$	$1,23348 \cdot 10^{-1}$
A_7	$4,85727 \cdot 10^{-1}$	$5,23046 \cdot 10^{-1}$	A_{I5}	$6,36004 \cdot 10^{-2}$	$8,2I975 \cdot 10^{-2}$
A_8	$4,297I9 \cdot 10^{-1}$	$4,6I490 \cdot 10^{-1}$	A_{I6}	$3,62373 \cdot 10^{-2}$	$5,I8454 \cdot 10^{-2}$

TABLE 1. Continued.

Coeff.	Neutron energy		Coeff.	Neutron energy	
	18 MeV	20 MeV		18 MeV	20 MeV
A_{17}	$1,83986 \cdot 10^{-2}$	$2,98687 \cdot 10^{-2}$	A_{21}	$3,13794 \cdot 10^{-4}$	$9,06811 \cdot 10^{-4}$
A_{18}	$8,11315 \cdot 10^{-3}$	$1,51456 \cdot 10^{-2}$	A_{22}	$6,73673 \cdot 10^{-5}$	$2,25244 \cdot 10^{-4}$
A_{19}	$3,18625 \cdot 10^{-3}$	$6,84642 \cdot 10^{-3}$	A_{23}	$9,02055 \cdot 10^{-6}$	$3,72883 \cdot 10^{-5}$
A_{20}	$1,10037 \cdot 10^{-3}$	$2,73710 \cdot 10^{-3}$			

TABLE 2. LEGENDRE POLYNOMIAL COEFFICIENTS A_l FOR THE ANGULAR DISTRIBUTION OF ELASTICALLY SCATTERED NEUTRONS ON THE 2^+, 45 keV LEVEL.

Coeff.	Neutron energy				
	0.10 MeV	0.25 MeV	0.50 MeV	0.75 MeV	1.0 MeV
A_1	$-2,05533 \cdot 10^{-3}$	$-6,91094 \cdot 10^{-3}$	$-4,63830 \cdot 10^{-2}$	$-1,56093 \cdot 10^{-2}$	$-1,96029 \cdot 10^{-2}$
A_2	$-2,28283 \cdot 10^{-3}$	$-4,14829 \cdot 10^{-3}$	$-4,05373 \cdot 10^{-2}$	$-1,26642 \cdot 10^{-2}$	$-1,43527 \cdot 10^{-2}$
A_3	$1,51597 \cdot 10^{-4}$	$1,69867 \cdot 10^{-3}$	$1,21853 \cdot 10^{-3}$	$1,98257 \cdot 10^{-3}$	$2,06837 \cdot 10^{-3}$
A_4	$-2,36161 \cdot 10^{-6}$	$3,80452 \cdot 10^{-6}$	$-2,59449 \cdot 10^{-3}$	$-1,59455 \cdot 10^{-3}$	$3,14904 \cdot 10^{-3}$
A_5	$-1,03763 \cdot 10^{-8}$	$-6,10698 \cdot 10^{-6}$	$-2,35363 \cdot 10^{-4}$	$1,63589 \cdot 10^{-5}$	$7,32876 \cdot 10^{-5}$
A_6	-	$2,59586 \cdot 10^{-7}$	$3,94117 \cdot 10^{-5}$	$9,49381 \cdot 10^{-5}$	$3,72995 \cdot 10^{-4}$
A_7	-	-	$-6,65061 \cdot 10^{-7}$	$-1,27985 \cdot 10^{-6}$	$-1,00843 \cdot 10^{-5}$
A_8	-	-	-	$8,33400 \cdot 10^{-7}$	$6,12047 \cdot 10^{-6}$
A_9	-	-	-	-	$1,20627 \cdot 10^{-7}$

Coeff.	Neutron energy				
	2 MeV	3 MeV	4 MeV	5 Mev	6 MeV
A_1	$-1,67703 \cdot 10^{-2}$	$8,07438 \cdot 10^{-2}$	$1,44031 \cdot 10^{-1}$	$1,60497 \cdot 10^{-1}$	$1,79966 \cdot 10^{-1}$
A_2	$-6,17596 \cdot 10^{-2}$	$-5,38122 \cdot 10^{-2}$	$-4,50894 \cdot 10^{-2}$	$-5,29772 \cdot 10^{-2}$	$-5,78545 \cdot 10^{-2}$
A_3	$2,85599 \cdot 10^{-2}$	$2,19046 \cdot 10^{-2}$	$-4,98799 \cdot 10^{-3}$	$-3,17340 \cdot 10^{-2}$	$-5,37606 \cdot 10^{-2}$
A_4	$6,28864 \cdot 10^{-3}$	$2,19618 \cdot 10^{-2}$	$2,79823 \cdot 10^{-2}$	$2,75450 \cdot 10^{-2}$	$1,34778 \cdot 10^{-2}$
A_5	$1,38170 \cdot 10^{-2}$	$3,69904 \cdot 10^{-2}$	$3,27866 \cdot 10^{-2}$	$1,88669 \cdot 10^{-2}$	$2,27675 \cdot 10^{-2}$
A_6	$1,96331 \cdot 10^{-3}$	$-1,14563 \cdot 10^{-3}$	$-1,98872 \cdot 10^{-2}$	$-2,80216 \cdot 10^{-2}$	$-1,98519 \cdot 10^{-2}$
A_7	$8,51545 \cdot 10^{-4}$	$4,60506 \cdot 10^{-3}$	$-1,19236 \cdot 10^{-2}$	$-3,03507 \cdot 10^{-2}$	$-3,61706 \cdot 10^{-2}$
A_8	$8,46872 \cdot 10^{-4}$	$2,91856 \cdot 10^{-3}$	$2,81202 \cdot 10^{-4}$	$-1,42716 \cdot 10^{-2}$	$-3,09743 \cdot 10^{-2}$
A_9	$-9,62784 \cdot 10^{-5}$	$1,41688 \cdot 10^{-3}$	$7,81993 \cdot 10^{-3}$	$1,11172 \cdot 10^{-2}$	$4,98525 \cdot 10^{-3}$
A_{10}	$4,13223 \cdot 10^{-5}$	$1,03286 \cdot 10^{-3}$	$4,13345 \cdot 10^{-3}$	$7,09164 \cdot 10^{-3}$	$3,72266 \cdot 10^{-3}$
A_{11}	$-4,70900 \cdot 10^{-6}$	$2,54284 \cdot 10^{-5}$	$4,65528 \cdot 10^{-4}$	$2,11953 \cdot 10^{-3}$	$4,78237 \cdot 10^{-3}$
A_{12}	-	$6,75052 \cdot 10^{-5}$	$5,83793 \cdot 10^{-4}$	$2,22005 \cdot 10^{-3}$	$5,70361 \cdot 10^{-3}$
A_{13}	-	$1,64818 \cdot 10^{-6}$	$7,21855 \cdot 10^{-5}$	$2,37252 \cdot 10^{-4}$	$4,92684 \cdot 10^{-4}$
A_{14}	-	-	$-4,32386 \cdot 10^{-5}$	$-1,86566 \cdot 10^{-4}$	$-1,62230 \cdot 10^{-4}$
A_{15}	-	-	$-5,79066 \cdot 10^{-7}$	$9,51463 \cdot 10^{-6}$	$9,13650 \cdot 10^{-5}$

TABLE 2. Continued.

Coeff.	Neutron energy				
	7 MeV	8 MeV	9 MeV	10 MeV	11 MeV
A_1	2,07603·10^{-1}	2,44200·10^{-1}	2,89946·10^{-1}	3,39292·10^{-1}	3,75822·10^{-1}
A_2	-5,11072·10^{-2}	-3,32067·10^{-2}	-5,07327·10^{-3}	2,80457·10^{-2}	5,57923·10^{-2}
A_3	-6,66596·10^{-2}	-7,16087·10^{-2}	-6,86459·10^{-2}	-6,03790·10^{-2}	-4,84173·10^{-2}
A_4	-5,02945·10^{-5}	-1,47386·10^{-2}	-2,47189·10^{-2}	-2,67995·10^{-2}	-2,24035·10^{-2}
A_5	3,02198·10^{-2}	2,29111·10^{-2}	1,12443·10^{-2}	4,60982·10^{-3}	2,79597·10^{-3}
A_6	-8,42648·10^{-3}	-1,68116·10^{-3}	3,86386·10^{-3}	9,53563·10^{-3}	1,33459·10^{-2}
A_7	-3,60140·10^{-2}	-2,00743·10^{-2}	-2,72070·10^{-2}	-1,96402·10^{-2}	-1,17661·10^{-2}
A_8	-4,05241·10^{-2}	-4,69471·10^{-2}	-5,01362·10^{-2}	-4,84508·10^{-2}	-4,10540·10^{-2}
A_9	-7,33697·10^{-3}	-1,88954·10^{-2}	-2,64829·10^{-2}	-3,07277·10^{-2}	-3,07820·10^{-2}
A_{10}	-4,76933·10^{-3}	-1,08121·10^{-2}	-1,22582·10^{-2}	-1,24863·10^{-2}	-1,24507·10^{-2}
A_{11}	8,85890·10^{-3}	1,32548·10^{-2}	1,44549·10^{-2}	1,21444·10^{-2}	8,40500·10^{-3}
A_{12}	9,68057·10^{-3}	1,25559·10^{-2}	1,20408·10^{-2}	9,24076·10^{-3}	4,36815·10^{-3}
A_{13}	8,98479·10^{-4}	1,98110·10^{-3}	4,16396·10^{-3}	6,49461·10^{-3}	7,26526·10^{-3}
A_{14}	2,03946·10^{-4}	2,40623·10^{-3}	5,92642·10^{-3}	1,01916·10^{-2}	1,41471·10^{-2}
A_{15}	3,73947·10^{-4}	1,05162·10^{-3}	2,14855·10^{-3}	3,82994·10^{-3}	5,71449·10^{-3}
A_{16}	-	-1,37486·10^{-4}	-1,10842·10^{-4}	3,25337·10^{-4}	8,33296·10^{-4}
A_{17}	-	1,86738·10^{-5}	7,46198·10^{-5}	2,54689·10^{-4}	6,29871·10^{-4}

Coeff.	Neutron energy				
	12 MeV	14 MeV	16 MeV	18 MeV	20 MeV
A_1	4,07811·10^{-1}	4,56321·10^{-1}	4,92858·10^{-1}	5,24776·10^{-1}	5,46980·10^{-1}
A_2	8,77723·10^{-2}	1,36571·10^{-1}	1,87325·10^{-1}	2,24720·10^{-1}	2,52788·10^{-1}
A_3	-2,45767·10^{-2}	1,00224·10^{-2}	5,06951·10^{-2}	7,56911·10^{-2}	9,26714·10^{-2}
A_4	-9,85182·10^{-3}	9,25719·10^{-3}	3,51549·10^{-2}	4,90628·10^{-2}	5,56688·10^{-2}
A_5	6,54097·10^{-3}	2,10474·10^{-2}	4,35145·10^{-2}	5,31926·10^{-2}	5,33033·10^{-2}
A_6	1,47829·10^{-2}	2,45839·10^{-2}	4,38831·10^{-2}	5,71561·10^{-2}	6,09818·10^{-2}
A_7	-6,13054·10^{-3}	1,09218·10^{-2}	2,98806·10^{-2}	4,17096·10^{-2}	4,76329·10^{-2}
A_8	-3,16093·10^{-2}	-1,26508·10^{-2}	6,06315·10^{-3}	1,89097·10^{-2}	2,67782·10^{-2}
A_9	-2,79937·10^{-2}	-1,71748·10^{-2}	-2,58917·10^{-4}	1,07027·10^{-2}	1,63949·10^{-2}
A_{10}	-1,26954·10^{-2}	-8,11638·10^{-3}	7,51504·10^{-4}	6,99679·10^{-3}	9,52256·10^{-3}
A_{11}	5,80164·10^{-3}	9,18213·10^{-3}	1,59882·10^{-2}	1,77384·10^{-2}	1,57977·10^{-2}
A_{12}	4,81483·10^{-4}	3,36630·10^{-3}	1,16451·10^{-2}	1,37554·10^{-2}	1,35548·10^{-2}
A_{13}	6,40595·10^{-3}	7,01638·10^{-3}	4,73120·10^{-3}	2,51996·10^{-3}	2,97274·10^{-3}
A_{14}	1,76054·10^{-2}	1,78580·10^{-2}	6,31329·10^{-3}	-2,22407·10^{-3}	-5,34758·10^{-3}
A_{15}	1,02776·10^{-2}	1,16175·10^{-2}	4,07636·10^{-3}	-3,11071·10^{-3}	-7,11198·10^{-3}
A_{16}	3,32503·10^{-3}	7,20170·10^{-3}	1,36246·10^{-2}	1,17681·10^{-2}	4,74499·10^{-3}
A_{17}	1,45998·10^{-3}	4,75798·10^{-3}	1,29230·10^{-2}	1,36798·10^{-2}	8,83451·10^{-3}
A_{18}	1,14708·10^{-4}	9,66005·10^{-4}	3,73865·10^{-3}	8,29066·10^{-3}	1,07728·10^{-2}
A_{19}	5,41422·10^{-5}	1,05526·10^{-4}	2,60367·10^{-3}	7,24937·10^{-3}	1,14158·10^{-2}

TABLE 2. Continued.

Coeff.	Neutron energy				
	12 MeV	14 MeV	16 MeV	18 MeV	20 MeV
A_{20}	-	-	$5,46369 \cdot 10^{-4}$	$2,82615 \cdot 10^{-3}$	$5,37896 \cdot 10^{-3}$
A_{21}	-	-	$1,88384 \cdot 10^{-4}$	$1,07757 \cdot 10^{-3}$	$2,85965 \cdot 10^{-3}$
A_{22}	-	-	-	$3,13116 \cdot 10^{-4}$	$8,48425 \cdot 10^{-4}$
A_{23}	-	-	-	$8,22000 \cdot 10^{-5}$	$3,05715 \cdot 10^{-4}$

TABLE 3. LEGENDRE POLYNOMIAL COEFFICIENTS A_I FOR THE ANGULAR DISTRIBUTION OF ELASTICALLY SCATTERED NEUTRONS ON THE 4^+, 148 keV LEVEL.

Coeff.	Neutron energy				
	0.25 MeV	0.50 MeV	0.75 MeV	1.0 MeV	2.0 MeV
A_1	$6,60383 \cdot 10^{-3}$	$2,97305 \cdot 10^{-2}$	$3,75420 \cdot 10^{-2}$	$4,73167 \cdot 10^{-2}$	$1,13906 \cdot 10^{-1}$
A_2	$-4,50741 \cdot 10^{-4}$	$-2,55705 \cdot 10^{-3}$	$-9,09802 \cdot 10^{-3}$	$-1,60823 \cdot 10^{-2}$	$-9,16530 \cdot 10^{-2}$
A_3	$-1,41272 \cdot 10^{-3}$	$-5,76225 \cdot 10^{-3}$	$-6,94510 \cdot 10^{-3}$	$-7,25792 \cdot 10^{-3}$	$-1,71602 \cdot 10^{-3}$
A_4	$-2,68513 \cdot 10^{-4}$	$-1,04890 \cdot 10^{-3}$	$3,35294 \cdot 10^{-4}$	$1,83705 \cdot 10^{-3}$	$5,85170 \cdot 10^{-3}$
A_5	$1,41053 \cdot 10^{-5}$	$1,64502 \cdot 10^{-4}$	$4,40459 \cdot 10^{-4}$	$5,28366 \cdot 10^{-4}$	$-7,68476 \cdot 10^{-3}$
A_6	$-1,21642 \cdot 10^{-7}$	$-3,78814 \cdot 10^{-6}$	$-8,46816 \cdot 10^{-5}$	$-2,08116 \cdot 10^{-4}$	$8,84151 \cdot 10^{-4}$
A_7	-	-	$7,49456 \cdot 10^{-6}$	$2,86487 \cdot 10^{-5}$	$7,62341 \cdot 10^{-4}$
A_8	-	-	$-4,11674 \cdot 10^{-7}$	$-2,00343 \cdot 10^{-6}$	$-4,62973 \cdot 10^{-4}$
A_9	-	-	-	-	$5,64285 \cdot 10^{-5}$
A_{10}	-	-	-	-	$-2,80152 \cdot 10^{-6}$
A_{11}	-	-	-	-	$3,24557 \cdot 10^{-6}$
	3.0 MeV	4.0 MeV	5 MeV	6 MeV	7 MeV
A_1	$1,44494 \cdot 10^{-1}$	$1,53235 \cdot 10^{-1}$	$1,55676 \cdot 10^{-1}$	$1,62687 \cdot 10^{-1}$	$1,61752 \cdot 10^{-1}$
A_2	$-1,18222 \cdot 10^{-1}$	$-1,07749 \cdot 10^{-1}$	$-9,06485 \cdot 10^{-2}$	$-7,58029 \cdot 10^{-2}$	$-6,25151 \cdot 10^{-2}$
A_3	$-2,44409 \cdot 10^{-2}$	$-1,24834 \cdot 10^{-2}$	$-9,53659 \cdot 10^{-3}$	$-2,34019 \cdot 10^{-2}$	$-4,17788 \cdot 10^{-2}$
A_4	$-1,84676 \cdot 10^{-2}$	$-1,80455 \cdot 10^{-2}$	$-2,75223 \cdot 10^{-2}$	$-3,11307 \cdot 10^{-2}$	$-3,25657 \cdot 10^{-2}$
A_5	$-3,88562 \cdot 10^{-3}$	$-6,12815 \cdot 10^{-3}$	$-7,33796 \cdot 10^{-3}$	$6,54673 \cdot 10^{-3}$	$1,72441 \cdot 10^{-2}$
A_6	$6,08319 \cdot 10^{-3}$	$4,49711 \cdot 10^{-4}$	$1,77743 \cdot 10^{-3}$	$6,92502 \cdot 10^{-3}$	$2,89563 \cdot 10^{-3}$
A_7	$-3,24815 \cdot 10^{-3}$	$-4,87790 \cdot 10^{-3}$	$-1,02763 \cdot 10^{-3}$	$9,19852 \cdot 10^{-4}$	$-1,28058 \cdot 10^{-3}$
A_8	$-5,61885 \cdot 10^{-4}$	$4,26467 \cdot 10^{-3}$	$1,10805 \cdot 10^{-2}$	$9,08616 \cdot 10^{-3}$	$2,42021 \cdot 10^{-3}$
A_9	$3,85679 \cdot 10^{-4}$	$3,62952 \cdot 10^{-4}$	$-1,54520 \cdot 10^{-4}$	$-3,47922 \cdot 10^{-3}$	$-5,27969 \cdot 10^{-3}$
A_{10}	$-1,85704 \cdot 10^{-4}$	$-3,88304 \cdot 10^{-4}$	$-1,33247 \cdot 10^{-3}$	$-1,20652 \cdot 10^{-3}$	$3,64979 \cdot 10^{-4}$
A_{11}	$4,35942 \cdot 10^{-5}$	$1,54917 \cdot 10^{-4}$	$3,09293 \cdot 10^{-4}$	$5,50460 \cdot 10^{-4}$	$4,63498 \cdot 10^{-4}$
A_{12}	$-1,28576 \cdot 10^{-5}$	$-1,00590 \cdot 10^{-4}$	$1,20849 \cdot 10^{-4}$	$3,56987 \cdot 10^{-4}$	$4,35344 \cdot 10^{-4}$
A_{13}	$-2,46564 \cdot 10^{-6}$	$-5,99643 \cdot 10^{-5}$	$-1,99648 \cdot 10^{-4}$	$-1,46592 \cdot 10^{-4}$	$2,06168 \cdot 10^{-4}$
A_{14}	-	$3,17933 \cdot 10^{-5}$	$7,99205 \cdot 10^{-5}$	$3,84715 \cdot 10^{-5}$	$-1,65752 \cdot 10^{-4}$
A_{15}	-	$-7,07207 \cdot 10^{-7}$	$-2,32738 \cdot 10^{-5}$	$-1,34338 \cdot 10^{-4}$	$-5,03967 \cdot 10^{-4}$

TABLE 3. Continued.

Coeff.	Neutron energy				
	8 MeV	9 MeV	10 MeV	11 MeV	12 MeV
A_1	$2,13907 \cdot 10^{-1}$	$2,45491 \cdot 10^{-1}$	$2,74822 \cdot 10^{-1}$	$2,93735 \cdot 10^{-1}$	$3,07224 \cdot 10^{-1}$
A_2	$-4,91007 \cdot 10^{-2}$	$-3,45947 \cdot 10^{-2}$	$-2,02205 \cdot 10^{-2}$	$-5,82493 \cdot 10^{-3}$	$9,74145 \cdot 10^{-3}$
A_3	$-5,96584 \cdot 10^{-2}$	$-7,07942 \cdot 10^{-2}$	$-7,42228 \cdot 10^{-2}$	$-7,43958 \cdot 10^{-2}$	$-6,95390 \cdot 10^{-2}$
A_4	$-4,06771 \cdot 10^{-2}$	$-4,48931 \cdot 10^{-2}$	$-4,47246 \cdot 10^{-2}$	$-4,58418 \cdot 10^{-2}$	$-4,57755 \cdot 10^{-2}$
A_5	$1,63499 \cdot 10^{-2}$	$1,56591 \cdot 10^{-2}$	$1,49145 \cdot 10^{-2}$	$1,45028 \cdot 10^{-2}$	$1,16887 \cdot 10^{-2}$
A_6	$-3,96492 \cdot 10^{-3}$	$-6,88060 \cdot 10^{-3}$	$-5,98988 \cdot 10^{-3}$	$-4,12996 \cdot 10^{-3}$	$-6,49925 \cdot 10^{-2}$
A_7	$1,33357 \cdot 10^{-5}$	$3,42005 \cdot 10^{-3}$	$3,12730 \cdot 10^{-3}$	$1,47672 \cdot 10^{-3}$	$-1,83429 \cdot 10^{-3}$
A_8	$4,77982 \cdot 10^{-3}$	$7,39119 \cdot 10^{-3}$	$4,96163 \cdot 10^{-3}$	$2,00666 \cdot 10^{-3}$	$8,79090 \cdot 10^{-4}$
A_9	$-1,31202 \cdot 10^{-3}$	$2,38335 \cdot 10^{-3}$	$3,18296 \cdot 10^{-3}$	$2,82024 \cdot 10^{-3}$	$3,97980 \cdot 10^{-3}$
A_{10}	$2,25657 \cdot 10^{-3}$	$4,53989 \cdot 10^{-3}$	$8,73637 \cdot 10^{-3}$	$1,29760 \cdot 10^{-2}$	$1,49095 \cdot 10^{-2}$
A_{11}	$-8,68465 \cdot 10^{-5}$	$-9,50446 \cdot 10^{-4}$	$-7,38829 \cdot 10^{-4}$	$3,13895 \cdot 10^{-4}$	$1,55907 \cdot 10^{-3}$
A_{12}	$-2,47119 \cdot 10^{-4}$	$-1,59130 \cdot 10^{-3}$	$-4,30632 \cdot 10^{-3}$	$-6,17818 \cdot 10^{-3}$	$-7,64195 \cdot 10^{-3}$
A_{13}	$-1,28758 \cdot 10^{-4}$	$1,40963 \cdot 10^{-5}$	$-8,75253 \cdot 10^{-4}$	$-1,56539 \cdot 10^{-4}$	$-8,34133 \cdot 10^{-4}$
A_{14}	$-6,94767 \cdot 10^{-4}$	$-5,26982 \cdot 10^{-4}$	$6,75061 \cdot 10^{-4}$	$2,37855 \cdot 10^{-3}$	$4,31894 \cdot 10^{-3}$
A_{15}	$-5,66311 \cdot 10^{-4}$	$-4,90604 \cdot 10^{-4}$	$-3,00183 \cdot 10^{-4}$	$9,29565 \cdot 10^{-4}$	$9,25026 \cdot 10^{-4}$
A_{16}	$-5,19118 \cdot 10^{-5}$	$-3,68725 \cdot 10^{-4}$	$-1,17577 \cdot 10^{-3}$	$-2,15991 \cdot 10^{-3}$	$-2,63486 \cdot 10^{-3}$
A_{17}	$9,45215 \cdot 10^{-6}$	$-1,10975 \cdot 10^{-5}$	$-1,98076 \cdot 10^{-4}$	$-6,61766 \cdot 10^{-4}$	$-7,75606 \cdot 10^{-4}$
A_{18}	-	-	-	-	$-1,13278 \cdot 10^{-4}$
A_{19}	-	-	-	-	$2,56046 \cdot 10^{-4}$

	14 MeV	16 MeV	18 MeV	20 MeV
A_1	$3,55189 \cdot 10^{-1}$	$3,86491 \cdot 10^{-1}$	$4,04901 \cdot 10^{-1}$	$4,26834 \cdot 10^{-1}$
A_2	$5,46726 \cdot 10^{-2}$	$1,02811 \cdot 10^{-1}$	$1,32004 \cdot 10^{-1}$	$1,63458 \cdot 10^{-1}$
A_3	$-5,93838 \cdot 10^{-2}$	$-3,76109 \cdot 10^{-2}$	$-1,63487 \cdot 10^{-2}$	$6,56068 \cdot 10^{-3}$
A_4	$-5,48919 \cdot 10^{-2}$	$-6,00851 \cdot 10^{-2}$	$-5,70750 \cdot 10^{-2}$	$-5,24940 \cdot 10^{-2}$
A_5	$4,22430 \cdot 10^{-4}$	$-9,54353 \cdot 10^{-3}$	$-1,36688 \cdot 10^{-2}$	$-1,80515 \cdot 10^{-2}$
A_6	$-4,69763 \cdot 10^{-3}$	$-1,45102 \cdot 10^{-2}$	$-1,97441 \cdot 10^{-2}$	$-2,30265 \cdot 10^{-2}$
A_7	$-1,17686 \cdot 10^{-3}$	$-9,83492 \cdot 10^{-3}$	$-1,19099 \cdot 10^{-2}$	$-8,84962 \cdot 10^{-3}$
A_8	$-4,07513 \cdot 10^{-3}$	$-1,36939 \cdot 10^{-2}$	$-1,88986 \cdot 10^{-2}$	$-1,71026 \cdot 10^{-2}$
A_9	$3,09660 \cdot 10^{-3}$	$-2,96829 \cdot 10^{-3}$	$-8,93267 \cdot 10^{-3}$	$-1,21812 \cdot 10^{-2}$
A_{10}	$1,58091 \cdot 10^{-2}$	$1,48821 \cdot 10^{-2}$	$1,29780 \cdot 10^{-2}$	$7,35240 \cdot 10^{-3}$
A_{11}	$6,06495 \cdot 10^{-3}$	$8,52190 \cdot 10^{-3}$	$1,00802 \cdot 10^{-2}$	$9,79040 \cdot 10^{-3}$
A_{12}	$-1,46198 \cdot 10^{-3}$	$5,57826 \cdot 10^{-3}$	$8,72034 \cdot 10^{-3}$	$1,14370 \cdot 10^{-2}$
A_{13}	$2,27202 \cdot 10^{-3}$	$3,56478 \cdot 10^{-3}$	$3,07263 \cdot 10^{-3}$	$5,40567 \cdot 10^{-3}$
A_{14}	$5,42538 \cdot 10^{-4}$	$-7,24949 \cdot 10^{-3}$	$-7,60994 \cdot 10^{-3}$	$-1,98753 \cdot 10^{-3}$
A_{15}	$-1,55029 \cdot 10^{-3}$	$-5,52038 \cdot 10^{-3}$	$-4,08630 \cdot 10^{-3}$	$-2,10266 \cdot 10^{-3}$
A_{16}	$-2,23491 \cdot 10^{-3}$	$5,32675 \cdot 10^{-4}$	$-5,90160 \cdot 10^{-4}$	$-4,73347 \cdot 10^{-3}$
A_{17}	$-1,45674 \cdot 10^{-3}$	$-5,02964 \cdot 10^{-3}$	$-7,33597 \cdot 10^{-3}$	$-7,32857 \cdot 10^{-3}$
A_{18}	$-1,51567 \cdot 10^{-3}$	$-3,31941 \cdot 10^{-3}$	$-5,90536 \cdot 10^{-3}$	$-5,52230 \cdot 10^{-3}$
A_{19}	$3,06764 \cdot 10^{-4}$	$6,46102 \cdot 10^{-4}$	$-1,87799 \cdot 10^{-3}$	$-4,72617 \cdot 10^{-3}$

TABLE 3. Continued.

Coeff.	Neutron energy			
	14 MeV	16 MeV	18 MeV	20 MeV
A_{20}	-	$5,4I907 \cdot I0^{-4}$	$I,I2005 \cdot I0^{-3}$	$-8,29404 \cdot I0^{-4}$
A_{2I}	-	$8,33378 \cdot I0^{-4}$	$I,8I33I \cdot I0^{-3}$	$2,22935 \cdot I0^{-3}$
A_{22}	-	-	$2,04I65 \cdot I0^{-4}$	$7,47427 \cdot I0^{-4}$
A_{23}	-	-	$I,670I3 \cdot I0^{-4}$	$3,36549 \cdot I0^{-4}$

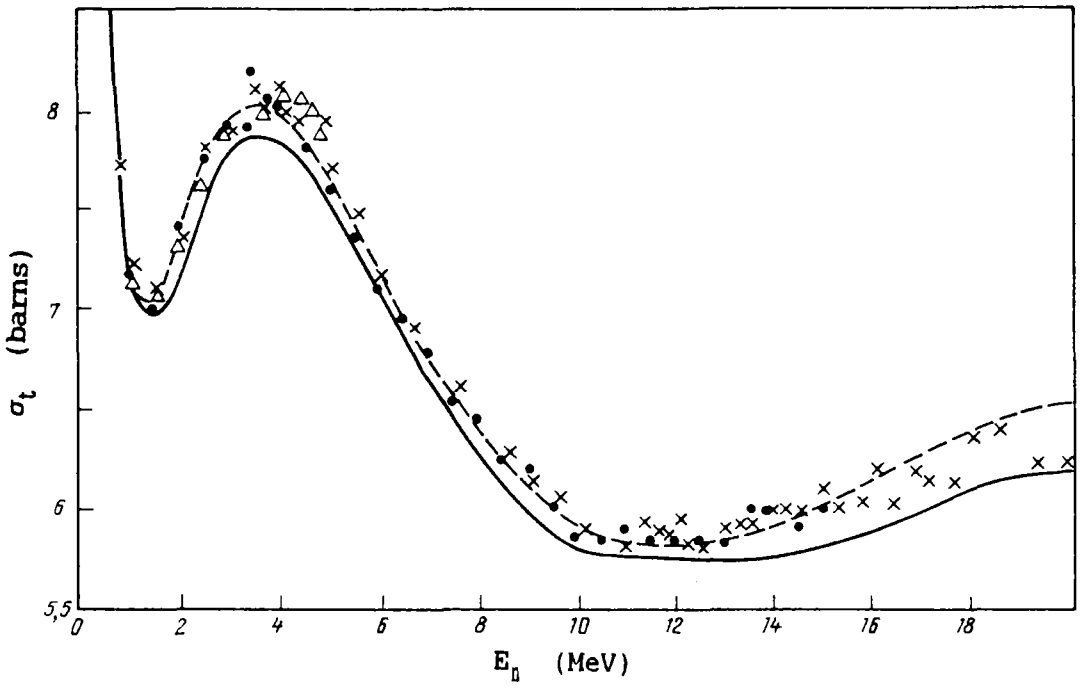

FIG. 6. Total ^{238}U cross-section: —— ref.[1] evaluation, — — — authors' coupled channel calculations. Experimental data: x - ref.[7], ● - ref.[8], △ - ref.[9].

The (n,3n) reaction cross-section

The currently available (n,3n) reaction cross-section data, published in references [10-12], agree with each other, and cover the full energy range, from threshold to the upper boundary of the file energy. In the region of the (n,3n) reaction cross-section maximum, these data lie approximately 30% lower than the reference [1] evaluation. It is therefore suggested to change the evaluated curve [1] above 15 MeV to agree with the experimental data. The data resulting from this analysis with the evaluation in reference [1] are tabulated in Table 5 and shown graphically in Figure 7.

TABLE 4. COMPARISON OF THE TOTAL CROSS-SECTION IN THE 1-20 MeV ENERGY RANGE BETWEEN RESULTS OF THIS EVALUATION AND THOSE OF THE REFERENCE [1] EVALUATION (given in barns)

E_n (MeV)	This evaluation	Ref.[1] evaluation	E_n (MeV)	This evaluation	Ref.[1] evaluation
1.0	7.14	7.14	8.5	6.25	6.14
1.6	7.10	6.99	9.0	6.11	6.0
2.0	7.40	7.13	9.5	6.00	5.9
2.5	7.75	7.51	10.0	5.90	5.82
3.0	7.95	7.80	11.0	5.85	5.78
3.5	8.02	7.84	12.0	5.85	5.76
4.0	7.98	7.84	13.0	5.86	5.76
4.5	7.82	7.73	14.0	5.92	5.78
5.0	7.60	7.56	15.0	5.98	5.83
5.5	7.37	7.34	16.0	6.05	5.90
6.0	7.19	7.10	17.0	6.11	6.00
6.5	6.95	6.85	18.0	6.20	6.09
7.0	6.75	6.65	19.0	6.27	6.16
7.5	6.55	6.45	20.0	6.28	6.19
8.0	6.38	6.29	-	-	-

TABLE 5. COMPARISON OF REF.[1] EVALUATED (n,3n) CROSS-SECTION WITH THIS EVALUATION (in barns)

E_n MeV	This evaluation	Ref.[1] evaluation
13.0	0.240	0.240
14.0	0.479	0.479
15.0	0.650	0.690
15.5	0.720	0.790
16.0	0.760	0.872
16.5	0.790	0.938
17.0	0.800	0.993
17.5	0.810	1.043
18.0	0.815	1.076
18.5	0.810	1.055
19.0	0.790	0.960
19.5	0.720	0.840
20.0	0.650	0.700

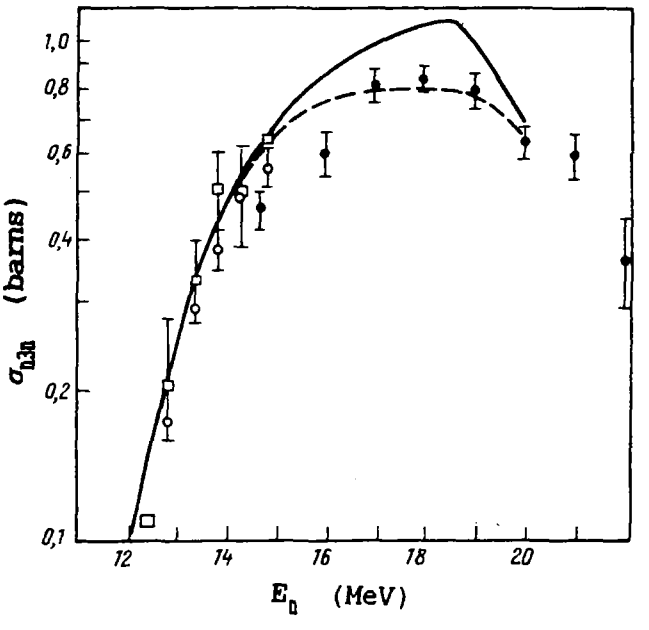

FIG. 7. The ^{238}U (n,3n) reaction cross-section: —— ref.[1] evaluation, – – – this evaluation. Experimental data: □ - ref.[10], o - ref.[11], ● - ref.[12].

Conclusion

The following conclusions can be made as a result of this analysis:

1. The use of the coupled channel method in the evaluation of the angular distribution of elastically and inelastically scattered neutrons leads to a better agreement with experimental data and improves the reliability of the evaluated data.

2. Consideration of the new experimental σ_t and $\sigma_{n,in}$ cross-section data points to the need to reevaluate the reference [1] evaluation of these cross-sections in the MeV energy range.

REFERENCES

[1] NIKOLAEV, M.N., ABAGYAN, L.P., KORCHAGENA, ZH.A., Neutron Data for Uranium-238., Part 1, Institute of Physics and Power Engineering, Obninsk (1979) (in Russian).
NIKOLAEV, M.I., BAZAZYANTS, N.O., GORBACHEVA, L.V., ibid. Part 2.

[2] KLEPATSKIJ, A.B., KONSHIN, V.A., SUKHOVITSKIJ, E.Sh., The coupled channel method and the evaluation of neutron data of fissile nuclei, Izv. Akad. Nauk BSSR, Ser. Fiz. Ehnerg. 2 (1984) 21 (in Russian).

[3] BEGHIAN, L.E., KEGEL, G.H.R., MARCELLA, T.V., et al., Neutron scattering cross-sections of uranium-238, Nucl. Sci. and Eng. 69 (1979) 191.

[4] HAOUAT, G., SIGAUD, J., LACHKAR, J., et al., Differential cross-section measurements of fast neutron scattering or ^{208}Pb, ^{232}Th and ^{238}U at 2.5 MeV, Rep. NEANDC(E)-180-L (1977).

[5] HAOUAT, G., LACHKAR, J., LAGRANGE, Ch., et al., Differential cross-section measurements for 3.4 MeV neutron scattering from ^{208}Pb, ^{232}Th, ^{235}U, ^{238}U and ^{239}Pu, Rep. NEANDC(E)-196-L (1978).

[6] KIKUCHI, Ya., Research of the best running conditions of nuclear codes for coupled channel calculations of neutron interactions with heavy deformed nuclei, IAEA Rep. INDC(FR)-5/L (1972).

[7] HAYES, S.H., STOLER, P., KLEMENT, J.M., et al., The total neutron cross-section of uranium-238 from 0.8 to 30 MeV, Nucl. Sci. and Eng. 50 (1973) 243.

[8] SCHWARTZ, R.B., SCHRACK, R.A., HEATON, H.T., Total neutron cross-sections of ^{235}U, ^{238}U and ^{239}Pu from 0.5 to 15 MeV, Nucl. Sci and Eng. 54 (1974) 322.

[9] POENITZ, W.P., WHALEN, J.F., SMITH, A.B., " Total neutron cross-sections of heavy nuclei", in Proc. Int. Conf. on Nuclear Data for Science and Technology, Knoxville, TE (1979) 698.

[10] FREHAUT, J., MOZHINSKI, G., "Measurement of (n,2n) and (n,3n) cross-sections for incident energies between 6 and 15 MeV", in Proc. of Conf. on Nuclear Cross-sections and Technology, Washington, DC., Vol.2 (1975) 855.

[11] FREHAUT, J., Status of (n,xn) cross-section data at Bruyeres-le-Chatel in the actinide region, Rep. NEANDC(E)-211-L (1981) 29.

[12] VEESER, L.R., ARTHUR, E.D., "Measurements of (n,3n) cross-sections for ^{235}U and ^{238}U", in Proc. of Int. Conf. on Nuclear Physics and Nuclear Data, Harwell, UK (1978) 1054.

EVALUATION OF THE AVERAGE ^{238}U RESONANCE PARAMETERS IN THE RESOLVED RESONANCE ENERGY RANGE

V.A. Konshin, N.K. Salyakhov

Abstract

The average <D>, <gΓ_n^0> and <S_0> resonance parameters have been evaluated for ^{238}U using Froehner's method of recognition of omitted levels. This study concludes that due to the considerable uncertainty in the number and widths of p-wave resonances in ^{238}U, the suggested dependence of the level density on parity is questionable.

The diversity of evaluated average parameters for one and the same set of resonance parameters bears witness to the variety of methods used to determine these quantities [1]. This problem has been avoided in this analysis by the combined utilization of the latest methods and a subsequent analysis of the results. The following analytical methods are currently used in the determination of average resonance parameters:

- Δ_3 statistics [2],
- spin distribution of the derived neutron widths [3],
- maximum likelihood analysis with consideration of omitted weak resonances [4,5],
- maximum likelihood analysis with consideration of omitted weak and multiplet resonances [6],

The basis of these methods lies in obtaining average parameters for part of the data in which it is assumed that resonance transmission is absent, and using some or all [6] of the following resonance parameter properties:

- independence of the actual resonance density on energy,
- spin independence of the strength function S(1,J)=S(J),
- the χ^2 distribution of the reduced neutron widths for ν=1 degrees of freedom,
- distribution of the distances between resonances according to Wigner's law.

Two of the more perfected above-mentioned methods are considered in this analysis, namely that of Coceva [4], and that of Froehner [6]. The main emphasis of this analysis is on the application of these methods to the evaluation of ^{238}U data in the resolved resonance region.

The Δ_3 statistical method [2] is devoted to the region in which resonance transmission is absent. This region is actually characterized by the linear dependence of the increasing number of resonances on energy, and falls within the special conditions described in reference [2]. In reference [3], it is assumed that reduced widths of all experimentally determined resonances are larger than a limiting fraction α of the actual average width $\langle g\Gamma_n^0 \rangle$. The basis of this method consists in comparing the expected theoretical factor, determined by the spin distribution parameter α, with the experimentally determined value of the number of widths n_i for which $g\Gamma_n^0 \geq \alpha \langle g\Gamma_n^0 \rangle$.

The average parameters calculated in reference [4], are determined from the conditions which maximize the value of the likelihood function $L(\langle g\Gamma_n^0 \rangle, \langle g\Gamma_n^1 \rangle, D^0, \nu)$. This method allows one to determine the magnitude of the average reduced neutron width $\langle g\Gamma_n^1 \rangle$ for p-waves and the number of degrees of freedom of the neutron width distribution at the same time as the determination of the $\langle g\Gamma_n^0 \rangle$ and $\langle D^0 \rangle$ quantities. It is assumed that all resonances whose widths lie above the conditional threshold $\eta(E)$ are taken into account. The likelihood function is defined as the probability that there exists a set of resonances $(E_i, g\Gamma_{ni})$ in which the number of observed resonances N_{obs} have widths for which $g\Gamma_{ni} \geq \eta(E)$; the widths of the remaining resonances lie below that threshold.

In order to simplify the calculation and the analysis, the likelihood function is represented in the form of a sum of independent contributions summed over discrete energy intervals; that is, rather than determining the specific position of resonances, the calculation determines the probability that a given number of resonances will fall in a given energy interval:

$$L(D_1^0 \ell ist) = \prod_{k=1}^{m} \left[\prod^{n_k} (g\Gamma_{n_{i_k}} | \ell ist)(n_k | D^0, \ell ist) \right] = \prod_{i=1}^{N_{obs}} (g\Gamma_{n_i} | \ell ist) \prod_{k=1}^{m} (n_k | D^0, \ell ist), \qquad (1)$$

where A/B is the probability for event A to occur under the condition that event B had occurred first; where *list* is the set of parameters $\langle g\Gamma_n^0 \rangle$, $\langle g\Gamma_n^1 \rangle$, ν ; and n_i is the number of resonances observed in the interval k. The existence of the energy dependent threshold $\eta(E)$ is taken into account by introducing the

so-called truncated χ^2 distribution for neutron widths $\Gamma_{ni} \geq \eta(E)$ in the evaluation of the explicit form of equation (1). The likelihood function for the set of s-resonance parameters has the following form:

$$L(\langle g\Gamma_n^0\rangle, D^0, \nu) = \prod_{i=1}^{N_{obs}} \frac{\nu}{2\langle g\Gamma_n^0\rangle}\left(\frac{g\Gamma_{n_i}^0}{2\langle g\Gamma_n^0\rangle}\right)^{\nu/2-1} \prod_{k=1}^{m}\left[\sum_{N>n}(N/D^0)\binom{N}{n}P_0^n(1-P)^{N-n}\right];$$

$$\binom{N}{n} = \frac{N!}{(N-n)!\,n!};$$

$$\alpha_0[\eta(E)] = \frac{1}{\Gamma(\nu/2)}\int_{\frac{\nu\eta(E)}{2\langle g\Gamma_n^0\rangle}}^{\infty} \exp(-z)z^{\nu/2-1}dz,$$

Here P_0 represents the probability that a given resonance satisfies the condition that $g\Gamma_{ni} > \eta(E)$ (it is assumed that $P_0=\alpha_0[\eta(E)]$ is constant over the whole interval); E is the centre of the interval; (N/D^0) is the distribution of the possible total number of resonances in a given interval: $(N/D^0)\approx\exp[(N-\langle N\rangle)/2\sigma^2]$, where $\langle N\rangle=\Delta\varepsilon_i/D^0$ ($\Delta\varepsilon_i$ being the interval width); and the variance σ^2 is equal to $0.203[\ln(2\pi\,\Delta\varepsilon_i/D^0)+0.343]$.

The reliability of the average resonance parameters can be improved by studying their dependence on the position of the $\eta(E)$ threshold by varying its parameters within reasonable limits. In the present analysis, this reliability was determined under the condition that it satisfies the approximations used in this approach, and that not less than 80% of the initially selected sample falls within the region which satisfies the condition that $g\Gamma_{ni} > \eta(E)$. The following expression is used to determine the variance of the average parameters for this particular case:

$$\sigma^2(\langle g\Gamma_n^0\rangle)/\langle g\Gamma_n^0\rangle^2 = 2/N; \quad \sigma^2(D^0)/(D^0)^2 = (0{,}8 + N - N_{obs})/N_{obs}, \qquad (2)$$

where N is the evaluated number of resonances. Note that this expression can be used only for s-resonance parameters.

An important aspect of this analysis lies in the choice of the shape and magnitude of the conditional threshold $\eta(E)$. On one hand the shape of this function must guarantee the absence of

transmitted resonances for which $g\Gamma_n \geq \eta(E)$, and on the other, it must preserve a large enough sampling capacity. Reference [5] has adopted the following expression for this function:

$$\eta(E) = (AE^B + C)\ tE^{\frac{1}{2}}$$

where A, B, C are chosen for t=1, on the basis of the correspondence of $\eta(E)$ to the actual resonance acceptance threshold based on their neutron width. The dependence of the result as a function of the threshold position was studied by varying the t parameter only. This showed that results, not dependent on the t parameter, are evidently statistically dependable.

In references [6] and [4], the values of the average parameters are derived from the conditions which maximize the likelihood function. What singles out the method used in reference [6] is that it groups the resonances before they are screened. A parameter which takes the diffuseness of the peak registration threshold into account is introduced, and the threshold parameter is coupled to the quantity D^0. In the calculation of resonance transmissions, the multiplet nature of the peaks is taken care of by the introduction of their neutron width distribution:

$$P(G)dG = (1-q)(1+V)\exp(-x)(\pi x)^{-1/2}dx\,,$$

where $G = g\Gamma_n^0$; $G_0 = \langle g\Gamma_n^0 \rangle$; $x = G/2G_0$; $V = z\sqrt{\pi}\exp(z^2)(1+erf\,z)$; $z = q\sqrt{x}$.

The fraction of the distance between resonances q(E), which is smaller than the experimental resolution threshold, is represented by the author of reference [6] in the form of:

$$q(E) = \bar{q}\,\frac{\rho - \rho_0}{\rho - \rho_0}\,.$$

Here $\bar{q} = \int_0^{D_c} P(D)dD$

where D_c is the minimal experimentally resolved distance and P(D) is the distribution of distances between resonances. Taking ρ to be the actual resonance density, and $\rho_0(E)$ the observed peak density, we have:

$$\rho_0(E) = \frac{dN(E)}{dE} = \rho_0\left[1 - k\,\frac{2(\bar{E}-E)}{\Delta E}\right];$$

where ρ_0 and k are derived from the second degree polynomial N(E).

The calculation of the average parameters is thus reduced to the solution of the following set of equations which satisfy the conditions for maximizing the likelihood function:

$$1 - 1/N \sum_{i=1}^{N} \frac{\bar{U}_c}{S_i} \frac{\partial S_i}{\partial \bar{U}_c} = 0 \ ;$$

$$G^\circ = \bar{G} \left[1 - 2/N \sum_{i=1}^{N} \left(\frac{G_0}{S_i} \frac{dS_i}{\partial G^\circ} + \frac{G^\circ}{1+V_i} \frac{\partial V_i}{\partial G^\circ} \right) \right]^{-1} ,$$

where $\bar{U}_c = \rho_0 D^\circ = \bar{\rho}_0 / \rho$; and S_i is the parameter which reflects the diffuseness of the resonance registration threshold:

$$S_i = 1/2 \left(1 - \tanh \frac{U_i - \bar{U}_c}{k \bar{U}_c} \right) .$$

An attempt to generalize this method for the case of a mixed set of s- and p- resonances is described in reference [7].

The average resonance parameters of ^{238}U were evaluated with the use of evaluated parameters for 164 s-wave and 280 p-wave levels that were calculated in reference [8] up to an energy of 4.04 keV, and for 428 resonances calculated in reference [9] up to 4.04 keV. Out of 302 resonances that lie below 2 keV, 206 were p-type according to reference [9], and 183 according to reference [8]. The determination of the parity of those states having a small neutron width is quite complicated, and to determine whether they belonged to the s- or p- type was possible for only a small number of weak resonances with the aid of differences between experimentally determined capture gamma-ray spectra.

Since the average reduced neutron widths for s- and p-resonances are significantly different, they are separated from each other in references [8] and [9] by using a quantitative criterium based on Baes's theorem (that all levels for which $P(p, g\Gamma_n^0) < 0.5$ are s-levels). In the energy range below 2 keV, approximately 10% (23 levels) were identified in references [8] and [9] as p-levels. This difference is explained by the fact that in reference [8], contrary to reference [9], five levels for which $P(p, g\Gamma_n^0) > 0.5$ were considered as s-levels in order to satisfy the Δ_3 statistics condition in the energy range of 0 - 2 keV; also, all levels which were observed to take part in sub-threshold fission were considered to belong to s-type levels.

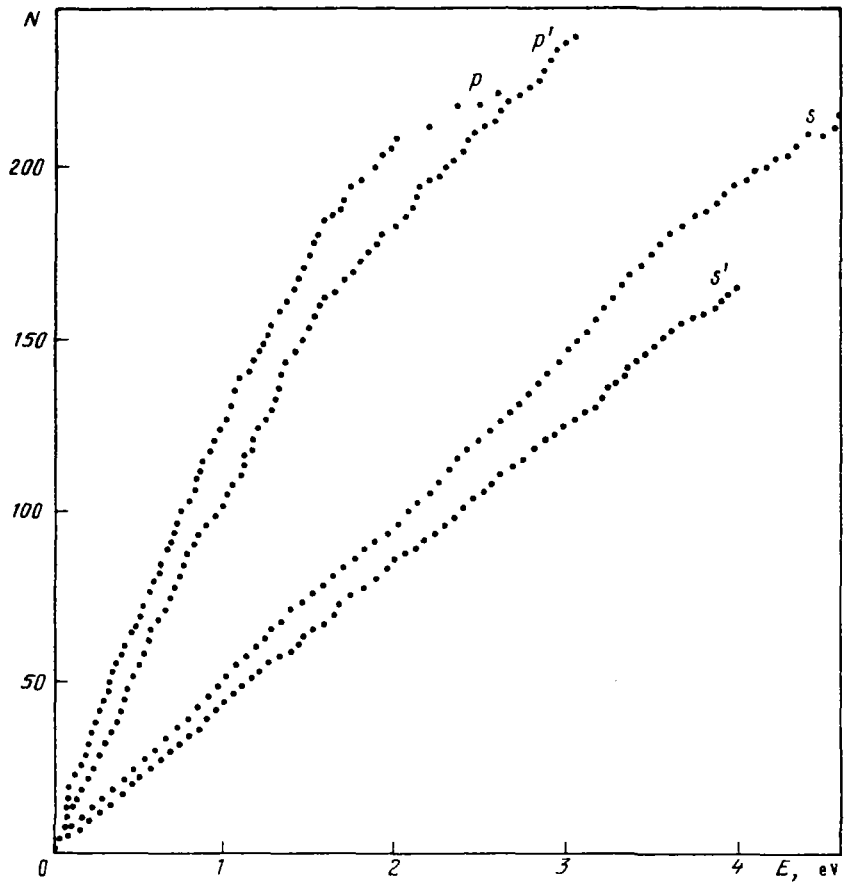

Fig. 1. Increase in the number of s- and p-resonances [8], and s'- and p'-resonances [9] for ^{238}U.

Figure 1 shows the growing sums of s- and p-type resonances as given in references [8] and [9]. One can see a substantial difference in the slopes of these curves. Differences in the data of references [8] and [9] can be seen in the diagrams showing the distribution of reduced neutron widths (Figure 2), and particularly in the diagrams of p-resonance widths distribution which are given in units of $g\Gamma_n^l$ (see Figure 3, where $g\Gamma_n^l = g\Gamma_n / \{(k_0R)^2/[1+(k_0R)^2]\}$).

Figures 4 a,b and c show the average values of $\langle g\Gamma_n^0 \rangle$ for s- and p-waves, as well as the values of $\langle D \rangle$ for s-waves as a function of the parameter α, derived from the analysis of the data from reference [9] using the method described in reference [4]. The dependence of the average values of $\langle g\Gamma_n^0 \rangle$ and $\langle g\Gamma_n^1 \rangle$ on the α parameter is particularly noticeable where the approximate value of the ratio D_0/D_1 is assumed to be equal to 3 in the method used in reference [4] (see Figure 4a).

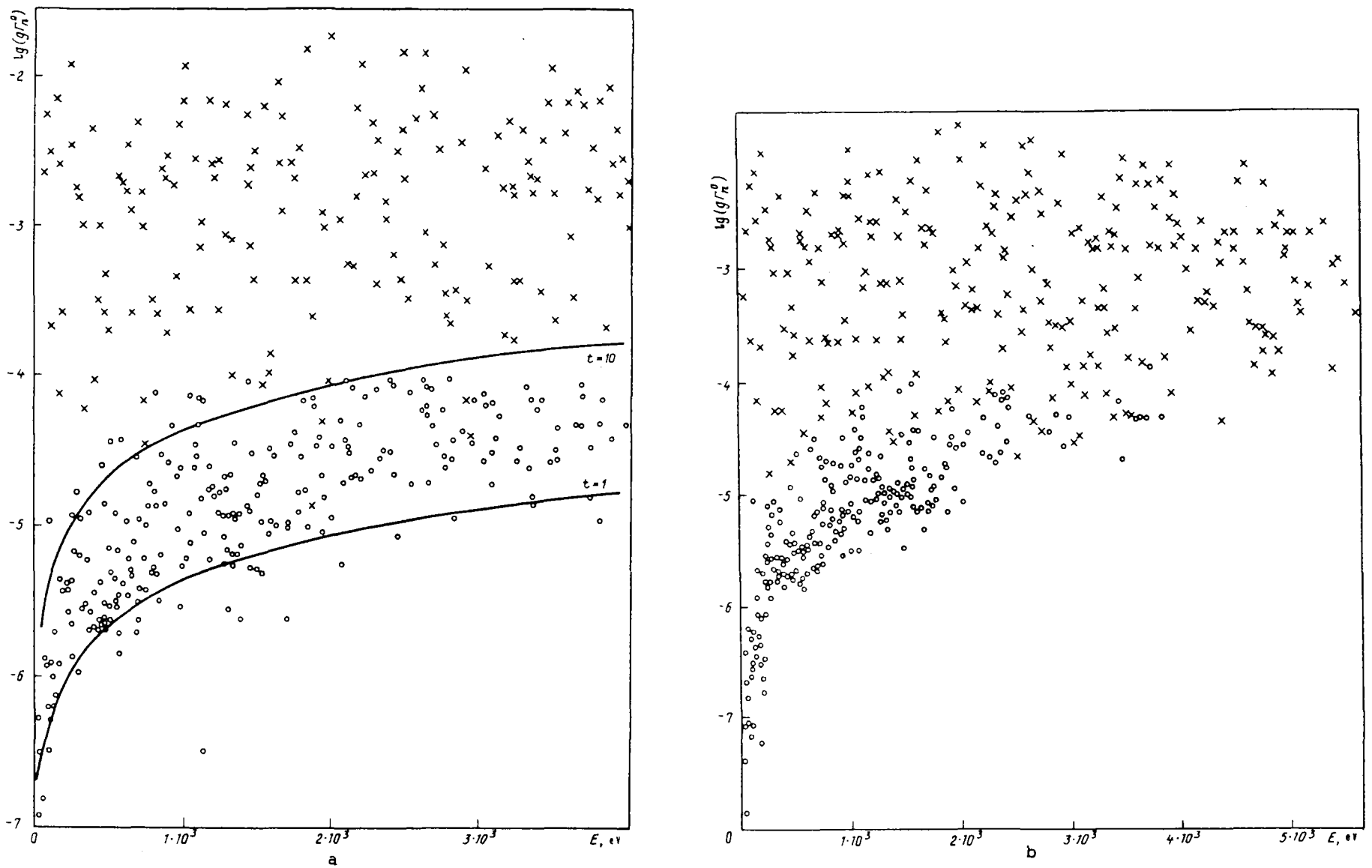

Fig. 2. Reduced neutron widths for s-levels (x) and for p-levels (o) of ^{238}U: (a) according to reference [8], and (b) according to reference [9]. Solid curves represent different levels of the conditional resonance registration threshold.

The analysis of the p-resonances using the reference [4] method (Figure 5) and that of reference [6] confirms the proposition that the given ratio is not substantiated if one used the data given in reference [9]. The result of the analysis of the s-resonances [9] over various energy ranges (see Figure 6), using the reference [6] method, confirms the proposition that, because of the multiplet character of the peaks, the method applied in this case allows one to take the transmission of resonances into account, whereas the reference [4] method does not give this possibility.

The results of the evaluation of the average resonance parameters are given in Table 1. Contrary to the approach taken in references [4] and [5], the error in the values of the evaluated parameters were estimated as follows: for the reference [4] method the error was estimated from the spread of the results averaged over different ranges of the t parameter; for the reference [6] method, the errors were estimated from the oscillations of the evaluated values which resulted from the choice of coefficients to fit the approximating parabola over different energy intervals. The values taken as the basis in the process of deriving the final values of the evaluated averaged parameters, were those that were obtained within narrow energy intervals, and which at the same time, offered a wide enough choice. The following average resonance parameters, based on the evaluated data given in reference [9], can be adopted on the basis of these results:

$$\langle g\Gamma_n^0 \rangle = (1.9 \pm 0.20) \cdot 10^{-3} \text{ eV (for s-wave } g=1)$$
$$\langle D_0 \rangle = (19.2 \pm 0.5) \text{ eV}$$
$$\langle g\Gamma_n^1 \rangle = (1.55 \pm 0.17) \cdot 10^{-3} \text{ eV}$$
$$\langle D_1 \rangle = (4.5 \pm 0.25) \text{ eV}$$

In comparison, the following are the values of the same quantites as given by the authors of reference [9]:

$$\langle g\Gamma_n^0 \rangle = (2.30 \pm 0.23) \cdot 10^{-3} \text{ eV}$$
$$\langle D \rangle_0 = (20.8 \pm 0.6) \text{ eV}$$
$$\langle \Gamma_n \rangle_1 = 2.1 \cdot 10^{-3} \text{ eV}$$
$$\langle D \rangle_1 = 4.4 \pm 0.4 \text{ eV}$$

From the values obtained for $\langle D \rangle_0$ and $\langle D \rangle_1$ it can be seen that the value for the ratio $\langle D \rangle_0 / \langle D \rangle_1 \approx 4$.

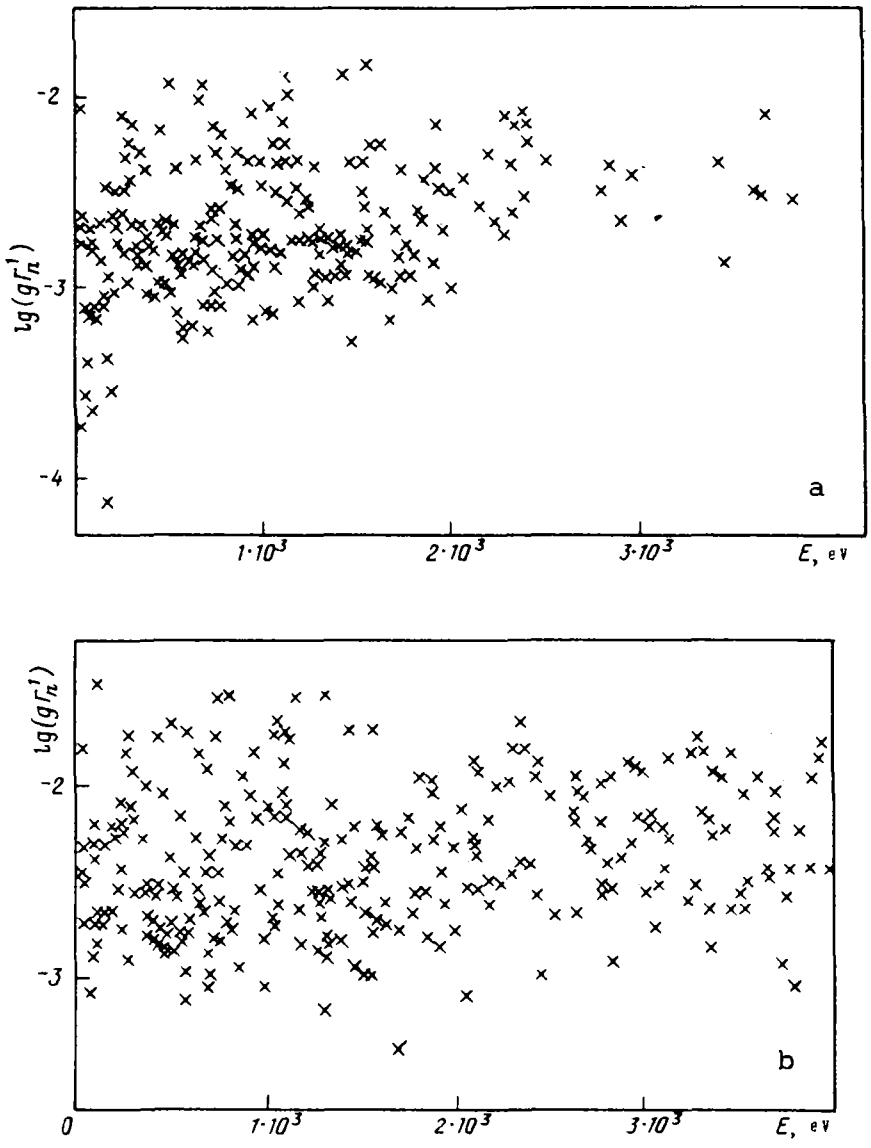

Fig. 3. Normalized $g\Gamma_n^1$ neutron widths for ^{238}U p-resonances: (a) according to reference [8], (b) according to reference [9].

The application of reference [4] method to the set of resonance parameters given in reference [8] indicates that there is weak dependence of the average s- and p-wave parameters on the registration threshold parameter $\eta(E)$ (see Figure 7). The application of Froehner's method to the s-resonance set of reference [8] shows a weak tendency for a group-wise resonance transmission. The average value for $\langle D \rangle_0$ turns out to be equal to (21.7±0.4) eV and $\langle g\Gamma_n^0 \rangle = (2.43 \pm 0.15) \cdot 10^{-3}$ eV. The application of reference [6] method to the p-resonance set of reference [8] shows a complete agreement with the group-wise representation of resonance transmission. Corresponding calculations have yielded the following values: $\langle D \rangle_1 = (6.9 \pm 0.4)$

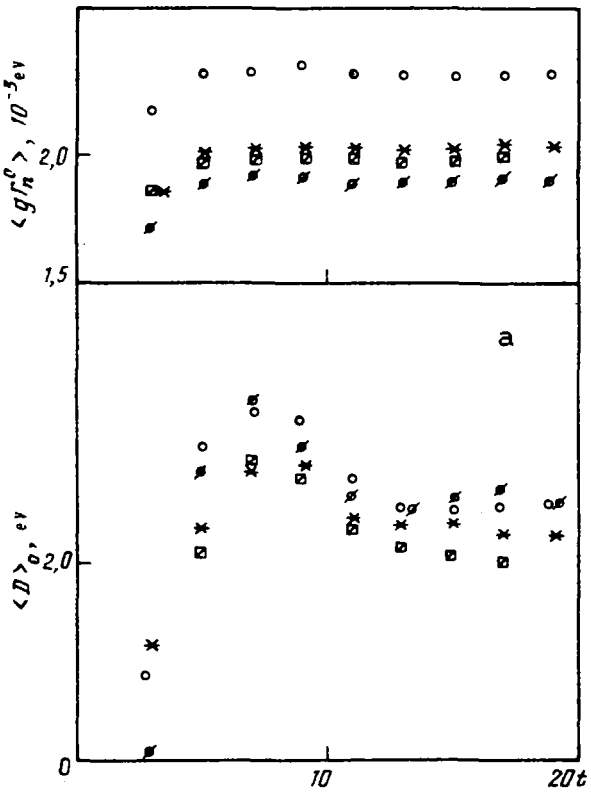

*Fig. 4. Dependence of the average values of parameters as a function of the conditional threshold level for resonance registration, and as a function of the energy interval using reference [4] method: (a) for the un-separated set of -s resonance data from reference [9], (b) for p-resonance data, and (c) for s-resonances in the α range of 20-60 and for a fixed value of $\langle g\Gamma_n^0\rangle_1 = 2.0 \cdot 10^{-3}$ eV, all given for the following energy ranges: x - 0 to 4.042 keV, Δ - 0 to 3.0 keV, o - 0 to 2.0 keV, Φ - 0 to 1.5 keV, * - o to 1.25 keV, ⊠ - 0 to 1.0 keV.*

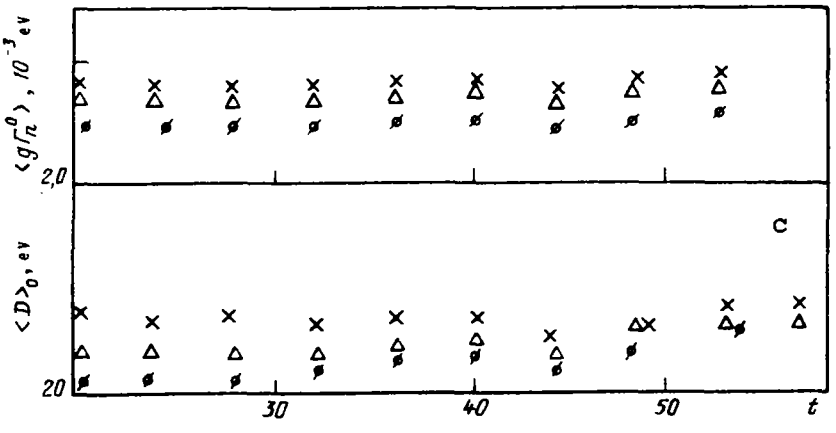

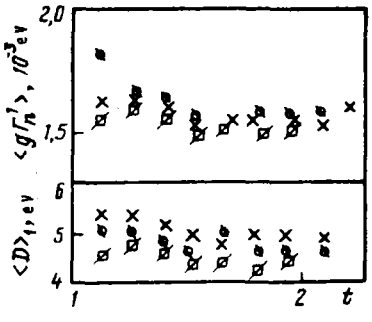

Fig. 5. Results of calculations using the reference [4] method on the ^{238}U s-resonance set from reference [9] for the following energy intervals: Φ - 0 to 1.5 keV, x - 0 to 1.0 keV, ⊠ - 0 to 0.8 keV.

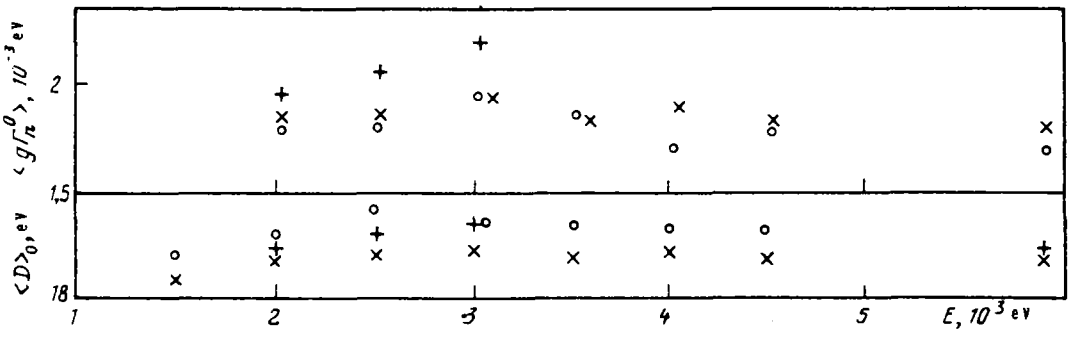

Fig. 6. Results of calculations using the reference [6] method on the ^{238}U s-resonance set from reference [9] for various energy intervals, whereby the coefficients of the parabola, which approximates the increasing sum of the s-resonances, are chosen according to the following energy intervals: x - 0 to 5.756 keV, + - 0 to 3.0 keV, and o - 0 to 2.5 keV.

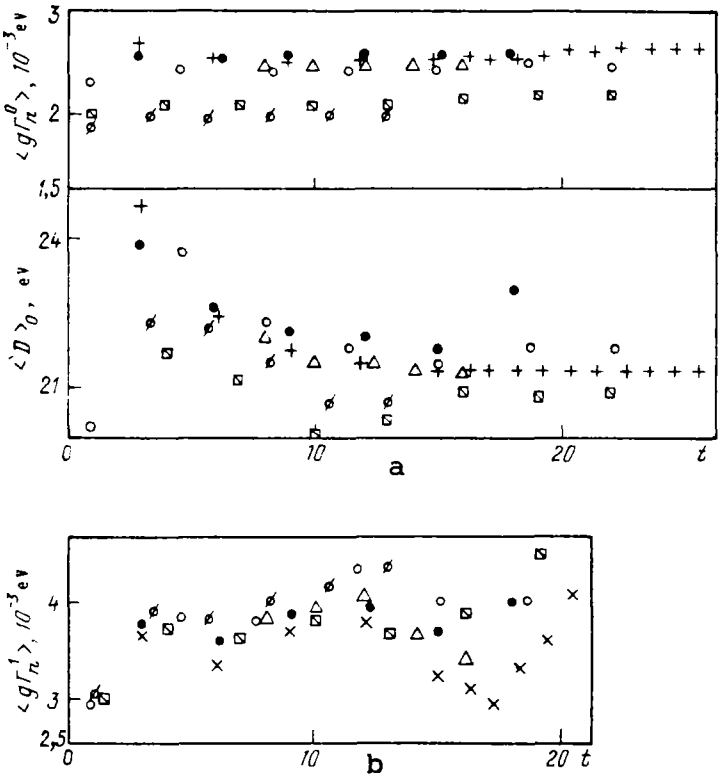

Fig. 7. Results of calculations using the reference [4] method on the ^{238}U resonance parameter data from reference [8]: (a) where a is chosen for s-resonances, and (b) for p-resonances, given for the following intervals: + - 0 to 4.023 keV, Δ - 0 to 3.5 keV, ● - 0 to

TABLE I. RESULTS OF THE EVALUATION OF ^{238}U AVERAGE RESONANCE PARAMETERS BASED ON DATA PUBLISHED IN REFERENCES [8] AND [9]

Parameter	Energy interval (keV)	Coceva's Method [4] applied to references		Froehner's Method [6] applied to references	
		[8]	[9]	[8]	[9]
A	0-1.0	20.5±0.5	20.4±0.4	-	-
A	0-1.5	21.4±0.6	21.3±0.3	-	18.7±0.5
A	0-2.0	21.5±0.7	21.0±0.3	-	19.0±0.3
A	0-2.0	-	20.6±0.5	21.9±0.4	19.2±0.5
A	0-3.0	21.2±0.3	20.8±0.3	21.98±0.40	19.2±0.4
A	0-3.5	21.5±0.3	-	22.1±0.4	19.0±0.5
A	0-4.0	21.30±0.25	21.5±0.3	22.1±0.4	19.2±0.3
B	0-1.0	2.00±0.15	1.98±0.10	-	-
B	0-1.5	1.75±0.10	1.90±0.10	-	1.50±0.30
B	0-2.0	1.98±0.15	2.30±0.15	-	1.88±0.12
B	0-2.5	-	2.25±0.10	2.30±0.15	1.90±0.15
B	0-3.0	2.50±0.15	2.35±0.15	2.45±0.15	2.00±0.15
B	0-3.5	2.50±0.15	2.40±0.15	2.50±0.15	1.82±0.15
B	0-4.0	2.50±0.15	2.40±0.15	2.55±0.15	1.80±0.15
C	0-1.0	3.15±0.25	2.00±0.10	-	-
C	0-1.5	3.90±0.25	1.90±0.10	-	-
C	0-2.0	3.90±0.50	2.30±0.10	-	-
C	0-2.5	-	-	-	-
C	0-3.0	3.75±0.25	-	-	-
C	0-3.5	3.90±0.15	-	-	-
C	0-4.0	3.60±0.25	-	-	-
D	0-1.0	3.50±0.40	1.55±0.10	2.50±0.25	1.64±0.15
D	0-1.5	3.75±0.25	1.58±0.10	2.25±0.20	1.56±0.15
D	0-2.0	3.50±0.30	1.55±0.15	1.90±0.35	1.40±0.20
D	0-2.5	3.60±0.25	-	-	-
E	0-1.0	7.0±0.8	-	6.50±0.60	4.75±0.25
E	0-1.5	6.5±0.5	-	7.25±0.40	4.55±0.30
E	0-2.0	7.0±0.5	-	6.75±0.30	4.22±0.40
E	0-2.5	7.5±0.0	-	-	-

Annotation: Reference [6] method is applicable only to separate s- and p-resonance parameter sets.

Parameters (first column Table 1)

A - $\langle D \rangle_0$ (eV) s-wave

B - $\langle g\Gamma_n^0 \rangle$ (10^{-3} eV) s-wave

C - $\langle g\Gamma_n \rangle_1$ (10^{-3} eV) p-wave

D - $\langle g\Gamma_n \rangle_1$ (10^{-3} eV) p-wave, separate p-resonance file

E - $\langle D \rangle_1$ (eV) p-wave, separate p-resonance file

TABLE 2. COMPARISON OF ^{238}U P-RESONANCE WIDTHS

E_r (eV)	Results published in different references		
	Ref.[8]	Ref.[9]	Ref.[10]
4.41	0.1121 - 06	0.0550 - 06 (0.1100 - 06)	0.110 - 06
10.22	0.1674 - 05	0.080 - 05 (0.600 - 05)	0.1670 - 05
11.32	0.4002 - 06	0.180 - 06 (0.3600 - 06)	0.420 - 06
16.30	0.4966 - 07	0.5300 - 07 (0.5300 - 07)	0.5000 - 07
19.52	0.1393 - 05	0.0600 - 05 (0.1200 - 05)	0.1170 - 05
45.166	0.1963 - 05	0.065 - 05 (0.1300 - 05)	-
49.626	0.9691 - 06	0.6000 - 06 (0.600 - 06)	-
57.100	-	0.500 - 06 (0.500 - 06)	-
63.505	0.1013 - 04	0.0300 - 04 (0.600 - 04)	0.1600 - 04
72.780 (72.60)	0.1000 - 04	0.0300 - 04 (0.0600 - 04)	-
74.380	0.2700 - 05	0.200 - 05 (0.2000 - 05)	-
83.683	0.1081 - 04	0.035 - 04 (0.0700 - 04)	0.1400 - 04
89.289	0.9489 - 04	0.8900 - 04 (0.8900 - 04)	0.9900 - 04
90.976	0.6000 - 05	-	-
93.097 (93.25)	0.5932 - 05	0.1700 - 05 (0.3400 - 05)	-
93.174	0.4800 - 05	0.3000 - 05 (0.3000 - 05)	-
111.205	0.8399 - 05	0.2400 - 05 (0.4800 - 05)	1.0000 - 05
121.5	-	0.300 - 05 (0.6000 - 05)	-
124.975 (124.600)	0.2208 - 04	0.0850 - 04 (0.1700 - 04)	0.2600 - 04
127.40	-	0.500 - 05 (0.5000 - 05)	-

TABLE 2. COMPARISON OF ^{238}U P-RESONANCE WIDTHS

133.292	0.8651 - 05	0.6200 - 05 (0.2400 - 05)	-
136.0	-	0.6000 - 05 (0.6000 - 05)	-
152.419	0.5075 - 04	0.1800 - 04 (0.3600 - 04)	0.5000 - 04
158.90	0.1533 - 04	0.1000 - 04 (0.1000 - 04)	0.2000 - 04
173.187	0.4677 - 04	0.1500 - 04 (0.3000 - 04)	0.5000 - 04

Note: values of $g\Gamma_n$ are given in parentheses in column 3.

eV and $\langle g\Gamma_n \rangle_1 = (2.25 \pm 0.25) \cdot 10^{-3}$, which evidently satisfy the ratio $\langle D \rangle_0 / \langle D \rangle_1 \approx 3$. The results of the evaluation using methods [4] and [6] are listed in Table 1.

The analysis of the data given in references [8] and [9] seems to indicate that the reason for the differences in the values of the ratio $\langle D \rangle_0 / \langle D \rangle_1$ (which is a factor of 3 for reference [8] and a factor of 4 for reference [9]), do not arise as a result of using one or the other method of data analysis, but are due to the values of the basic data themselves. In particular, the values of the p-resonance widths, given in reference [9], are 2 to 2.5 times smaller than those listed in references [8] and [10]. In addition, it must be noted that although values for Γ_n are given in reference [10], no information is given as to the origin of the p-level spins. This leads one to suspect that the values for Γ_n quoted in these references are actually values for $g\Gamma_n$. Authors of reference [9] quote values for $g\Gamma_n$ and derive values for Γ_n on the basis of arbitrary values of p-resonance spins on the assumption that the level density is proportional to (2J+1). But even in this case, if one compares values of $g\Gamma_n$, it turns out that the p-resonances given in reference [9] are on the average 20-30% smaller than those given in references [8] and [10]. The number of identified p-resonances in the energy range up to 2 keV in the evaluation described in reference [9] is larger than the number quoted in reference [8] by 23 resonances. Therefore, in view of such significant discrepancies in the number of p-resonances and in the values of their widths, there is not enough evidence within the framework of this analysis to

arrive at a definitive conclusion regarding the actual value of the $\langle D \rangle_0 / \langle D \rangle_1$ ratio.

An important criterion to test the validity of these evaluations is whether the results are in agreement; a disagreement in these results could have two reasons: an incorrect use of the methods to evaluate the average parameters, or the inaplicability of the data to the initial conditions of the method.

It must be noted that the results of the evaluation of $\langle g\Gamma_n \rangle_1$ (obtained with the use of Coceva's method [4] and the data given in reference [8]), which were performed for a mix of s- and p-data as well as for p-resonance data only, are practically the same; this, however, cannot be said in the case of results obtained on the basis of data published by Nikolaev et al. [9].

After a thorough analysis of the results, the first of the two reasons for such a disagreement was rejected. The conclusion can be made that the noted disagreement between the evaluations of $\langle g\Gamma_n \rangle_1$ using reference [9] data, namely that the premise of the method used in reference [4] is inconsistent with the results, is due to the fact that $\langle D \rangle_0 / \langle D \rangle_1 \approx 3$. It is possible that this disagreement would not have arisen if the partition of the resonances according to their parity in reference [9] would have been done differently.

The following conclusions can be made on the basis of this analysis:

1. Because of the small number of widths and the multiplicity of peaks, it is possible to improve the accuracy of the average parameter values by using methods for the introduction of level transmission corrections. The simultaneous application of the methods described in references [4] and [6], would also increase the reliability of the average parameter evaluation.

2. The dependence of ^{238}U resonance density on parity can be solved only by setting up a rigorous experiment which would eliminate the ambiguity in the interpretation of derived resonance parameters.

However, if one were to take reference [8] and [9] data as initial parameters, it could be stated with certainty that $\langle D \rangle_0 / \langle D \rangle_1$ is equal to ≈ 3 in the first case, and to ≈ 4 in the second case.

REFERENCES

[1] RIBON, P., Intercomparison of methods used to determine average parameters from sets of resonance parameters, Rep. NEANDC(E)-213-AL, Centre d'Etudes Nucleaires de Saclay, Gif-sur-Yvette (1981) 1-12.

[2] DYSON, F.T., MEHTA M.L., Statistical theory of the energy levels of complex systems, J. Math. Phys., 4 (1963) 701.

[3] MOORE, M.S., MOSES, I.D., KEYWORTH, G.A., et al., Spin determination of resonance structure in (^{235}U+n) below 25 keV, Phys. Rev. C18 (1978) 1328-1348.

[4] COCEVA, C., STEFANON, M., Experimental aspects of the statistical theory of nuclear spectra fluctuations, Nucl. Phys. 315 (1979) 1-20.

[5] DELFINI, G., GRUPPELAAR, H., "Maximum likelihood analysis of resolved resonance parameters for some fission product nuclei", (Proc. of Specialists' meeting on Neutron Cross-sections of Fission Product Nuclei, Bologna, 1979) Rezione Technica Intern. (1979) 169-178.

[6] FROEHNER, F.H., "Level density estimation with account of unrecognized mutiplets applied to uraniun and plutonium resonance data", (Proc. IAEA Consultants' meeting on Uranium and Plutonium Isotope Resonance Parameters, Vienna, 1981), IAEA Rep. INDC(NDS)-129 (1982) 103-111.

[7] FROEHNER, F.H., "Statistical inference of level densities from resolved resonance parameters", (Proc. IAEA Advisory Group meeting on Basic and Applied Problems of Nuclear Level Densities, Brookhaven National Lab., 1983), BNL Report (1983) 219-244.

[8] DE SAUSSURE G., OLSEN, D.K., PEREZ, R.B., et al., Evaluation of the ^{238}U Neutron Cross-Sections for Incident Neutron Energies up to 4 keV, Progr. Nucl. Energy 3 (1979) 87-124.

[9] NIKOLAEV, M.N., ABAGYAN, L.P., KORCHAGINA, Zh.A., et al., Neutron Data for ^{238}U, Part 1, FEI, Obninsk (1978) (in Russian).

[10] POORTMANS, F., MEWISSEN, L., ROHR, G., et al., "Resonance parameters of ^{238}U below 4.2 keV", (Proc. IAEA Consultants' meeting on Uranium and Plutonium Isotope Resonance Parameters, Vienna, 1981), IAEA Rep. INDC(NDS)-129 (1982) 125.

EVALUATION OF ^{238}U NEUTRON DATA IN THE RESONANCE REGION

A.A. Van'kov

Abstract

The evaluation of neutron data and the generation of group constants in the resolved and unresolved resonance region of ^{238}U are discussed in connection with the development of the USSR nuclear data library for reactor materials.

The resonance region of ^{238}U is generally defined to lie within the following energy ranges: 4.65 keV $\leq E_n \leq$ 100 keV for the region of unresolved resonances, and $E_n <$ 4.65 keV for the resolved resonance region. The upper energy boundary of 100 keV is chosen somewhat arbitrarily, because of the small number of resonance effects above that energy, and also because it is the logical energy point for the transition from the R-matrix model to the optical potential model to describe neutron cross-sections. It is evident that there must be an energy transition region in which the results from the two theoretical models must match. In the process of preparing the ^{238}U file for the nuclear data library of the Nuclear Data Centre of the USSR State Committee on the Utilization of Atomic Energy, questions arose regarding the choice of neutron cross-section models, and the dependability of existing evaluated model parameters, such as the strength functions and the average resonance parameters (e.g., neutron widths, radiation widths, distances between resonances, etc.).

Resolved resonance region. Experience has shown that the single level Breit-Wigner formalism gives a satisfactory description of ^{238}U resonance cross-sections. However, should it be desirable to have a single representation of resonance cross-sections of fissile and even-even nuclides, it is advisable to evaluate these parameters using the s-matrix (Adler-Adler) formalism as well.

The resonance region of the ^{238}U neutron data file, referred to above, is based on the Breit-Wigner model. The corresponding evaluations of resolved resonances and of average resonance

parameters are described in references [1-3]. The basic shortcoming of these evaluations is that they are based on references published before 1978, and are in need of a re-evaluation taking the most recent data into account. Considerations of the reliability of current s-resonance parameter evaluations, discussed in reference [4], indicate that differences in the data could be as high as 10% or more. More serious is the state of the evaluated p-resonance parameters. For instance, as reported in references [5] and [6], the values of earlier p-resonance neutron width evaluations [1-3] are significantly different from more recent data; some of these observed differences are as large as an order of magnitude. It is therefore evident that the conclusion arrived at by the authors of references [1-3], that the observed p-resonance neutron widths cannot be described by the Porter-Thomas distribution, is groundless. It also follows from reference [7] that current p-resonance data do not contradict the Porter-Thomas law. For the same reason, evaluations of average resonance parameters described in reference [8] can not be compared with the evaluation scheme used in references [1-3]. As a result, it is necessary to reject the aforementioned propositions put forward by the authors of references [1-3], consisting of omitting a significant number of p-levels, of assuming the dependence of ^{238}U level densities on parity, and of assuming the dependence of the radiation width on the orbital momentum. These assumptions can be substantiated only on the basis of experimental data which, however, do not exist at the present time.

Unresolved resonance region. The following values for the average resonance parameters were adopted in references [1-3]:

- for s-neutrons: $D_{1+} = 20.8$ eV, $\overline{\Gamma}_\gamma = 23.5$ MeV, $R_0 = 9.35$ fm (fm is equal to 10^{-15} m);
- for p-neutrons: $D_{1-} = 13.2$ eV, $\overline{\Gamma}_\gamma = 13.2$ MeV, $R_0 = 4.5$ fm (or up to 6.9 fm in some cases).

In most references relating to ^{231}U data, these parameters were applied irrespectively for s- and p-neutrons. The problems are that theoretical models do not always take the spin dependence of level densities for such nuclei as ^{238}U into consideration, and

that reliable p-resonance radiation width data are not existent. The situation regarding the potential scattering radius R is more complicated. According to the authors of reference [8], the effect that is more "observable" is not the dependence of R on the orbital momentum, but on the neutron energy. The question arises as to what is the effect on the calculational parameters of all these differences which result from the evaluation of average resonance parameters reported in references [1-3] and [8]. Above of all it affects the resonance self-shielding factors and their temperature dependence. As an example, the effect of an increase in temperature on the effective absorption cross-section can be as high as 30% [9].

Evaluation of the average radiation capture cross-section. In the region of unresolved resonances of the current BNAB-78 [3] library of multigroup data, the σ_γ cross-sections are lower than those resulting from the evaluation of microscopic data on the basis of integral data. This leads to a certain degree of compensation of the errors which are introduced in the interpretation of the integral data. These effects must be taken into account in the formulation of the data files. One way to take integral data into account is to introduce correcting coefficients at the production stage of the multigroup data files. So far, the existing problems in the calculational procedures to produce data files have not been resolved. It is unfortunate that the solution to this crucial problem has not been found and that the underlying reasons for these discrepancies have not been brought to light. Considering that divergencies in other respects (such as in the neutron spectrum, in the reactivity of ^{238}U and of other samples, etc.) are observed in the process of testing the evaluated neutron files against results of integral experiments, and considering the complex procedure involved in the introduction of various corrections, one should expect that a more thorough analysis of integral data would lead to a reduction in the differences between the values of corresponding quantities calculated from the data files and the integral data. Even so, it is not clear at the present time whether it is possible to use average radiative capture cross-sections calculated from the files for practical applications without adjusting them with the use of correcting factors.

REFERENCES

[1] NIKOLAEV, M.N., ABAGYAN, L.P., KORCHAGINA, Zh.A. et al., ^{238}U Neutron Data, Part 1, FEI, Obninsk (1978) (in Russian).
NIKOLAEV, M.N., BAZAZYANTS, N.O., GORBACHEVA, L.V., ^{238}U Neutron Data, Part 2, FEI, Obninsk (1979) (in Russian).

[2] MANTUROV, T.N., NIKOLAEV, M.N., Evaluation of the ^{238}U radiative capture cross-section in the unresolved resonance region, Preprint FEI-666, Obninsk (1976) (in Russian).

[3] ABAGYAN,L.P., BAZAZYANTS, N.O., NIKOLAEV, M.N., TSIBULYA, A.M., Multigroup data for reactor and shielding calculations, Ehnergoizdat, Moscow (1981) (in Russian).

[4] DE SAUSSURE, G., SMITH, A.B.,"^{238}U issues, resolved and unresolved", (Proc. Intern. Conf. on Nuclear Data for Science and Technology, Anterp, 1982), North Holland, Amsterdam (1983) 9-20.

[5] POORTMANS, F., MEWISSEN, L., "Resonance parameters of ^{238}U below 4.2 keV", (Proc. IAEA Consultants Mtg. on Uranium and Plutonium Isotope Resonance Parameters, IAEA, Vienna, 1981), IAEA Rep. INDC(NDS)-129 (1982) 112-123.

[6] MOXON, M.C., JOLY, J.E., "The neutron capture cross-section of ^{238}U", ibid. pp. 124-135.

[7] DE SAUSSURE, G., Progress in Nuclear Energy 3 (1979) 87.

[8] VAN'KOV, A.A., GOSTEVA, L.S., UKRAINTSEV, V.F., Analysis of Transmission Experiments on ^{238}U in the Unresolved Resonance Region, Problems of Atomic Science and Technology, Ser. Nuclear Constants 3(52) (1983) 27-32 (in Russian).

[9] VAN'KOV, A.A., VOROPAEV, A.I., CHUKHLOVA, O.P., The effect of improved ^{238}U and ^{239}Pu nuclear data on the computational characteristics of a test model of a fast reactor, At. Ehnerg. 58(6) (1985) 463 (in Russian).

NEUTRON TRANSMISSION IN NATURAL URANIUM IN THE 10 keV TO 2.5 MeV ENERGY RANGE

V.V. Filippov

Abstract

The measurement of neutron transmission in natural uranium, performed in nine series of experiments using T(p,n)^{3}He neutrons is summarized, and compared to data from other authors. The results of this analysis confirm the multigroup values of the total cross-section and of the self-shielding factors of the BNAB-78 data library for natural uranium.

This article describes the evaluation of the total cross-section of natural uranium at energies above 10 keV on the basis of earlier measurements reported in references [1-3] which used T(p,n) neutrons to perform the measurements for different sample thicknesses. The experiment was conducted on a van de Graaff electrostatic generator at angles of 100^0-140^0 to the proton beam (for neutron energies below 350 keV) and in the direction of the proton beam for neutron energies above 300 keV, as described in references [1-3].

The experiment, performed under conditions of good geometry, consisted in the measurement of the decrease of the neutron count (measured with a battery of paraffin shielded boron counters) upon the introduction of the sample in the collimated neutron beam for neutron energies ranging from 10-300 keV, determined primarily by varying the thickness of the tritium-titanium target. The metallic uranium samples had a diameter of 46 mm and a density of $0.0473 \cdot 10^{24}$ atoms/cm^3. The accuracies of the transmission functions ranged from 0.7%-1.5% for sample thicknesses of 0.3 to 1 cm, and to 5%-10% for higher values (see last column of Table I). Reference measurements of the transmission function were made on polyethylene and beryllium for energies below 200 keV, and with tungsten and molybdenum for energies above 1 MeV. These showed that the background does not depend on sample thickness, but primarily on the detector noise and the imperfections of the paraffin shielding. The background level varied from 0.009 to 0.002 of the counting level for neutron beam energy of E<0.35 MeV, and from 0.0005 to 0.001 for higher beam energies [2].

Only those data points for which the background correction did not exceed 40% were included in the subsequent analysis. Altogether, 1069 individual transmission values measured at 136 different energies (from 5 keV to 3.0 Mev) for 31 sample thicknesses (from 0.3 to 25 cm) were included in the analysis. A large part of the analyzed neutron transmission data is shown in Fig. 1, where data for a given sample thickness are connected by a curve. The degree of reproducibility of the observed cross-sections for indicated sample thicknesses is illustrated (by means of different symbols) in Fig. 2. The data reported in reference [1] for 4 cm samples are represented in Fig. 2 by the black circles. The actual values of the average total cross-sections, obtained by extrapolating the dependence of the measured cross-sections to zero sample thickness, are given in the upper part of that figure. The monotonic character of the dependence of the cross-section on sample thickness simplified the extrapolation procedure considerably.

TABLE I. CHARACTERISTICS OF THE NEUTRON TRANSMISSION FUNCTION EXPERIMENT

Exp. Series	Sample thickness (mg/cm^2)	Angle to proton beam	Number of values		Range of sample thickness
			Energy	Thick.	
1	0.11	100	12	12	0.5-13
2	0.32	100	5	10	0.5-13
3	0.62	100	6	11	0.5-13
4	0.71	120	10	21	0.5-16
5	0.74	139	12	18	0.3-13
6	0.62	139	55	1	4
7	1.8	0	5	10	1-23
8	2.6	0	17	11	1-18
9	2.6	0	2	47	0.3-30

In the regions of overlap, the values of the average total cross-sections were consolidated; their values are tabulated in Table II, and compared to some existing evaluations in Fig.2. As can be seen from Fig 2, this evaluation agrees with the ENDF/B-IV evaluation over the full range except from 150-300 keV where our values are 2%-3% higher. Above 200 keV there is a tendency for the KFK-750 data to be somewhat higher than the ENDFB-IV data, which is supported by the results of this evaluation.

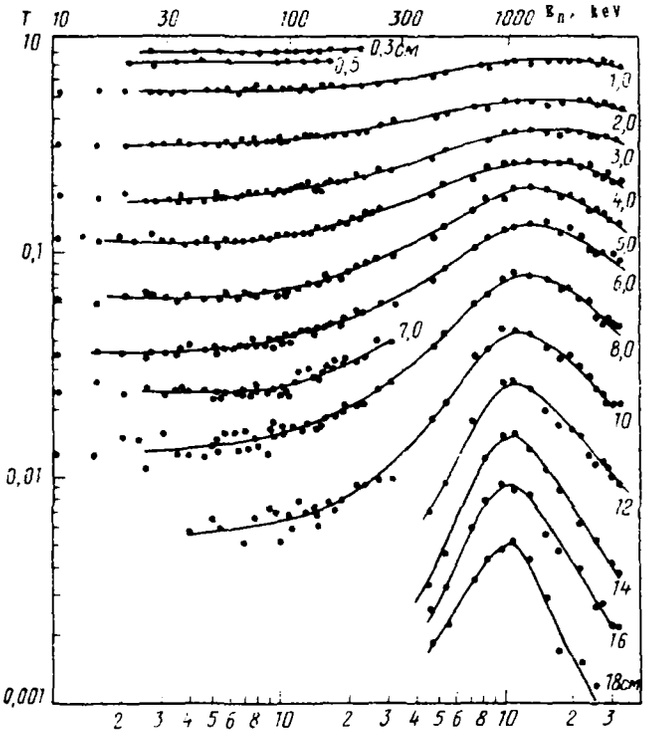

Fig. 1. Summary results of $T(p,n)^3He$ neutron transmission in natural uranium.

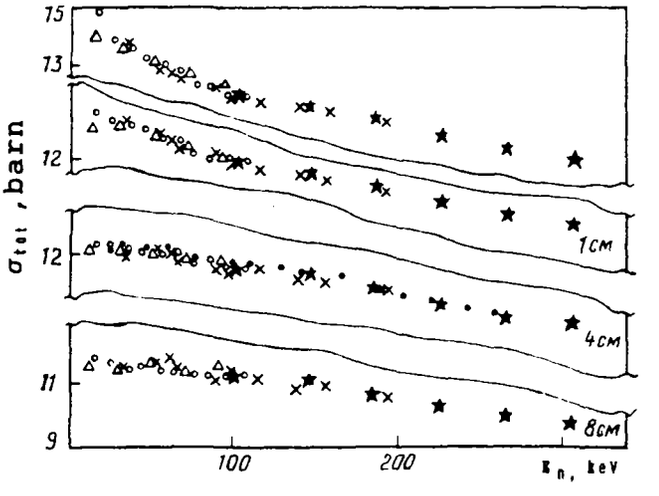

Fig. 2. Reproducibility of observed values of the total neutron cross-section in different measurement series.

TABLE 2. ENERGY DEPENDENCE OF THE TOTAL NEUTRON CROSS-SECTION FOR NATURAL URANIUM

E_n (keV)	σ_t (barns)	E_n (MeV)	σ_t (barns)
15	14.5±0.2	0.46	8.9±0.1
27	13.7±0.2	0.52	8.4±0.1
35	13.6±0.2	0.71	7.8±0.1
48	13.1±0.2	0.82	7.5±0.1
54	12.95±0.2	1.08	7.1±0.1
63	12.8±0.2	1.28	7.03±0.07
69	12.6±0.2	1.50	7.00±0.07
80	12.4±0.2	1.76	7.05±0.07
91	12.3±0.2	1.90	7.11±0.07
98	12.2±0.2	2.12	7.18±0.07
103	12.05±0.15	2.33	7.38±0.07
115	11.9±0.15	2.52	7.70±0.07
128	11.8±0.15	2.69	7.85±0.07
145	11.7±0.15	3.02	7.69±0.07
156	11.5±0.15		
185	11.2±0.15		
225	10.8±0.15		
265	10.4±0.15		
305	10.05±0.15		

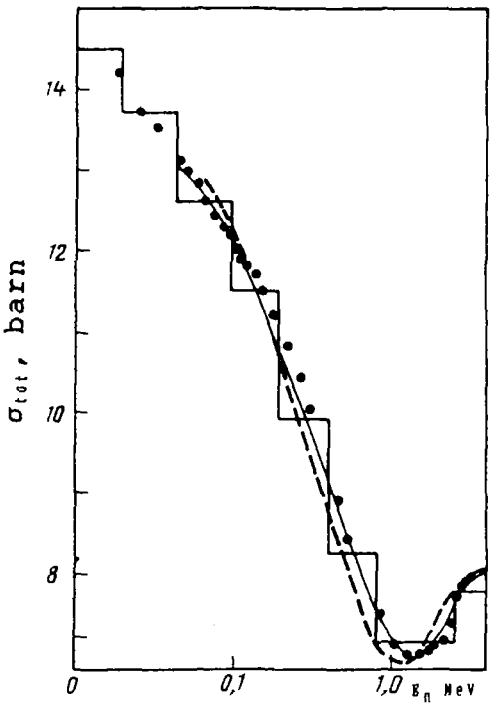

Fig. 3. Comparison of the total cross-section obtained by extrapolating to zero sample thickness with the following evaluations: ENDF/B-IV (solid curve), KFK-750 (dashed curve), BNAB-78 (histogram).

At ≈130 keV, the ENDF/B-IV recommended cross-section curve turns up sharply; our data shows the same behavior, except that the up-turn is more pronounced. At energies below 300 keV, the energy dependence of the total cross-section as recommended in the BNAB [4] data library agrees with the data given in Table 2; however, above that energy (up to E_n=1 MeV) it is lower than the values recommended in ENDF/B-IV. A comparison of the energy dependence of this evaluation with the latest experimental data [5] shows good agreement up to E_n≈200 keV; above that energy, our values are higher. The experimental data given in reference [5] are in full agreement with ENDF/B-IV data up to an energy of 400 keV, but drop below the ENDF/B-IV data above that energy, and agree with the BNAB [4] evaluation up to E_n=1 MeV. The total cross-sections for different sample thicknesses, calculated by averaging the experimental transmission data over the energy intervals used in the BNAB [4] system, are tabulated in Table 3.

TABLE 3. GROUP-AVERAGED VALUES OF THE TOTAL CROSS-SECTION (IN BARNS) AS A FUNCTION OF SAMPLE THICKNESS.

Sample thickness (cm)	Energy interval (keV) (BNAB group number)				
	4.6-10(12)	10-21(11)	21-46(10)	46-100(9)	100-200(8)
0	16.4±0.3	14.5	13.6	12.7	11.75±0.10
0.5	15.1±0.3	13.95	13.2	12.6	11.7±0.08
1	14.4±0.2	13.58	12.9	12.45	11.6±0.07
1.5	13.7±0.2	13.20	12.7	12.4	11.55±0.07
2	13.2±0.15	12.85	12.5	12.3	11.5±0.06
3	12.5±0.15	12.4	12.2	12.15	11.4±0.06
5	11.9±0.15	11.75	11.74	11.9	11.25±0.06
8	11.2±0.15	11.15	11.20	11.5	11.0±0.05
10	10.8±0.15	10.8	10.95	11.35	10.9±0.05
13	10.4±0.15	10.5	10.65	11.15	10.8±0.05

Annotation. The data for group 12 (energy interval 4.6-10 keV) are given here as illustration only; they are not reliable because of the considerable uncertainty of the data in that energy interval.

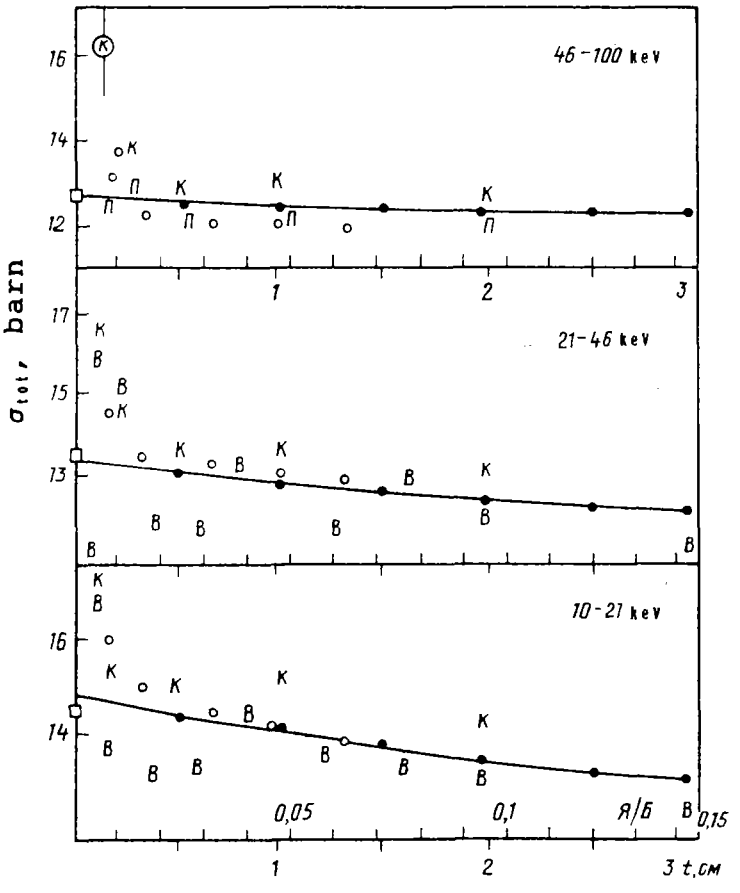

Fig. 4. Comparison of observed total cross-section values: ● this evaluation, k - [3], □ - [4], П - [5], B - [6], ∘ - [7]

The general state of the measured non-exponential character of neutron transmission in uranium in the 10-100 keV energy range as reported in the literature is shown in Fig. 4. Measurements with samples thicker than 2 cm were performed only by this author [6]. Generally, the data are in good agreement, however, their diversity increases the uncertainty of our results. The situation is more complex for measurements with thinner samples. In this case the author assumed that the reliability of the observed dependence is inversely proportionate to the scatter of the data. The author's data below 50 keV are in good agreement with the data given in reference [7] after they had been averaged according to the 1/E law over energy intervals defined by the BNAB [4] energy groups. For the top energy group (see Fig. 4) the author's data agree with the values reported in reference [5]. Extrapolation of the data of this evaluation to zero sample thickness (as given in Table 4), result in values which are close to the evaluated data adopted in the BNAB [4] data library.

The data given in Table 3 were processed using the method of directed divergence minima [8] for the unfolding of the probability distribution density of the total neutron cross-section within the confines of the energy group. The processed data are shown in Fig.5. The accuracy of the reconstituted distribution density values which is determined by the random value of the analyzed transmission within the limits of their uncertainty, ranges fron 5-7% for largest density values to 40-60% for the smallest values. The sharp narrowing of the resultant distributions above 50 keV can be explained by the manifestation of the inelastic scattering channel.

Multigroup data (total neutron cross-sections and the self-shielding factors) for natural uranium are listed in Table 4. The average cross-section data which have resulted from this analysis agree with the BNAB data, and as mentioned above, with the ENDF/B-IV data except the 7th energy group. ENDL-78 group values below the 10th group are somewhat lower. The values of the evaluated resonance parameters, which are proposed in this evaluation are corroborated by the analysis reported in reference [9]. The data processed by the authors of reference [6] using theoretical models yield somewhat higher values. The values of

our self-shielding factors, which were derived from the reconstituted distribution momentum, are in good agreement with our self-shielding factors, which were derived from the reconstituted distribution momentum, are in good agreement with the accepted BNAB [4] values below the 8th energy group. At higher energies the resonance self-shielding effects are ignored in the BNAB data library. Although the values of the measured self-shielding factors are not much different than unity, it must be noted that the calculations yield but a small fraction of this effect if one assumes a monotonically varying dependence of the cross-section within a group. Our results do not confirm those proposed in reference [6] that there is a sharp reduction (of approximately 30%) of the value of the self-shielding factor below 50 keV.

Calculations show that the assumption of a breakdown in the initial part of the observed dependence of the cross-section as a function of sample thickness [6,7,10] (see Fig.4), leads to even larger differences than reported in reference [6], in the values of both cross-sections and self-shielding factors from those given in the BNAB library. However, the extent of the manifestation of this breakdown is insufficient in order to radically change the accepted concept of the way self-shielding affects the characteristics of the total uranium neutron cross-section in the unresolved region.

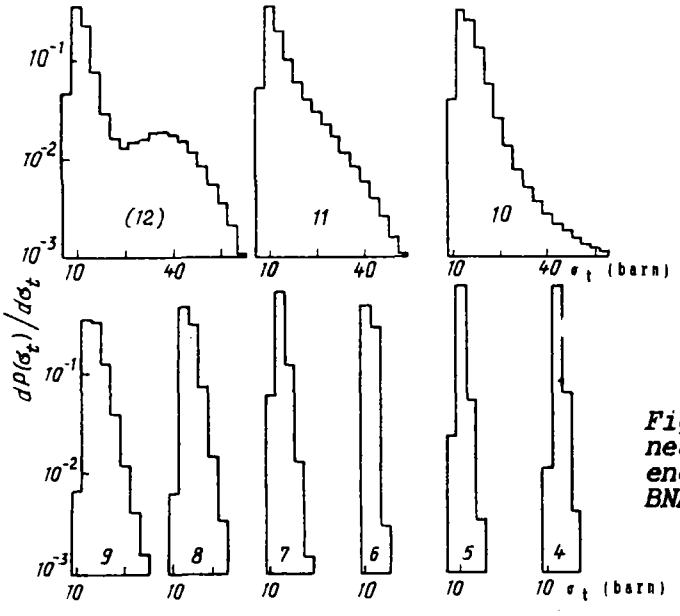

Fig. 5. Distribution density of the total neutron cross-section of uranium in the energy intervals corresponding to the nine BNAB energy groups [4].

TABLE 4A. MULTIGROUP DATA FOR NATURAL URANIUM: TOTAL CROSS-SECTIONS

BNAB Group	Origin of the data					
	BNAB-78	ENDL-78	ENDF/B-IV	Ref.[9]	Ref.[6]	This evaluation
12	15.88	14.41	16.0	16.0	17.0	16.4±0.3
11	14.48	14.02	14.4	14.6	15.1	14.5±0.2
10	13.46	13.53	13.4	13.6	13.9	13.5±0.2
9	12.57	12.79	12.7	12.8	-	12.7±0.1
8	11.53	11.52	11.5	11.7	-	11.7±0.1
7	9.90	10.02	10.0	-	-	10.30±0.08
6	8.23	8.34	8.33	-	-	8.30±0.07
5	7.13	7.17	7.16	-	-	7.12±0.05
4	7.13	7.20	7.18	-	-	7.21±0.05

TABLE 4B. MULTIGROUP DATA FOR NATURAL URANIUM. SELF-SHIELDING FACTORS

BNAB Group	Origin of the data		
	BNAB-78	Ref.[6]	This evaluation
12	0.668	0.410(139%)	(0.68)
11	0.755	0.523(-31%)	0.76±0.02
10	0.885	0.682(-20%)	0.83±0.02
9	0.915	-	0.914
8	0.950	-	0.94
7	1.0	-	0.96
6	1.0	-	0.941
5	1.0	-	0.96
4	1.0	-	0.97

REFERENCES

[1] FILIPPOV, V.V., Total neutron cross-sections for uranium and thorium in the 10-250 keV energy range, Problems of Atomic Science and Technology. Ser. Nuclear Constants 26 (1977) 5 (in Russian).

[2] FILIPPOV, V.V., " Moments of total neutron cross-section", Resonance Absorption of Neutrons (Proc. of All-Union Seminar on Resonance Absorption of Neutrons, Moscow, 1977), Moscow (1978) (in Russian).

[3] FILIPPOV, V.V., NIKOLAEV, M.N., "Measurement of the structure of the total neutron cross-section", (Proc. of Anglo-Soviet Seminar on Nuclear Constants for Reactor Calculations, Dubna, 1968), Paper ACC-68/17 (in Russian).

[4] ABAGYAN, L.P., BAZAZYANTS, N.O., NIKOLAEV, M.N., TSIBULYA, A.M., Group Constants for Reactor and Shielding Calculations, Ehnergoizdat, Moscow (1981) (in Russian).

[5] POENITZ, W., WHALEN, J., SMITH, A., Total Neutron Cross-sections of Heavy Nuclei, Nucl. Sci. and Eng. 78 (1981) 333.

[6] VAN'KOV, A.A., GOSTEVA, L.S., UKRAINTSEV. V.F., Analysis of transmission experiments in uranium in the unresolved energy region, Problems in Atomic Science and Technology. Ser. Nuclear Constants 3(52) (1983) 27 (in Russian).

[7] BYOUN, T., BLOCK, R., SEMLER, T., in Proc. of National Topical Meeting on New Developments in Reactor Physics and Shielding, New York, 1972. Part 2 (1972) 1115.

[8] TARASKO, M.Z., The method of directed divergence minima for distribution unfolding, Preprint FEI-1446, Obninsk (1983) (in Russian).

[9] MANTUROV, G.N., LUNEV, V.P., GORBACHEVA, L.V., "Evaluation of Uranium-238 and Thorium-232 in the Unresolved Resonance Region", (Proc. of Sixth All-Union Conference on Neutron Physics, Kiev, 1983), TsNIIatominform, Moscow, Vol.2 (1984) 231 (in Russian).

[10] KONONOV, V.N., POLETAEV, E.D., "Measurement of the ^{238}U total cross-section and resonance self-shielding of the capture cross-section in the 5-80 keV energy region", (Proc. of Second All-Union Conference on Neutron Physics, Kiev, 1973), Obninsk, Vol.2 (1974) 199 (in Russian).

COMPARISON OF THE BNAB-78 AND ENDF/B-V EVALUATED ^{238}U RADIATIVE CAPTURE DATA IN THE ENERGY RANGE FROM 0.5 TO 15 MeV.

V.A. Tolstikov

Abstract

Evaluations of the ^{238}U capture cross-section as given in the BNAB-78 and ENDF/B-V evaluated data libraries are intercompared and their values compared to recently published data which had not been included in these evaluations. It is concluded that there is a need to re-assess the earlier experimental data, particularly those based on activation measurements, taking secondary neutron reactions and scattering effects into account. It is recommended that a precision measurement of the capture cross-section and its dependence on energy be done in the 1-7 MeV energy range.

The accuracy requirements of the evaluated values of radiative capture cross-sections for ^{238}U in nuclear technology are considerable: 2% in the 1 keV-1 MeV energy range, and at most 3% to 5% in the 1-5 MeV energy range [1].

The evaluations which were done for the BNAB-78 [2,3] and the ENDF/B-V [4] nuclear data libraries were performed some time ago: the BNAB-78 file during the years 1975-1978, and the ENDF/B-V file in 1977[1] .

In view of the development of improved methods for the evaluation of cross-sections and their uncertainties, the publication of new experimental data, and the development of new methodologies for the measurement of cross-sections, there is a need to revise these earlier evaluations and to re-assess the reliability of the data used as input to these earlier evaluations. In addition, there is also a need to perform a high-precision measurement of the ^{238}U radiative capture cross-section over a wide energy range. The reason for these measures is that the required accuracies of these evaluated data have not yet been met.

---

[1] Subsequently, ENDF/B data [4] were adjusted according to changes in the evaluated values of the ^{235}U fission cross-section (see citation [17] in reference [7]).

A comparison of the BNAB-78 and ENDF/B-V evaluated data is given below. In the BNAB-78 library, data for E_n>0.4 MeV were taken directly from the evaluation reported in references [5] and [6], which was obtained with the use of the "fractional-rational" approximation method; for energies below 0.4 MeV, the total, inelastic and radiative capture cross-sections were evaluated simultaneously using the maximum likelihood method complemented by the nuclear reaction statistical theory. In the regions of overlap, the data were matched "manually".

The ENDF/B-V evaluation used the following procedure: groups of ^{238}U radiative capture cross-sections were evaluated separately, determined absolutely or relative to the scattering cross-section, or to the $\sigma_{n,\gamma}{}^{197}Au$, the $\sigma_{n,f}{}^{235}U$ and the $\sigma_{n,\alpha}{}^{10}B$ cross-sections. The final recommended ^{238}U $\sigma_{n,\gamma}(E_n)$ curve was derived from the combination and correlation of four such separately evaluated groups of data. Both the BNAB-78 and ENDF/B-V evaluations used similar compilations of experimental data.

The results of these evaluations are plotted on a linear-linear scale in the figures below for the following energy ranges: 0.5-1.5, 1-5 MeV and 5-15 Mev. The figures also show experimental results of relatively recent experiments which were either not included in the evaluations [7] or accepted only partially [8] (the results quoted in the initial publication were preliminary and were not given at all of the energies which were included in subsequent publications [8]). The measurement reported in reference [7] was made relative to the ^{235}U fission cross-section, and the measurement reported in reference [8] was made relative to the hydrogen scattering cross-section. The figure also shows data measured in earlier experiments [9-11] which are normalized at $E_n \approx 350$ keV to the absolute average data value reported in reference [8]. This normalization energy is more reliable than the 30 keV point (kinematic collimation) used to normalize absolute cross-sections obtained by the authors or derived from results of other authors for given neutron energies.

More complex situations, such as those related to the spectrum of incident neutrons and other considerations, have forced the authors to review their method of normalization. The following

experimental results of the ^{238}U radiative capture cross-section are reported in reference [8] for the corresponding neutron energies: 117.4±3.6 mb at 352±25 keV, 119.9±3.4 mb at 348±23 keV, 122.3±3.7 mb at 348±15 keV and 124.8±3.1 mb at 350±24 keV. The average value of these data differs from the maximum limiting values by 3%, which is in agreement with the experimental uncertainty. Consequently, the data were renormalized using the average value of 121.1±3.3 mb at the neutron energy of 349 keV. It must be noted, however, that a normalization to the value of 452.2±19.9 mb at the energy of 30 keV [6] (which is the average of seven experiments published before 1976) yields a cross-section value of 121.3 mb at E_n=350 keV.

Although both normalization methods arrived at similar results, normalization of the data in the 300-400 keV energy region is more reliable because of the weak dependence of the radiative capture cross-section on neutron energy leads to a reduced dependence on the uncertainties of the neutron energy, and consequently on the incident neutron spectrum.

As can be seen in Figs. (a) and (b), the BNAB-78 and ENDF/B-V evaluations in the 0.5 to 1.5 MeV are in good agreement. Their maximum difference does not exceed 4%, the ENDF/B-V data lying somewhat higher. Even though earlier ^{238}U $\sigma_{n,\gamma}$ cross-section measurements relative to the ^{235}U σ_f cross-section [9,10], agree with both evaluations within the limits of their uncertainties, they lie systematically lower, and closer to the BNAB-78 evaluation (in which they are included). Our data, measured relative to the elastic (n,p) scattering cross-section [8] in the 0.5 to 1.05 MeV neutron energy range, lie on the average systematically above both evaluations, but closer to the ENDF/B-V evaluation (with which they almost overlap within the limit of their uncertainty). An exception to this general agreement, is the value of four data points in the vicinity of 600 keV, namely:127.1±5 mb(H=1) at 597±16 keV, 130.8±4.7 mb(K=1) at 590±23 keV, 114.6±3.1 mb(K=1) at 603±23 keV, and 114.0±2,9 mb(K=15) at 600±36 keV (where H=1, K=1 and K=15 are the identification of the hydrogen counters of different construction used for the measurement of the neutron flux). For reasons unclear to the authors, the measurement results are grouped around two cross-

section values: 129 mb and 114 mb, which differ by approximately two measurement uncertainty values. The average value, however, lies above the ENDF/B-V evaluation[1]. This tendency is also supported by the experimental data reported in reference [7], except for the data point in the vicinity of 830 keV.

However, an experimental value at 1196 keV and two at 1400 keV given in reference [8] lie significantly lower (12% and 8% respectively) than both evaluations. The reasons for these differences are being investigated.

Both evaluations are in good agreement with each other in the 1.5 to 5.0 MeV energy, which is not surprising as both evaluations are based on the same sets of data. Experimental data at neutron energies of 2.053 and 3.033 MeV, quoted in reference [7], lie significantly higher than either one of the two evaluations. As there are no reliable theoretical data in this energy range, the odd values of these cross-sections can only be verified by means of a precise experiment.

It seems that earlier experimental data for neutron energies larger than approximately 2.5 MeV, have a number of systematic errors (which tend to raise the values of the data) which are apparently due to insufficient consideration given to scattering effects in the structure of the target, the sample holder and the sample itself. Substantial errors of this type in the experiment described in reference [12] are reported on in reference [13]. According to the analysis described in reference [13], the corrections of the data reported in reference [12] amounted to 7.4%, 16.4% and 42% at energies of 3 and 7.6 MeV. Considering the similarity of the methods used in activation measurements performed at earlier times (e.g.,in the year 1978), similar errors can be expected to be found in other such measurements. Irrespective of their apparent simplicity, activation measurements at E_n>1.5 MeV are difficult enough. Adequate consideration of scattering effects are difficult to take into account by either calculation or experiment. This problem was

---

[1] An analogous situation was observed for reference [7] data at E_n≈500 keV.

recognized a long time ago, and addressed in references [14] and [15]. For these reasons, the energy dependence of the ^{238}U capture cross-section in the energy region above 1 MeV still has to be resolved.

The data of both evaluations differ significantly in the energy range of 5-15 MeV: ranging from 20% at 5 MeV to more than 100% at 14 MeV. Experimental data exist only up to 7 MeV. As there are no data between 7 MeV and 14 MeV, the character of the cross-section curve in this energy interval is based on the extrapolation of the recommended data at 14 MeV. In the BNAB-78 data library [3], the end point of the extrapolation at 14 MeV is taken to be 2.6 mb. This value is based on the available data that existed at that time: namely, 3.3±0.5 mb at 14 MeV [16], and 3.45±1.5 mb at 15 MeV [11]. Apparently, as these data are considerably inflated because of scattering effects, the cross-section value at 15 MeV is taken to be artificially lower than the experimental value (namely 2.7 mb). However, based on the analysis reported in reference [17], it is recognized that over a wide range of mass numbers (50-240), the magnitude of the capture cross-section is approximately 1 mb at $E_n \approx 14$ MeV. This is the value used in the ENDF/B-V data library. For this reason, the BNAB-78 data in the energy range from 5 MeV to 15 MeV, can be expected to be lower as a result of their re-assessment.

The following conclusions can be drawn as a result of these considerations:

1. The state of the experimental data and the evaluations on which they are based in the energy range of 1.5 MeV and 7 MeV is not satisfactory. It is therefore deemed necessary that a precise measurement of the ^{238}U capture cross-section be performed so as to satisfy the data requirements for practical applications, and for the purpose of checking the methods used for the computation of actinide cross-sections which will be difficult to obtain by experimental means in the near future. For that purpose, it will be necessary to improve the activation method of measurement, particularly regarding the improvement of methods for the determination and calculation of errors due to the effects of neutron scattering and the generation of neutrons from secondary reactions.

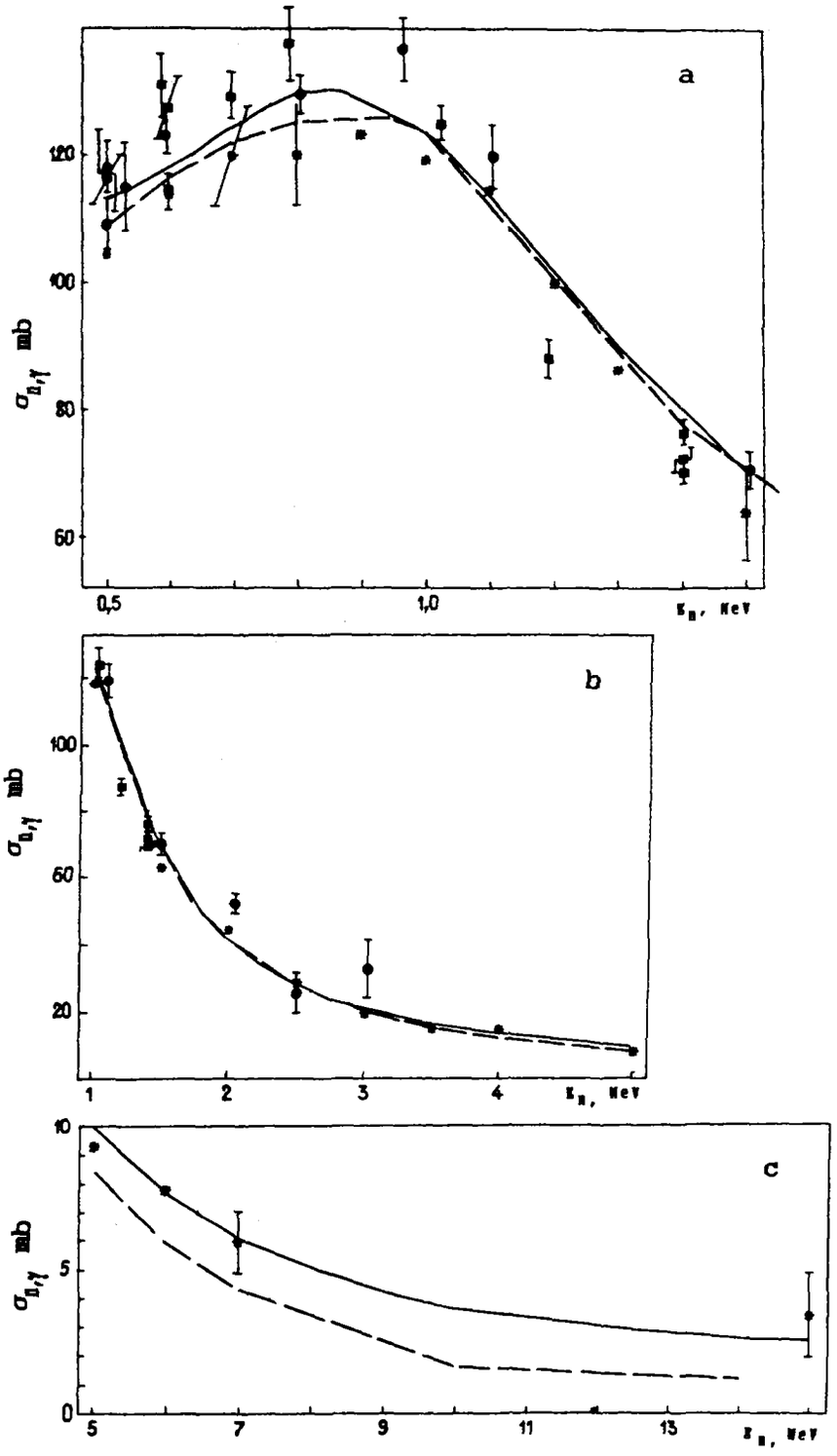

*Neutron radiative capture cross-sections for ^{238}U in the following energy ranges:Fig.(a) 0.5-1.5 MeV, Fig.(b) 1-5 MeV, Fig.(c) 5-15 MeV, for data from the following references: • [7], ■ [8], * in Figs.(a,b) [9,10], * in Fig.(c) [11]; continuous curve in Figs.(a,b) BNAB-78 [2]; continuous curve in Fig.(c) BNAB-78 [3]; dashed curve in all Figs. ENDF/B-V [4].*

2. An exact measurement is needed in the energy range of 1-7 MeV of the ^{238}U $\sigma_{n,\gamma}$ cross-section at 100 keV intervals so as to identify any non-monotonic behavior of the cross-section.

3. At energies ranging from 0.3-1.5 MeV. it is now already possible to determine the ^{238}U radiative capture cross-section to an accuracy of better than 3% using the activation method. So far, other methods are not able to achieve such accuracies.

It is only with the aid of a comprehensive compilation of experimental data, obtained by different methods to accuracies of less than 3%, and in agreement with each other within the limits of their uncertainties, that it will be possible to satisfy the severe requirements imposed by the development of nuclear technology.

4. At the present time, it is necessary to improve the ^{238}U $\sigma_{n,\gamma}$ cross-section file of the BNAB-78 data library taking the following into consideration:

- the inclusion of experimental data published in references [7,8,9];
- the review of the reliability of the earlier data, considering in particular the remarks made in this article regarding the effect of neutron scattering;
- the re-normalization of the data to revised values of standard cross-sections;
- the inclusion of theoretical calculations in the determination of evaluated curves;
- the need to make a dependable assessment of the uncertainties of the evaluated data inasmuch as they are essentially non-existent in the BNAB-78 or the ENDF/B-V nuclear data libraries.

REFERENCES

[1] U.S. NATIONAL NUCLEAR DATA CENTER, Compilation of requests for nuclear data, Rep. BNL-NCS-51572, Brookhaven National Laboratory (1983).

[2] NIKOLAEV, M.N., ABAGYAN, L.P., KORCHAGINA, Zh.A., et al., "Neutron data for uranium-238", Part 1, Institute of Physics and Power Engineering, Obninsk (1978) (in Russian).

[3] NIKOLAEV, M.N., BAZAZYANTS, N.O., GORBACHEVA, L.V., et al., "Neutron data for uranium-238", Part 2, Institute of Physics and Power Engineering, Obninsk (1979) (in Russian).

[4] POENITZ, W.P., PENNINGTON, E., SMITH, A.B., The ^{238}U radiative capture cross-section evaluation for ENDF/B-V, Rep. ANL/NDM-32, Argonne National Laboratory (1977).

[5] VINOGRADOV, V.N., DAVLETSHIN, A.N., KRIVTSOV, A.S., et al., The evaluated average ^{238}U radiative capture cross-sections in the 0.001-7 MeV energy range, Nuclear-physical Research in the USSR, 22 (1976) 4 (in Russian).

[6] VINIGRADOV, V.N., DAVLETSHIN, A.N., PLATONOV, V.P., et al., "Radiative capture of fast neutrons by the uranium-238 nucleus", (in Proc. of 3rd All-Union Conf. on Neutron Physics, Kiev, 1975), Part 4, TsNIIatominform (1976) 104 (in Russian).

[7] FAWCETT, L.P., POENITZ, W.P., SMITH, D.L.,"Measurement of the fast neutron capture cross-section", Nuclear Cross-sections for Technology, (Proc. of Inter. Conf., Knoxville, TE, 1979), Washington, D.C. (1980).

[8] DAVLETSHIN, A.N., TIKHONOV, S.V., TIPUNKOV, A.O., TOLSTIKOV, V.A., Measurement of the neutron radiative capture cross-sections of ^{238}U and ^{197}Au relative to the elastic scattering cross-section of neutrons on protons, At. Ehnerg. 48(2) (1980) 87-91 (in Russian).

[9] PANITKIN, Yu.G., TOLSTIKOV, V.A., Radiative capture of 1.2-4 MeV neutrons, At. Ehnerg. 33 (1972) 782 (in Russian).

[10] PANITKIN, Yu. G., STAVISSKIJ, Yu.Ya., TOLSTIKOV, V.A., "Measurement of the ^{238}U neutron radiative capture cross-section in the 0.024-1.1 MeV energy range", (in Proc. of All-Union Conf. on Neutron Physics, Kiev, 1971),Part 1, Naukova Dumka, Kiev (1972) 321 (in Russian).

[11] PANITKIN, Yu.G., TOLSTIKOV, V.A., Radiative capture of neutrons in the 5-20 MeV energy range, At. Ehnerg. 33(4) (1972) 825 (in Russian).

[12] BARRY, J.F., BUNCE, I., WHITE, P.H., Cross-section for the reaction ^{238}U(n,γ)^{239}U in the energy range 0.12-8.6 MeV, J. Nucl. Energy A/B 18 (1964) 481.

[13] SOWERBY, M.G., PATRICK, B.H., MATHER, D.S., Simultaneous evaluation of the fission cross-section of ^{235}U, ^{239}Pu and ^{238}U, and the capture cross-section of ^{238}U in the energy range 100 eV to 20 MeV, Ann. Nucl. Sci. and Eng. 1(7/8) (1974) 409.

[14] DAVLETSHIN, A.N., TIPUNKOV, A.O., TIKHONOV, S.V., TOLSTIKOV, V.A., "Background corrections in sample activation on electrostatic accelerators", Problems of Atomic Science and Technology. Ser. Nuclear Constants 3(38) (1980) 68-77 (in Russian).
DAVLETSHIN, A.N., TIPUNKOV, A.O., TOLSTIKOV, V.A., Analysis of the methodology of fast neutron interaction cross-section measurements by activation, At. Ehnerg. 48(2) (1980) 113 (in Russian).

[15] ANDERSEN, P., ZORRO, R., BERGQVIST, I., The influence of background neutrons on (n,γ) activation measurements in the neutron energy region 2.0-7.7 MeV, Lund University report (1984).

[16] PERKIN, J.Z., O'CONNOR, Z.P., COLEMAN, R.F., Radiative capture cross-section for 14.5 MeV neutrons, Proc. Phys. Soc. 72 (1958) 505.

[17] DRAKE, D., BERGQVIST, I., McDANIELS, D.K., Dependence of 14 MeV radiative neutron capture on mass number, Phys. Letters 36B(6) (1979) 557-558.

[18] KONONOV, V.N., POLETAEV, E.D., BOKHOVKO, M.V., et al., Experimental determination of the resonance self-shielding factors for the ^{238}U radiative neutron capture cross-section in the 10-140 keV energy range, Problems of Atomic Science and Technology. Ser. Nuclear Constants 2 (1985) 41-44 (in Russian).

FAST NEUTRON FISSION CROSS-SECTION OF ^{238}U

A.A. Goverdovskij

Abstract

Experimental and evaluated ^{238}U neutron induced fission cross-section data are analyzed. It is shown that the BNAB-MICRO evaluation is preferable to the ENDF/B-V evaluation.

The ^{238}U fast neutron fission cross-section is often used as a standard in the measurement of threshold reaction cross-sections such as (n,α), (n,p), (n,2n) and other reactions. It is for this reason that information on the ^{238}U cross-section plays such an important role in the energy region above 5 MeV. Experimental results of the $^{238}U/^{235}U$ fission cross-section ratio have been plotted in Fig.1. The bulk of the data are grouped in a 7-10% wide band. If one takes the accuracy requirement of the ^{238}U cross-section into account (from the point of view of its importance as a standard as well as an important reaction in nuclear technology), then one gets an actual critical selection of experimental information which is taken as the basis of the evaluation.

The deviation of the ratios of the ^{238}U to ^{235}U fission cross-sections, measured by various authors, from the curve based on the currently recommended ENDF/B-V evaluated data is plotted in Fig. 2. All of the available experimental data were separated into two groups. The first group (Fig. 2a) includes data that were measured on electrostatic generators working in continuous as well as pulsed mode [1,2,4,7,8]. The procedures used in the normalization of the energy dependence of the considered class of relative measurements is achieved by various means: ranging from the method of isotopic impurities determination by analytical weighing, to the comparison of relative alpha activities of the ^{238}U and ^{235}U samples. The most reliable is the isotopic impurity method in which the ^{238}U to ^{235}U fission cross-section ratio can be determined from the following relationship: $\sigma_8/\sigma_5 = \eta[(R_f/R_f)-1]$, where η is the ratio of the number of ^{235}U and ^{238}U atoms in the

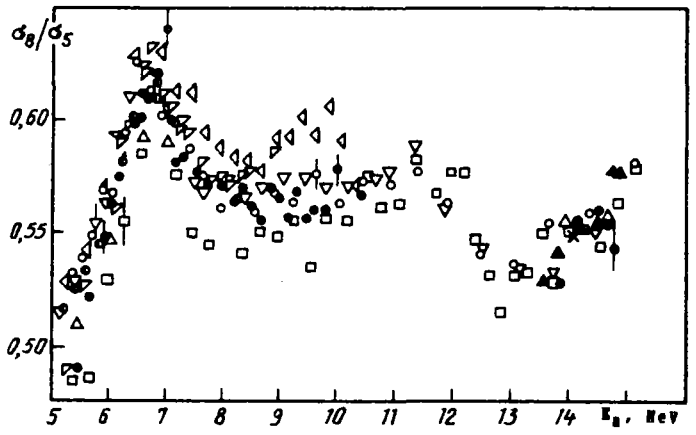

Fig. 1. ^{238}U to ^{235}U fission cross-section ratio from the following references: ● - [1], O - [2], ◐ - [3], △ - [4], □ - [5], ▽ - [6], ▷ - [8], x - [9], ▲ - [10]

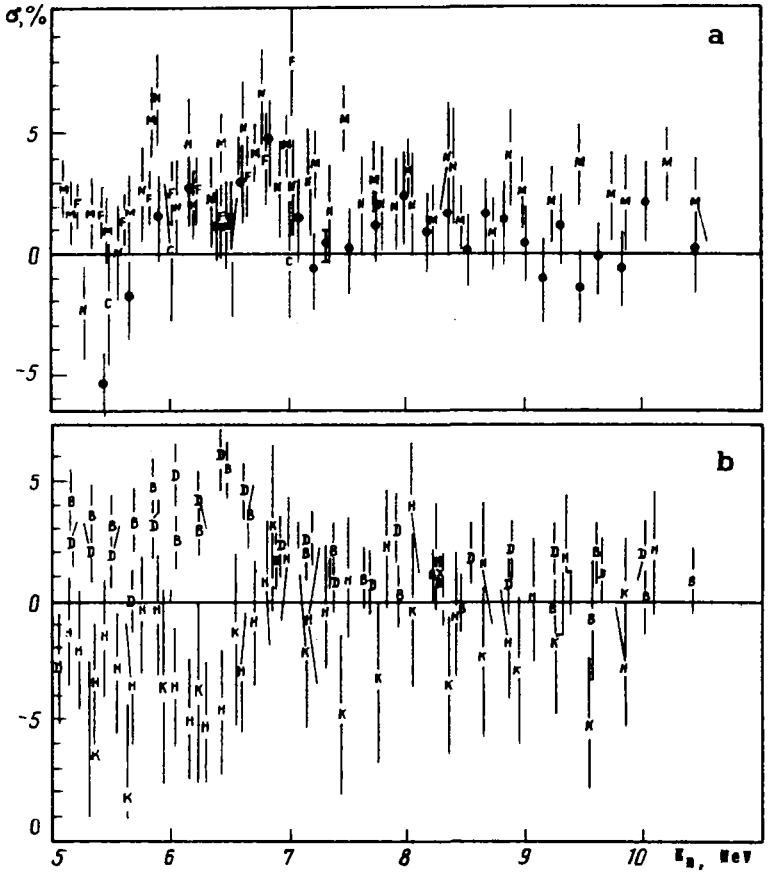

Fig. 2. Deviation of experimental data given by the following references from ENDF/B-V data: ● - [1], F - [2], B - [3], M - [4], K - [5], D - [6], N - [7], C - [8], H - [11]

investigated sample, and $R_{F\ and\ T}$ are the ratios of the effective number of recorded fission events in the investigated sample (^{235}U + ^{238}U) to the counts in a mono-isotopic (^{235}U) sample initiated by fast neutrons (F) and slowed down neutrons (T). The value for the quantity η is determined from data resulting from mass-spectroscopic analysis. As a result, the determination of the absolute value of the fission cross-section ratio can be executed at the same time as the measurement of the energy dependence.

One problem that arises in the use of neutron source reactions such as $^{7}Li(p,n)^{7}Be$, $D(d,n)^{3}He$ and others, is identifying the neutron background resulting from accompanying reactions (particularly for E_n>4 MeV). The authors of reference [2] solved this problem by the "dispersion" method, whose reliability decreases considerably in the energy region E_n>6.0 MeV. The separation of the background component due to reactions in the deuterium gas target by means of the same method [4], has apparently led to the elimination of a few data from the total number of points in the energy region E_n>8.5 MeV. The authors of reference [1] succeeded to separate the actual events from background counts using the time-of-flight method over a distance of 0.6-0.7 m without additional background measurements in the general vicinity of the samples. In their use of the $T(p,n)^{3}He$ reaction in a tritium gas target, the authors of reference [7] solved the problem in an analogous manner; in this case however, the neutron background differed considerably from the background in the experiments described in references [1,2,4]. The recording effectiveness of fission events in the quoted experiments was as high as 98-99%.

The second group of data (see Fig.2b) consists of results obtained from pulsed neutron fluxes having continuous energy spectra generated by linear electron accelerators [3,6] and cyclotrons [5,11]. The following methodological shortcomings in this group of experiments must be noted: a relatively low effectiveness (≈75%) in the detection of fission products [11], and the absence of an independent normalization procedure [6]. The isotopic impurity method (of threshold reactions) was used only in the experiment reported in reference [3]. In comparison to the data of the first group, in which the statistical

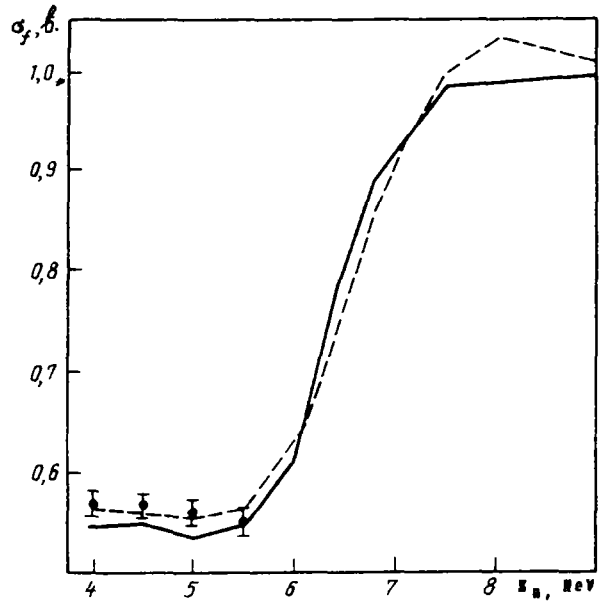

Fig. 3. Comparison of ENDF/B-V data (——) with reference [12] data (— — —) in the region of the first and second fission plateau; experimental data of reference [13] is given by a ●

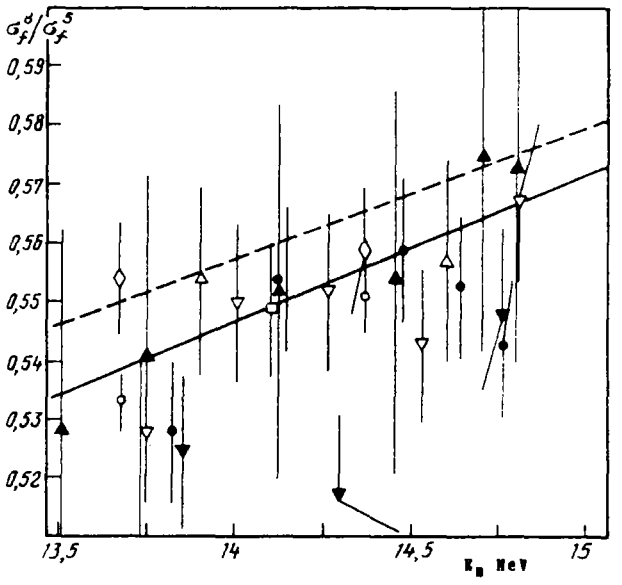

Fig. 4. ^{238}U to ^{235}U fission cross-section ratio for neutron energies around 14.6 MeV; ENDF/B-V data is given by ——; reference [12] data is given by — — —; experimental data from the following references: ● - [1], △ - [2], ◇ - [3], ▼ - [5], ○ - [6], □ - [9], ▲ - [10], ▽ - [11]

uncertainty ranged from 0.2% [2] to 1.1%[1,4] and 2% [7,8], the statistical uncertainty of the data in the second group is higher, ranging from 1.5% [3,5,6] to 3-4% [11]. Nevertheless, the basic data used in the ENDF/B-V evaluation are based on the second group of data. The inclusion of the data of the first group could bring about an increase of 1.5-2% in the values of the evaluated data.

Fig. 3 shows a comparison of the evaluated curve based on the ENDF/B-V data library with the evaluated curve given in reference [12]. The same figure also shows ^{238}U fission cross-section values reported in reference [13] (measured relative to the hydrogen scattering cross-section), which are in very good agreement with the evaluation of reference [12]. A comparison of Figs. 2 and 3, leads to the conclusion that the reference [12] evaluation gives a better representation of the existing experimental data than the evaluation given by the ENDF/B-V data library.

An analogous comparison is given in Fig. 4 for the data at energies around 14.6 MeV. This comparison shows that there is a need to correct the reference [12] evaluation, taking the new experimental data reported in references [1] and [13] into account.

REFERENCES

[1] GOVERDOVSKIJ, A.A., GORDYUSHIN, A.K., KUZMINOV, V.D., et al., At.Ehnerg. 56(3) (1984) 162 (in Russian).

[2] FURSSOV, B.I., KUPRIYANOV, V.M., SMIRENKIN, G.N., At. Ehnerg. 43 (1977) 181 (in Russian).

[3] BEHRENS, J.W., CARLSON, G.W., Nucl.Sci.and Eng. 63 (1977) 250.

[4] MEADOWS, J.W., Nucl.Sci.and Eng. 52 (1975) 255.

[5] CIERJACKS, S., et al., Nucl.Sci.and Eng. 52 (1975) 94.

[6] DIFILIPPO, F.S., et al., Nucl.Sci.and Eng. 68 (1978) 43.

[7] NORDBORG, C., et al., (Proc. of the NEANDC/NEACRP Spec. Mtg. on Fast Neutron Fission Cross-Sections of U-233, U-235, U-238 and Pu-239), Rep. ANL/90, Argonne National Laboratory (1976) 128.

[8] CANCE, M., GRENIER, G., Nucl.Sci.and Eng. 68 (1978) 197.

[9] WHITE, P., WARNER, G., J.Nucl.Energy 21 (1967) 671.

[10] VARNAGY, M., CSIKAI, J., J.Nucl.Instrum.and Methods 196 (1982) 465.

[11] COATES, M.S., et al., (Proc. Inter. Conf. on Nuclear Cross-Sections and Technology, Washington, DC, 1975) NBS Special Publication 425, Vol. 1 (1975) 568.

[12] NIKOLAEV, M.N., ABAGYAN, L.P., KORCHAGINA, Zh.A., et al., "Neutron data for uranium-238", Part 1, Institute of Physics and Power Engineering, Obninsk (1978) (in Russian).

[13] JINGXIA WU, et al, Chin.J.Nucl.Phys. 5 (1983) 158.

PROMPT FISSION NEUTRON SPECTRUM OF ^{238}U

N.V. Kornilov

Abstract

Experimental results of the prompt ^{238}U fission spectrum are analyzed. The energy dependence of the Maxwellian distribution T parameter and its uncertainty is calculated for incident neutron energies ranging from 1-15 MeV. It is concluded that pre-fission neutrons from the (n,nf) and (n,2nf) reactions must be included in the evaluation of fission neutron spectra.

The prompt fission neutron spectrum, whose mean value is characterized by the quantity $\bar{\nu}$, is the result of a number of different processes. In spontaneous fission as well as in fissions induced by neutrons with energies smaller than the energy of the (n,nf) reaction threshold, a single nucleus fissions and produces neutrons during the fission process. At higher energies, the probability exists for fissions to occur in various nuclei having different excitation energies generating additional neutrons emitted before the actual fission process by (n,xnf) reactions, referred to as emission neutrons. These processes must be taken into account when calculating prompt fission neutron spectra for a wide range of incident neutron energies.

There are many reports of experiments and reviews devoted to the study of prompt fission neutron spectra which contain analyses of fission data [1-4]. The spontaneous fission spectrum of ^{252}Cf has been studied extensively. The analysis of experimental data reported in reference [5] has shown that approximately 99% of neutrons having energies ranging from 20 keV to 8 MeV can be described by a Maxwellian distribution to an accuracy of approximately 5%. A change in this distribution is observed at higher energies which can amount to 20% for secondary neutron energies of E>10 MeV. For a large number of fissionable isotopes, and in those cases where the incident neutron energy falls in the range of secondary neutron energies, where emission neutrons are absent, prompt fission neutron spectra can be satisfactorily described by Maxwellian distributions [4].

The dependence of the Maxwell distribution parameter T (which is a measure of the hardness of the spectrum) on the incident energy is calculated on the basis of the well-known dependence, derived by Terrell, which establishes the relationship of $T(\bar{E}=1.5T)$ to the mean value of the number of prompt fission neutrons:

$$T = a + b\,(\bar{\nu} + 1)^{1/2} \qquad (1)$$

The sets of experimental data which have been used in this work have been practically the same since the beginning of the 70ies. Depending on the assumed initial conditions used as the basis for their analysis, the authors have obtained different values for the a and b coefficients. Thus, the values obtained in reference [4] are a=0.17±0.11 and b=0.60±0.05. In reference [1], the authors have assumed that the value for ν does not include the total number of neutrons, but only that fraction which is due to the emission from fission fragments, namely ν_f; this approach leads to the coefficient values: a=0.35 and b=0.51. The value for the T parameter must be derived from that part of the prompt fission neutron spectrum in which the emission neutrons are absent. For an incident energy E_0<9 MeV, the definition of this region is unambiguous (see Figure). The analysis of spectra for $E_0 \approx 14$ MeV, was performed by some authors on the assumption that the spectrum of emission neutrons was dependent on the condition of balanced evaporation and that their average energy was low (i.e., not higher than 1 MeV). A study of secondary neutron spectra, in which ^{238}U was bombarded with 6-14 MeV neutrons, has shown that a considerable fraction of neutrons (20-30%) are formed as a result of direct interactions, and that the observed spectrum has a high energy component which is practically constant at energies greater than 4 MeV. Such neutrons are also observed in prompt fission neutron spectra, which would cause an increase of the T value. Data presented in reference [1] together with the results of more recent experiments [3,7-11], which have initial energies lower than the fission reaction threshold and which are characterized by a preliminary release of neutrons ($E_0 < B_{f1}$), have been analyzed with due consideration given to the material presented in reference [3]. This has led to the following results:

$$a=0.41\pm0.15 \text{ and } b=0.47\pm0.08 \qquad (2)$$

The dependence of the prompt ^{238}U fission neutron spectrum as a function of initial energy can be constructed on the basis of the established relationships. The spectrum of neutrons emitted during fission can be described as a function of incident energy E_0 and end energy E by the following expression:

$$\nu(E,E_0)=\alpha_0(E_0)\nu_0(E,E_0)+\alpha_1(E_0)\left[\nu_1(E,E_0)+f_1(E,E_0)\right]+ \\ +\alpha_2(E_0)\left[\nu_2(E,E_0)+f_2(E,E_0)\right]+\cdots, \qquad (3)$$

where $\alpha_i(E_0)$ represents the fractional emission processes for the fission reactions (n,nf) and (n,2nf); $\nu_i(E,E_0)$ the average number of prompt fission neutrons emitted in these processes; $f_1(E,E_0)$ and $f_2(E,E_0)$ are the spectra of neutrons emitted prior to fission from the (n,nf) and (n,2nf) reactions respectively.

The prompt fission neutron spectrum which results from emission fission can be represented by a Maxwellian distribution using the value for T, calculated from equation (1), if the value for the average number of neutrons $\bar{\nu}_i(E_0)$ is known for the given process. However, there are no experimental values for the $\bar{\nu}_i(E_0)$ quantity. The only data that are available are the ones on $\alpha_1(E_0)$ for ^{238}U, for initial energies of 6-9 MeV, published in reference [3]. Being that the accuracy of these results is not high (17-50%), the authors of this experiment could only give a qualitative conclusion that the experimental data do not contradict the assumption that $\alpha_1(E_0)$ is constant over the energy range of 7 MeV$\leq E_0 \leq$9 MeV. The separation of the partial dependencies of $\bar{\nu}_i(E_0)$ in reference [3] is based on the fact that, as new fission reaction channels are considered, one could observe changes in the dependence of the total number of prompt fission neutrons as a function of incident energy. Taking the values of $\alpha_i(E_0)$ and $\bar{\nu}(E_0)$ from reference [12] and assuming that the behavior of $\bar{\nu}_i(E_0)$, for $E_0>B^{fi}$ (where B_{fi} is the (n,inf) reaction threshold) is the same as for $E_0<B_{fi}$, it is then possible to derive the following dependencies [3]:

$$\bar{\nu}_0(E_0)=2.23+0.16(E_0), \\ \bar{\nu}_1(E_0)=1.39+0.14(E_0),\ E_0>6\ Mev \qquad (4) \\ \bar{\nu}_2(E_0)=0.99+0.10(E_0),\ E_0>11\ Mev$$

If one assumes that the hardness of the prompt fission neutron spectrum of ^{239}U, ^{238}U and ^{237}U depends only on the excitation energy (i.e., on the quantity $\bar{\nu}_i(E_0)$), then it would be possible to determine the values of the $T_i(E_0)$ parameters for each fissionable nucleus from equations (1), (2) and (4). The hardness of the summed spectrum as a function of the initial energy can then be calculated from the following expression:

$$\bar{T}(E_0) = \frac{\sum_i T_i(E_0)\,\bar{\nu}_i(E_0)\,\alpha_i(E_0)}{\sum_i \bar{\nu}_i(E)\,\alpha_i(E_0)}$$

The value of $\bar{T}(E_0)$ is only weakly dependent on the quantities $\nu_i(E_0)$ and $\alpha_i(E_0)$ used in theses calculations. Using the evaluated quantity $\nu(E_0)$ given in reference [13], changes the quantity T by less than 0.8%. A change of 30% in the value of α_i affects the value of $\bar{T}$ by less than 3%. Thus, regardless of the values chosen for α_i and $\bar{\nu}_i$, it can be expected that the value of the average parameter $\bar{T}$ will be calculated to an acceptable accuracy. The results of this calculation are compared to experimental data in Table I.

TABLE I. EXPERIMENTAL AND CALCULATED VALUES OF THE PARAMETER T FOR ^{238}U

E^0, MeV	T_{exp}, MeV	$\bar{T}$, MeV	References
1.35	1.29±0.03	1.298	[9]
1.90	1.35±0.06	1.308	[14]
2.02	1.29±0.03	1.310	[9]
2.09	1.285±0.03	1.312	[15]
2.30	1.23±0.06	1.315	[14]
2.47	1.33±0.04	1.318	[7]
4.09	1.42±0.04	1.348	[15]
6.01	1.36±0.03	1.370	[3]
7.00	1.29±0.05*	1.359	[16]
7.0	1.33±0.08	-	[1]
7.02	1.31±0.03	-	[3]
8.01	1.36±0.04	1.371	[3]
8.94	1.41±0.04	1.386	[3]

* The T value given in reference [16] was renormalized to T_{Cf} = 1.42 MeV.

The data listed in Table I shows a satisfactory agreement between the experimental data and the calculated dependence of the $\bar{T}$ parameter. The $\langle T_{exp}/\bar{T}\rangle$ ratio and its root-mean-square error are equal to 0.99±0.03. The uncertainty of the recommended dependence is taken to be ±3%, which is the root-mean-square error of the experimental data. The calculated values of the $\bar{T}$ parameter in the energy range 1-15 MeV are given in Table II together with the ENDF/B-V evaluated data, which have been incorporated in the BNAB-MICRO data library [17]. The ENDF/B-V $\bar{T}$ parameter was obtained from the average energy of the Watt distribution. A comparison of the tabulated results show that in the 1-15 MeV energy range, the data resulting from this calculation are in good agreement with the ENDF/B-V data. At lower energies one should give preference to the data of this evaluation inasmuch as they are closer to the experimental data.

The angular distribution of the prompt ^{238}U fission neutrons with respect to the direction of the incident neutron has been analyzed in great detail for E_0=2.47 MeV in reference [7]. Within the limits of the experimental uncertainties of $\Delta\bar{\nu}/\bar{\nu}\leq 6\%$ and $\Delta T/T\leq 4\%$, no angular dependence in the values of $\bar{\nu}$ or T have been observed.

TABLE II. RECOMMENDED VALUES OF THE $\bar{T}$ PARAMETER

	$\bar{T}$ Value			$\bar{T}$ Value	
E_0 MeV	This eval.	ENDF/B-V	E_0 MeV	This eval.	ENDF/B-V
1	1.292	1.345	9	1.387	1.407
2	1.310	1.351	10	1.403	1.415
3	1.328	1.358	11	1.420	1.424
4	1.346	1.367	12	1.433	1.432
5	1.363	1.376	13	1.444	1.440
6	1.370	1.385	14	1.448	1.450
7	1.358	1.392	15	1.451	1.458
8	1.371	1.399	-	-	-

The parametrization that has been performed so far describes only part of the prompt fission neutron spectrum. However, as it is customary for evaluated neutron data libraries to include the total value of the fission cross-section, it is expected that such libraries comprise neutron spectra corresponding to the entire fission process, e.g. as it is described in equation (3). For incdent energies exceeding the (n,nf) reaction threshold, a substantial fraction of neutrons (approximately 17%), are emitted prior to the fission event, and have a spectrum which departs from a Maxwellian distribution (see Figure). However, prompt neutron fission spectra given in both ENDF/B-V and BNAB-MICRO evaluated data libraries do not take this component into consideration.

A more detailed form of the emission spectrum in the energy interval of 7-9 MeV is analyzed in reference [18]. At those energies, only the $\alpha_1(E_0)[f_1(E,E_0)]$ component, related to the spectrum of the first neutron $\sigma_1(E,E_0)$, the ^{238}U fission probability $F_f(U)$ and the relationship $\alpha_1 f_1(E,E_0) \sim \sigma_1(E,E_0)P_f(U)$, where $U=E_0-E$, is considered in equation (3). The function $P_f(U)$ which is derived in reference [18] from the analysis of emission spectra, is in good agreement with results of statistical model calculations as well as with experimental data on the $^{236}U(t,pf)$ reaction.

Because of the paucity of experimental data on pre-fission neutrons spectra, it is not possible to derive an empirical dependence of the shape of such spectra from the incident energy. However, the analysis described in reference [18], and the positive results of the theoretical descriptions of reaction cross-sections and of neutron spectra of fissioning nuclei in reference [19], lead one to expect that neutron emission spectra for a broad range of initial energies could be calculated to a satisfactory degree of accuracy.

The following conclusions can be drawn as a result of these considerations:

1. Part of the ^{238}U prompt fission neutron spectrum attributed to fission neutrons can be described by a Maxwellian distribution with a single parameter T, and is weakly dependent

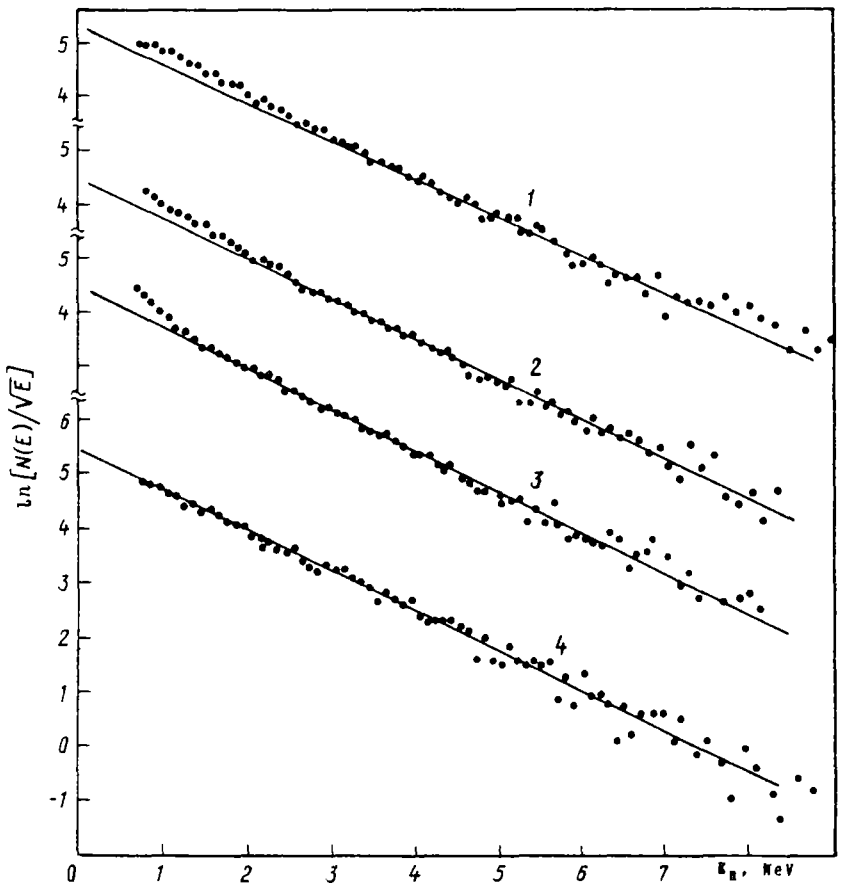

^{238}U prompt neutron fission spectrum for initial neutron energies of 8.94 MeV (curve #1), 8.01 MeV (curve #2), 7.02 MeV (curve #3) and 6.01 MeV (curve #4) [3]. The straight line represent the Mawellian distribution. The neutron surplus in the soft part of the spectrum is due to pre-fission neutrons from the (n,nf) reaction.

on the incident neutron energy. The low uncertainty of this parameter (~ 3%) allows one to calculate spectra to an accuracy of 3.5%, 7%, and 20% for secondary neutron energies of 0.5, 5 and 10 MeV respectively. The deviation from the Maxwellian distribution at energies greater than 10 MeV does not exceed the uncertainty of the calculation, and can therefore be ignored in the derivation of the evaluated data.

2. In order to give an accurate description of prompt fission neutron spectra it is essential to include the pre-fission neutron contribution. The spectrum of these emission neutrons for a wide range of initial energies can only be determined on the basis of rigorous theoretical calculations.

REFERENCES

[1] HOWERTON, R.J., DOYAS, R., Nucl.Sci.and Eng. 46 (1971) 414.

[2] STAROSTOV, B.I., SEMENOV, A.F., NEFEDOV, V.N., Problems of Atomic Science and Technology. Ser. Nuclear Constants 2(37) (1980) 3-44 (in Russian).

[3] KORNILOV, N.V., BARYBA, L.Ya., SALNIKOV, O.A., (Proc. of 5th All-Union Conf. on Neutron Physics, Kiev, 1980), Part 3, TsNIIatominform, (1980) 104 (in Russian).

[4] ZAMYATNIN, Yu.S., KROSHKIN, N.I., MELNIKOV, A.K., (Proc. of Second Intern. Conf. on Nuclear Data for Reactors, Helsinki, 1970), Vol.2, IAEA, Vienna, (1970) 183 (in Russian).

[5] INTERNATIONAL ATOMIC ENERGY AGENCY, (Proc. of IAEA Cons. Mtg. on The ^{235}U Fast Neutron Fission Crosss-Section and the ^{252}Cf Fission Neutron Spectrum, Smolenice, 1983), IAEA, Vienna, Rep. INDC(NDS)-146 (1983).

[6] KORNILOV, N.V., ZHURAVLEV, B.V., SALNIKOV, O.A., et al., (Proc. of 5th All-Union Conf. on Neutron Physics, Kiev, 1980), Part 2, TsNIIatominform, (1980) 44 (in Russian).

[7] BARYBA, V.Ya., ZHURAVLEV, B.V., KORNILOV, N.V., et al., At.Ehnerg. 43(4) (1977) 266 (in Russian).

[8] KNITTER, H.H., PAULSEN, A., LISKIEN, H., ISLAM, M.M., Atomkernenergie 22(2) (1973) 84-86.

[9] ALMEN, E., HOLMQVIST, T., WIEDLING, T., (Proc. of Second Intern. Conf. on Nuclear Data for Reactors, Helsinki, 1970), Vol.2, IAEA, Vienna (1970) 93.

[10] BOLDEMAN, J.W., CULLEY, D., in Proc. of Intern. Conf. on Neutron Physics and Nuclear Data for Reactors and Applied Purposes, Harwell, 1978.

[11] KOTELNIKOVA, G.V., LOVCHIKOVA, G.N., SALNIKOV, O.A., Preprint FEI-575, Institute of Physics and Power Engineering, Obninsk (1975) (in Russian).

[12] DAVEY, W.D., Nucl.Sci.and Eng. 44 (1971) 345.

[13] MALINOWSKIJ, V.V., TARASKO, M.Z., KUZMINOV, V.D., Problems of Atomic Science and Technology. Ser. Nuclear Constants 1 (1985) 24-35 (in Russian).

[14] KNITTER, H.H., Z.Phys. 244 (1971) 358.

[15] BARNARD, E., FERGUSON, A.T.F., McMURRAY, W.R., VAN HEERDEN, I.J., Nucl.Phys. 71 (1965) 228-240.

[16] BERTIN, A., BOIS, R., FREHAUT, J., HUDAS, P., (Proc. 3rd All-Union Conf. on Neutron Physics, Kiev, 1975), Vol.5, TsNIIatominform, Moscow (1976) 349-358.

[17] ABAGYAN, L.P., BAZAZYANTS, N.O., NIKOLAEV, M.N., et al., Group Constants for Reactor and Shielding Calculations, Ehnergoizdat, Moscow (1981) (in Russian).

[18] KORNILOV, N.V., SALNIKOV, O.A., (Proc. 3rd All-Union Conf. on Neutron Physics, Kiev, 1975), Vol.3, TsNIIatominform, Moscow (1976) 40 (in Russian).

[19] GRUZDEVICH, O.G., IGNATYUK, A.V., MASSLOV, V.M., PASHCHENKO, A.B., (Proc. 6th All-Union Conf. on Neutron Physics, Kiev, 1983), Vol.2, TsNIIatominform, Moscow (1984) 318-323 (in Russian).

ENERGY DEPENDENCE OF THE PROMPT NUMBER OF NEUTRONS FOR NEUTRON INDUCED FISSION OF ^{238}U

V.V. Malinovskij

Abstract

Several evaluations of the average number of prompt neutrons for the neutron-induced fission of ^{238}U are discussed. The current state of the experimental data are presented briefly. A new evaluation is recommended on the basis of a revision of old data and new experimental results.

The evaluated values of the energy dependence of the average number of prompt fission neutrons $\bar{\nu}_p$ used in reference [1] and in the BNAB-MIKRO evaluated nuclear data library is based on the evaluation described in reference [2]. In that evaluation [2], the data in the energy range of 1.2-15 MeV, data were extrapolated to lower energy and to energies up to 20 MeV, and were also renormalized to the spontaneous fission nu-bar value of 3.7347 [1] (while the value of ^{252}Cf nu-bar used in reference [2] was equal to 3.756).

The following information has become available in the last few years:

- the new accepted value of ^{252}Cf nu-bar, based on new experimental data and authoritative evaluations [3,4], is now 3.757±0.005;
- the data originally reported in reference [5], which were subsequently corrected in reference [6], have again been re-assessed [7] resulting in a change of nu-bar by 3% in the neutron energy range of 3-4 MeV;
- new results of nu-bar measurements in the 23-28 MeV neutron energy range have been published [8];
- new measurements have been published in reference [9], these data are shown in Figure 1.

A new evaluation of the energy dependence of ^{238}U nu-bar, which includes all of the changes listed above, has been reported in reference [10] and is also shown in Figure 1 up to the neutron

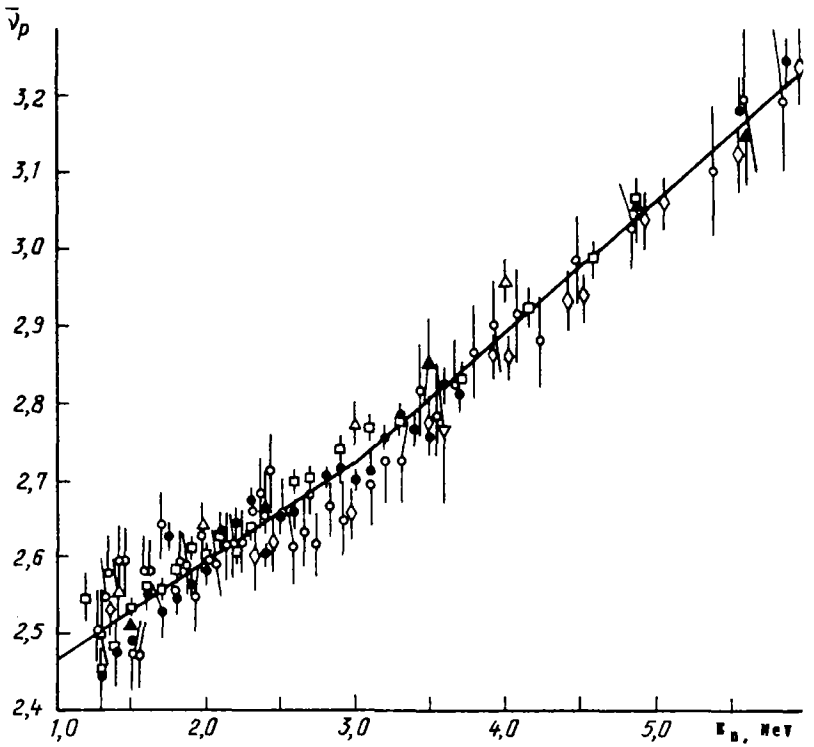

Fig. 1. Average number of prompt neutrons emitted in ^{238}U fission as a function of neutron energy. Experimental data: ▲ - Assplund-Nielsen, △ Masera et al., O - Savina et al., ◆ - [5,7], □ - [12]; ● - [9], —— Ref.[10] evaluation.

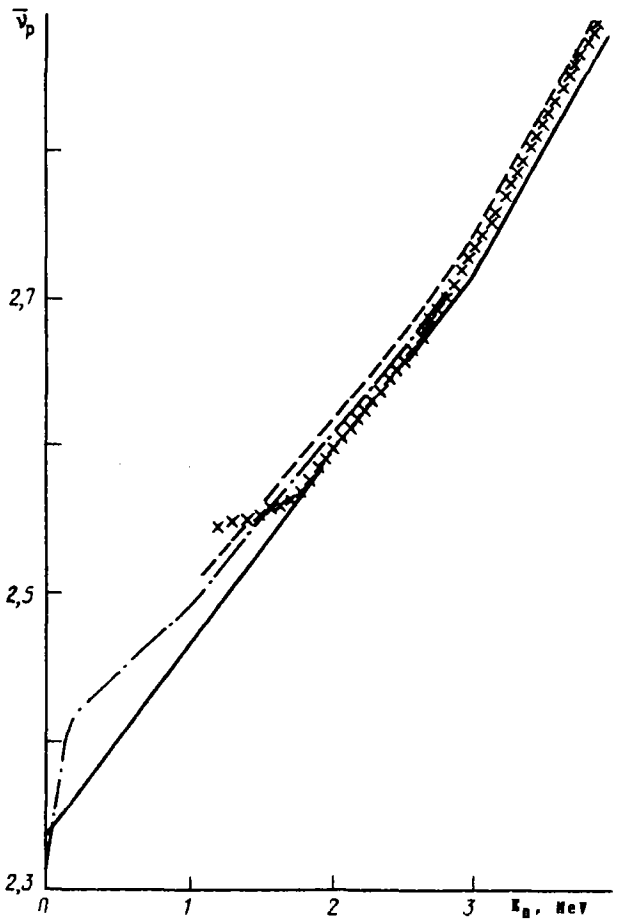

Fig. 2. Comparison of prompt ^{238}U nu-bar as a function of neutron energy for the following evaluations: — — — Ref.[2], — • — • — Ref.[8], xxxxxxx Ref.[11], —— Ref.[10].

energy of 6 MeV; this article [10] comprises the full numerical information as well as the complete set of references used in this evaluation. The result of this evaluation shows good agreement with the current experimental data (χ^2=10.2 for 14 degrees of freedom). The data reported in reference [8] were used to derive the prompt nu-bar value at E_n=20 MeV.

The results of different evaluations of the energy dependence of prompt nu-bar are plotted in Figure 2. The method of evaluation used by the authors of reference [2] has had a considerable influence on the evaluation reported in reference [5], which explains the 1% agreement of the nu-bar energy dependencies shown in the figure. A reduction of the prompt nu-bar value in reference [1] was obtained as a result of an unwarranted renormalization of the standard. The evaluation reported in reference [11] used old results [5] (after their first re-assessment) and does not include the data reported in references [9] and [12].

In view of the accuracy requirements of prompt nu-bar for ^{239}U set forth in WRENDA [13], the improvements which have been introduced by the new evaluation, reported in reference [10], are significant. It is therefore recommended that this new evaluation [10] be incorporated in the national evaluated nuclear data file.

REFERENCES

[1] ABAGYAN, L.P., BAZAZYANTS, N.O., NIKOLAEV, M.N., Multigroup Data for Reactor and Shielding Calculations, Moscow, Ehnergoizdat (1981) (in Russian).

[2] PROKHOROVA, L.I., PLATONOV, V.P., NURPEISSOV, B., SMIRENKIN, G.N., Problems in Atomic Science an Technology. Ser. Nuclear Constants 20(1) (1975) 104 (in Russian).

[3] AXTON, E.J., J. Europ.Sci.Technol. 5(4) (1984) 609.

[4] DIVADEENAM, M., STEHN, J.R., Ann.Nucl.Energy 11(8) (1984) 375.

[5] SOLEILHAC, M., FREHAUT, J., GAURIAU, J., J.Nucl.Energy 23 (1969) 257.

[6] FREHAUT, J., MOSINSKI, G., GAURIAU, J., (Proc. 2nd All-Union Conf. on Neutron Physics, Kiev, 1973), Vol.3, Obninsk (1974) 155 (in Russian).

[7] FREHAUT, J., MOSINSKI, G., SOLEILHAC, M., in International Experimental Neutron Data File, IAEA, Vienna, EXFOR 20.490 (1980).

[8] FREHAUT, J., Ibid., EXFOR 21.685 (1980).

[9] VOROBYEVA, B.G., KUZMINOV, V.D., MALINOVSKIJ, V.V., et al., Problems in Atomic Science and Technology. Ser. Nuclear Constants 1(40) (1981) 62 (in Russian).

[10] MALINOVSKIJ, V.V., TARASKO, M.Z., KUZMINOV V.D., Problems in Atomic Science and Technology. Ser. Nuclear Constants 1 (1985) 24-35 (in Russian).

[11] MANERO, F., KONSHIN, V.A., At.Energy Rev. 10 (1972) 637.

[12] NURPEISSOV, B., VOLODIN, K.E., NESTEROV, V.G., At.Ehnerg. 39 (1975) 199 (in Russian).

[13] INTERNATIONAL ATOMIC ENERGY AGENCY, WRENDA-83-84 World Request List for Nuclear Data (V.Piksaikin, Ed.), Rep. INDC(SEC)-88, IAEA, Vienna (1984).

EXPERIMENTAL AND EVALUATED DATA ON THE DISCRETE LEVEL EXCITATION FUNCTION OF THE ^{238}U(n,n') REACTION

S.P. Simakov

Abstract

Experimental data on the ^{238}U excitation function are compiled and analyzed. The experimental data are compared with the evaluated data from the BNAB, ENDF/B-IV and ENDL-78 evaluated data libraries. It is shown that the BNAB evaluated data are in good agreement with the existing experimental data, including new results from recent experiments.

Nuclear data in the energy region below 1 MeV have significant practical applications, since one third of all neutrons in the flux of a fast reactor fall in that energy range. In this energy range inelastic scattering contributes up to 25% to the total of all neutron interactions in ^{238}U. In addition, it is the only process that contributes to the softening of the neutron energy spectrum. As a result, this importance imposes rigorous requirements on the knowledge of the inelastic scattering cross-section and of the excitation functions of individual levels (the uncertainty in the cross-section must not exceed 3%) [1].

Let us examine the current state of the experimental and evaluated data on the excitation functions of discrete levels of the ^{238}U(n,n') reaction. At the present time, evaluated data of this reaction is included in the following data libraries: the Soviet evaluated data library BNAB-MIKRO, published in 1981 [2] (referred to hereafter simply as BNAB); the ENDL-78 evaluated nuclear data library of the Lawrence Livermore National Laboratory, issued in 1978 [3]; and the United States national nuclear data library ENDF/B-IV, published in 1975 [4].

The energies of the individual levels of the ^{238}U nucleus as adopted in these data libraries, and the latest published level scheme data [5], are listed in Table I. As seen from this table, starting with level of 680 keV, the values adopted in the data

libraries appear to be approximations of the actual level energies. Furthermore, excitation functions for the 307 keV, 827 keV and 966 keV levels are omitted entirely in the BNAB library, and the region of unresolved levels begins at the excitation energy of 1078 keV in the BNAB library, and at 2000 keV in the ENDL-78 and ENDF/B-IV libraries.

TABLE I. ^{238}U LEVEL ENERGIES (in keV)

BNAB	ENDL-78	ENDF/B-IV	Level Scheme data [5]
45	45	45	44.91 2^+
148	148	148	148.41 4^+
-	308	308	307.21 6^+
680	680	680	517.8 8^+, 680.1 1^+
732	732	732	731.9 3^+
-	827	827	827.1 5^+
939	930	930	927.0 0^+, 930.8 (1^-)
-	967	967	950 (2^-), 965.9 7^-, 966.3 2^+
1006	1000	1000	993 0^+, 998.3 (2^+), 997.5 3^+
1047	1041	1041	1037.3 2^+
1076	1060	1060	1055 (4^+), 1060.3 2^+, 1076 $5/2^+$

Let us now examine the experimental level excitation function data that have been published since the publication of these libraries.

References [6] and [7] describe the time-of-flight measurements of the level excitation cross-sections of the 45 keV and 148 keV levels of ^{238}U. The energy resolution achieved in experiments (approximately 10 keV) is considered to be good enough to separate the inelastically scattered neutrons from a significant elastic scattering background. In these experiments, the value of the cross-section was obtained by integrating the measured angular distributions of the scattered neutrons. This approach eliminates basic procedural problems, which is an essential condition in obtaining reliable results. The time-of-flight measurement of the excitation function of the first two levels of

^{238}U in the energy range 0.9 to 3.1 MeV is also reported in reference [8]. The fact that this experiment achieved a poorer resolution (of ~20 keV), and that the measurement was taken at one angle only (90°), makes this particular experiment less dependable. The data published in references [6-8] are compared with evaluated data in Tables II a and b. As can be seen, the BNAB evaluated data agree satisfactorily with the recently measured data for the 45 and 148 keV levels. It should be noted, however that the BNAB data fall below the experimental data for neutron energies above 2.5 MeV. This behavior is even more pronounced in the case of the earlier ENDF/B-IV evaluated data.

TABLE II a. NEUTRON INELASTIC SCATTERING CROSS-SECTION FOR THE EXCITATION OF THE 45 keV ENERGY LEVEL (in mb)

E, keV	Measured data	BNAB	ENDL-78	ENDF/B-IV
82	381±21 [6]	530	588	327
700	1530±100 [7]	1455	1460	1405
1500	700±100 [7]	605	693	285
-	630±60 [8]	-	-	-
2500	510±100 [7]	390	457	200
-	500±60 [8]	-	-	-
3400	570±100 [7]	300	418	165

TABLE II b. NEUTRON INELASTIC SCATTERING CROSS-SECTION FOR THE EXCITATION OF THE 148 keV ENERGY LEVEL (in mb)

E, keV	Measured data	BNAB	ENDL-78	ENDF/B-IV
82	-	-	-	-
700	350±40 [7]	317	365	395
1500	260±40 [7]	313	378	230
-	340±60 [8]	-	-	-
2500	130±40 [7]	120	179	30
-	120±20 [8]	-	-	-
3400	150±40 [7]	70	122	6

The excitation functions in references [7-9] were determined by measuring the gamma rays accompanying the neutron inelastic scattering process. Because of the better resolution (of ~4 keV) achieved by this method, it is possible to measure data for higher lying levels; however, because of the increase of the probability to populate the level under consideration as a result of cascade transitions from higher lying levels, this can be done only for a limited energy range. In addition, the high values of the internal conversion coefficients for low energy gamma rays prevents the measurement of the excitation function of the first three levels of the ^{238}U nucleus.

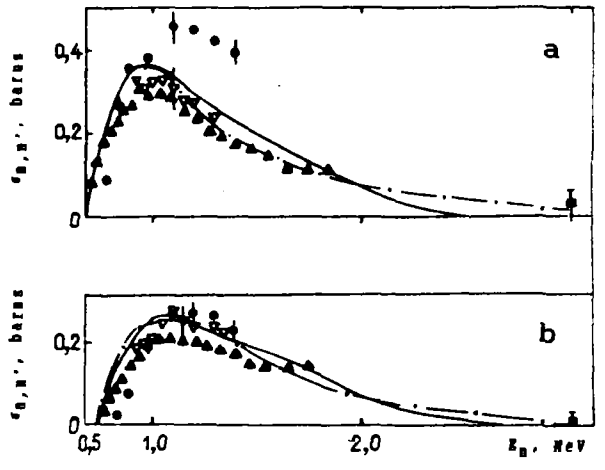

Figure 1

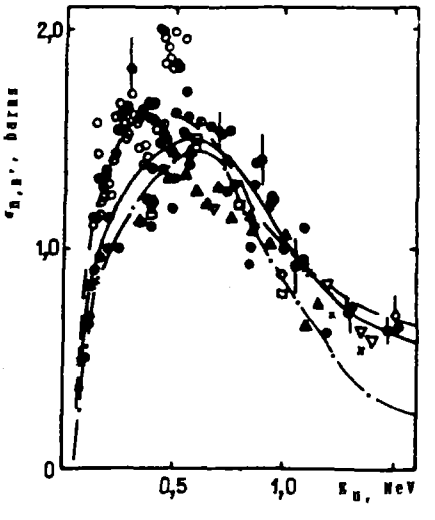

Figure 2

Fig. 1. Excitation functions for the 680 keV (a) and 733 keV (b) levels of ^{238}U. Experimental data: ▲ [9], ● [10], ■ [11], ▽ [12,13], ▼ [14]. Evaluated data : —— BNAB, — • — • — ENDL-78, ENDF/B-IV.

*Fig. 2. Excitation function for the first (45 keV) level of ^{238}U. Experimental data: ♦ [6], ◊ [7], 0 [8], △ [15], □ [16], ▲ [17], ● [18], 0 [19], 0 [20], 0 [21], 0 [22], ▽ [23], x [24], * [25]. Evaluated data: —— BNAB, — • — • — ENDF/B-IV, — — — ENDL-78.*

The data from references [9-11] for the 680 and 732 keV energy levels are compared with evaluated data in Fig. 1. The same figure also shows the results of measurements [12,13] of the same energy levels that were performed by using the gamma-ray detection method as well as the scattered neutron detection method. The agreement between the results of these two methods substantiates the reliability of the resulting excitation function. As seen from Fig. 1, the evaluated data are in satisfactory agreement with the results of the more recent

experiments. A comparison of the experimental and evaluated data for other ^{238}U levels shows a certain ambiguity as to which pseudo-level the level under consideration refers to.

Let us examine the excitation function of the first (45 keV) level of the ^{238}U nucleus in the 150-500 keV energy range in more detail. The accuracy with which this quantity can be predicted determines the accuracy of calculations of a number of fast neutron characteristics. As seen in Fig. 2, the scatter of the experimental and evaluated data in this energy range is considerable. However, as shown by the analysis of the latest experiments, there are no new experimental data other than those included in the BNAB library. In view of this situation, we undertook a critical analysis of all experimental data in the 150-500 keV energy range.

In the process of examining the data of each experiment, two factors which can give rise to significant errors in the measured data, must be given special consideration: inadequate energy resolution, and neglect of angular anisotropy of the scattered neutrons. On the basis of information gleaned from the available published literature, of all of the experiments described in references [15-25] there were only two [17 and 21] in which the energy resolution was adequate (i.e., 10-20 keV). As seen from Fig. 2, the results of these two experiments are in good agreement with each other, and yield the lowest cross-section values in the 150-500 keV energy range.

On the basis of this analysis, it can be concluded that the best description of the excitation function for the 45 keV level, from threshold to 0.5 MeV is given by the ENDF/B-IV or the BNAB libraries. This conclusion can also be substantiated by data from macroscopic experiments [2] or by results of theoretical calculations [26] which predict values for the cross-section in this energy range which correspond to the lower boundary of the scattered microscopic data. It is evident, however, that a definitive determination of the excitation function for the first level of the ^{238}U nucleus in the region of its maximum, and an agreement between experimental and theoretical results can only be achieved with the aid of new measurements.

As a result of this comparison and analysis of the experimental and evaluated data describing the excitation functions of separate levels of the ^{238}U nucleus in the (n,n') reaction, it can be concluded that in general, the BNAB evaluation gives a satisfactory representation of the experimental results, including the results of measurements performed in the last few years.

While this experiment was being conducted, a group at the Lowell Univerity (USA) reported the results of a measurement of the $^{238}U(n,n')$ reaction [14], using the scattered neutron detection method [12,13], including the results on the excitation function for the 680-1080 keV levels for neutron energies up to 2.2 MeV. As can be seen from the data plotted in Fig. 1, new results confirm earlier experimental data [9] and evaluations. The experimental results for the high excited states of ^{238}U reported in reference [14], for which there are hardly any experimental data, are in good agreement with the evaluated data given in the BNAB data library.

REFERENCES

[1] INTERNATIONAL ATOMIC ENERGY AGENCY, WRENDA 81/82 World Request List for Nuclear Data (N. Dayday, Ed.), Rep. INDC(SEC)-78, IAEA, Vienna (1981).

[2] ABAGYAN, L.P., BAZAZYANTS, N.O., NIKOLAEV, M.N., TSIBULYA, A.M., Multigroup Data for Reactor and Shielding Calculations, Moscow, Ehnergoizdat (1981) (in Russian).

[3] HOWERTON, R.J., Rep. UCRL-50400, Lawrence Livermore National Laboratory, Livermore CA. (1978).

[4] POENITZ, W.P., Rep. ANL/NDM-22, Argonne National Laboratory, Argonne, IL. (1977).

[5] ELLIS, Y.A., Nucl.Data Sheets 21 (1977) 549.

[6] WINTERS, R.R., HILL, N.W., MACKLIN, R.L., et al., Nucl.Sci and Eng. 78 (1981) 147.

[7] HAOUAT, G., LACHKAR, J., LAGRANGE, C.R., et al., Nucl.Sci. and Eng. 81 (1982) 491.

[8] BEGHIAN, L.E., KEGEL, G.H.R., MARCELLA, T.V., et al., Nucl.Sci. and Eng. 69 (1979) 191.

[9] OLSEN, D.K., MORGAN, G.L., McCONNELL, J.W., NBS Special Publication 594 (1980) 677.

[10] KAZYULYA, B.G., KOZULIN, Eh.M., POBEDONOSTSEV, L.A., et al., Problems of Atomic Science and Technology. Ser. Nuclear Constants 4(39) (1980) 14 (in Russian).

[11] BLINOV, M.V., STSIBORSKIJ, B.D., FILATENKOV, A.A.,in Neytronnaya Fizika (Proc. of 5th All-Union Conf. on Neutron Physics, Kiev, 1980), Part 2, TSNIIatominform, Moscow (1980) 308 (in Russian).

[12] COUCHELL, G.P., CIARCIA, C., EGAN, J.J., et al., in Nuclear Data for Science and Technology, (Proc. Intern. Conf., Antwerp, 1982) (BOECKHOFF, K.H., Ed.), D. Reidel Pub. Co., Boston (1983) 45.

[13] MITTLER, A., COUCHELL, G.P., EGAN, J.J., et al., NBS Special Publication 594 (1980) 680.

[14] EGAN, J.J., ARTHUR, E.D., KEGEL, G., in Nuclear Data for Basic and Applied Sci.,(Proc. Intern. Conf., Santa-Fe, NM., 1985), Gordon and Breach, New York (1986).

[15] CRANBERG, L., LEVIN, J.S., Phys. Rev. 109 (1958) 2063.

[16] GLASKOV, N.P., At. Ehnerg. 14(4) (1963) 400 (in Russian).

[17] SMITH, A.B., Nucl.Phys. 47 (1963) 633.

[18] BARNARD, E., FERGUSON, A.T.G., McMURRAY, W.R., et al., Nucl.Phys. 80 (1966) 46.

[19] BARNARD, E., DE VILLIERS, J.A.M., REITMAN, D., in Nuclear Data for Reactors (Proc. 2nd Intern. Conf. on Nuclear Data for Reactors, Helsinki, 1970), Vol.2 , IAEA, Vienna (1970).

[20] EGAN, J.J., PRINCE, A., et al., NBS Special Publication 425 (1975) 950.

[21] GUENTER, P., SMITH, A., NBS Special Publication 425 (1975) 862.

[22] GUENTER, P., HAVEL, D., SMITH, A., Rep. ANL/NDM-16, Argonne National Laboratory, Argonne (1975).

[23] VOROTNIKOV, P.E., VUKOLOV, V.A., KOLTYSHIN E.A., in Neytronnaya Fizika, (Proc. of 4th All-Union Conf. on Neutron Physics, Kiev, 1977), Part 2, TsNIIatominform, Moscow (1977) 119 (in Russian).

[24] ARMITAGE, B., SPENCER, W., Rep. INDC(UK)-29, IAEA, Vienna (1977) 3.

[25] TSANG, F.Y., BRUGGER, R.M., Nucl.Sci. and Eng. 65 (1978) 70.

[26] DE SAUSSURE, G., SMITH, A.B., in Nuclear Data for Science and Technology (Proc. Intern. Conf., Antwerp, 1982), D.Reidel Pub. Co., Boston (1983) 9.

THE ^{238}U (n,n') AND (n,2n) REACTION CROSS-SECTIONS AND ASSOCIATED NEUTRON SPECTRA

N.V. Kornilov

Abstract

The ^{238}U (n,n') and (n,2n) reaction cross-sections and the spectra and angular distribution of neutrons emitted from these reactions are discussed. The shortcomings of the description of the continuum neutron spectrum in the BNAB-MIKRO and ENDF/B-V is pointed out. It is found that the evaluated (n,n') and (n,2n) data included in the BNAB-MIKRO data library are in reasonable agreement with the results of recent experiments.

Let us examine the (n,n') and (n,2n) reaction cross-sections and the associated neutron spectra for initial energies E_0>4 MeV. This energy range which is characterized by a continuum of secondary neutrons presents certain difficulties in the study of these reactions. As a rule, the investigated energy range of secondary neutrons is bound at the lower end of the range by the detection threshold, which ranges typically from 0.2 to 0.5 MeV, and by the low energy tail of the elastic peak at the upper end of the spectrum. In order to correctly extrapolate the spectrum to the bounding energies it is essential to study the shape of the spectrum in great detail and to have a correct understanding of the reaction mechanisms.

The international ENDF format for the representation of evaluated data requires that neutron spectra for each partial process (e.g., (n,n'), (n,2n), etc.) be described separately. In view of the fact that there are no experimental neutron spectrum data for each individual reaction, the identification of each spectrum can only be derived from theoretical calculations which would guarantee that the experimental data for all reactions and composite spectra be properly taken into account. Since the determination of neutron spectra in the 10-14 MeV energy range by experimental means is difficult, a correct evaluation can only be done on the basis of theoretical models that have been tested in energy regions where data can be determined by experimental means. All of these factors underline the complexity of the

processes involved in the evaluation (including both experimental data and theoretical analysis) of the cross-sections and spectra of these quantities.

Neutron spectra and angular distributions. Among the numerous experiments performed during the 1970-ies, a number of them were dedicated to the measurement of double differential neutron scattering cross-sections on nuclei of $30<A<200$ for incident neutron energies of 14 MeV [1-3], 9 MeV [4,5] to 6-8 MeV [6]. A detailed study of ^{238}U neutron spectra for incident neutron energies of 6-9 MeV and 14 MeV are reported in references [7,8]. The analysis and systematization of these measurements are reported in references [9-13]. Theoretical methods to describe the neutron spectra were being developed at the same time [3,14,15]. As a result of these investigations it was possible to derive characteristics common to a large number of mass numbers, as well as to identify specific problems in describing experiments with theory.

Spectra of scattered neutrons are made up of two components: one determined by the equilibrium cross-section σ_e which predominates in the low energy region of secondary neutrons, and the other determined by the non-equilibrium cross-section σ_{di}. A good approximation for the description of the equilibrium cross-section is given by Weisskopf's evaporation model. In the earlier stages of these investigations, the non-equilibrium component was described by pre-equilibrium decay [2,4,5,10,11]. However, the inconsistency of this approach became apparent in the attempts to explain the asymmetrical nature of angular distributions, and the contribution of non-statistical processes in the (n,n') and (n,p) reactions which proceed through one and the same or neighboring compound nucleus [6,16]. A more consistent description of spectra and angular distributions was achieved by the direct reaction theory [3,10,13-15]. This approach, however, is limited to the description of scattering to low-lying states. It is difficult to know the extent of direct process contributions to the excitation of states whose energies are close to the incident energy. Various values of non-equilibrium process contributions have been derived from the analysis of experimental data: varying from 5-10% reported in

reference [13] to 30% given in references [3,11,12]. The uncertainty in estimating the extent of the direct process contribution to the excitation of high energy states is also related to the uncertainty in determining the energy dependence of nuclear level densities. Thus, in the process of describing neutron spectra generated by scattering from nuclei by direct process using the expression $\sigma_{di} \sim (E/E_0)^{\frac{1}{2}}(E_0-E)$, the authors of reference [13] also obtain a value for the nuclear level density parameter of $a \approx 32$ MeV^{-1}. Processing of the same experimental data on the assumption that (E_0-2) MeV$<U<E_0$ and that there is no direct process contribution yields a value of $a \approx 25$ MeV^{-1}. The non-existence of adequate theoretical calculations to determine the contribution of direct processes in ^{238}U over a wide energy range, makes it difficult to use these models for the evaluation of neutron spectra. As a consequence, cross-sections and neutron spectra are calculated as before with the use of the pre-equilibrium model [17].

Thus, regardless of the currently existing ambiguities which prevent a straightforward separation of the various reaction mechanisms, present day evaluations must take into account the non-equilibrium component of the neutron spectrum, which in the case of ^{238}U ranges from 70-100 mb/MeV for incident energies of 6-9 and 14 MeV.

Fig. 1 shows the distribution of inelastically scattered neutrons for $E_0 \approx 6$ MeV, first neutron spectra for ^{238}U for different incident energies [8,12], as well as their representation according to the following equation:

$$\sigma(E,E_0) = a_1 EU^{-n} \exp(2\sqrt{aU}) + a_2 (E/E_0)^{1/2} (E_0-E) \qquad (1)$$

These data are also represented satisfactorily by the pre-equilibrium decay model [17]. Existing evaluations of ^{238}U as well as of other nuclides, do not take the considerations outlined above into account. In both the ENDF/B-V and BNAB-MIKRO [18] evaluated data libraries, the spectra of scattered neutrons are represented by Maxwellian distributions which obviously do not agree with the experimentally observed distributions for ^{238}U.

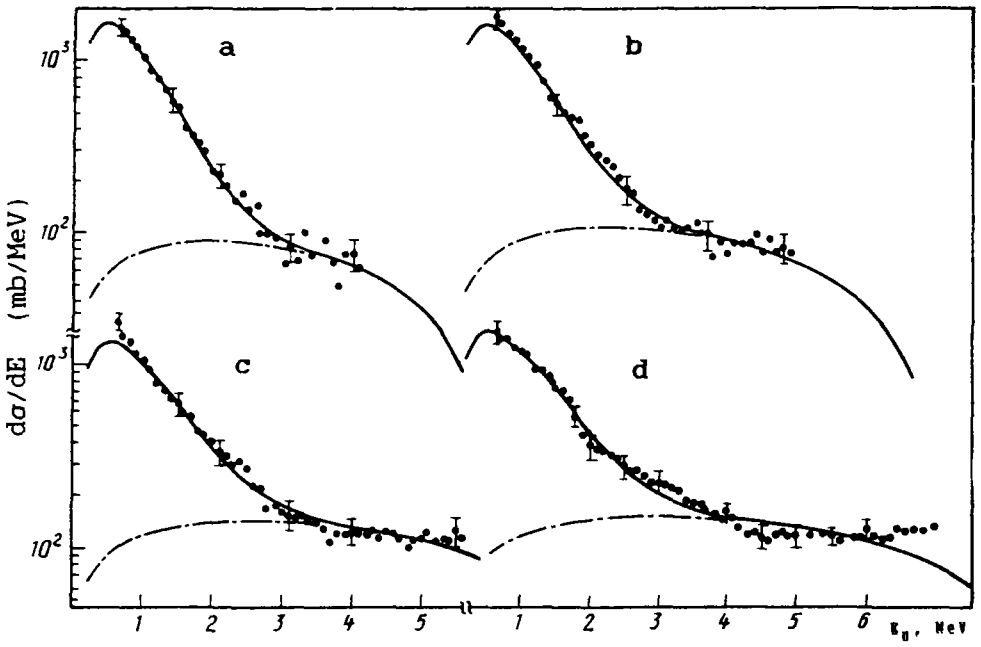

Fig. 1. Spectra of inelastically scattered neutrons integrated over angle (for E_0=6.02 Mev) and first neutron spectrum for ^{238}U for other incident energies: ● experimental data from Ref.[8,12], —— total spectrum; — • — • — non-equilibrium spectral component calculated with equation (1); E_0 values (MeV): a - 6.12, b - 6.98, c - 7.98, d - 8.94.

Another shortcoming common to existing evaluations is the incorrect use of the partial cross-sections in the separation of the individual spectral components. Neutron spectra from (n,n') reactions for $E_0>Q_{2n}$ must drop off rather sharply at energies of secondary neutrons $E<E_0-Q_{2n}$. In spite of these evident facts, the existing evaluations propose to describe these spectra by Maxwellian distributions for energies of $E_0>Q_{2n}$ as well. In addition, the spectra of neutrons emitted in the (n,xnf) reactions prior to fission, which should be part of the fission channel and included in the prompt neutron fission spectrum, are not identified separately in the evaluated data files.

The separation of spectral components according to individually contributing reactions can be done without any problem using current theoretical models. The capability of such theoretical calculations was demonstrated in reference [17]. However, although calculations were not done for individual partial cross-sections, there are no basic reasons why this cannot be done. The measurement of the angular distribution of secondary ^{238}U neutrons for $E_0\approx6.8$ MeV has been reported in reference [12]. These results showed a very weak angular dependence, which is

illustrated by the ratio of the Legendre polynomial coefficients $b_i/b_0 \leq 10\%$ (i=1,2). Since the experiment reported in reference [12] consisted in the measurement of total double differential cross-sections for all processes (fission included), it did not yield any data for the angular distribution of inelastically scattered neutrons.

The investigation of double differential inelastic scattering cross-sections on other nuclei shows that the angular distributions are symmetrical with respect to 90^0 for low secondary neutron energies. At higher energies, an increase in the number of neutrons scattered at small angles can be observed. A similar behavior can also be observed for (n,p), (α,n) and other reactions. For a wide range of incident particle energies, the angular distribution of neutrons can be described satisfactorily by the empirical systematics proposed in reference [19]. An important conclusion of this analysis is that, to a first approximation, the shape of angular distributions depends only on the energy of the emitted particles and is proportional to the contribution of the non-equilibrium emission. Furthermore, the authors of reference [20] show that the conclusion arrived at in reference [19] is also applicable to the description of the angular distribution in the (n,n') reaction. Extending these results to ^{231}U it is to be expected that for low energies, the distribution of neutrons would be described by $\sigma(0^0)/\sigma(90^0) \leq 1.15\text{-}1.20$. For higher energies, for instance $E \approx 10$ MeV and $E_0 \approx 14$ MeV, the ratio $\sigma(0^0)/\sigma(180^0)$ would be equal to approximately 3.

In the existing evaluations, the angular distribution of scattered neutrons is assumed to be isotropic. This assumption is justified only for low energy scattered neutrons and for accuracies not exceeding 20%. In the end, the need to include the non-isotropic dependence of these distributions in the data files must be determined by practical requirements.

The (n,n') reaction cross-section. Let us examine the experimental inelastic scattering cross-section data measured in the 1980-ies that have not been included in the evaluated data files [18]. In the experiment reported in reference [12], the

(n,n') reaction cross-section was measured for incident neutron energies of ~6 MeV. The experimental value of the cross-section for secondary neutron energies ranging from 0.62-4.1 MeV was determined to be equal to 1260±90 mb. In order to obtain a value for the total (n,n') reaction cross-section, the value of 326±60 mb (which is the cross-section for scattering on individual levels ranging from 0.045 MeV ≤ U ≤ 1.078 Mev), the value of 66±120 mb (which represent the contribution of the cross-sections for the scattering from the 3-4 MeV energy region to the 4.1-4.94 MeV interval) and the value of 800±160 mb (which is the value of the scattering cross-section for the 0-0.62 Mev energies, calculated with equation (1)) were added to the above-mentioned experimental value of 1260±90 mb. This resulted in an inelastic cross-section value of 2.45±0.23 b (see Fig.2). The errors of the different components were calculated independently. The (n,n') cross-section for the 6-11 MeV energy range was determined from the first neutron spectrum derived in reference [12] on the basis of the empirically determined spectral shape, and from evaporation model calculations used for the determination of the (n,nf) and (n,2n) reaction cross-sections. With the exception of the data required for the first neutron spectrum calculation, the parameters needed for the evaporation model calculations were obtained from the best experimentally determined values of the (n,2n) cross-section and from the fission characteristics of the ^{239}U nucleus.

Interesting results of inelastic scattering cross-section data were published in reference [21] for neutron energies ranging from 0.9 to 3.5 MeV. Pseudo-elastic scattering, in which the scattered neutrons fall into a controlled interval close to the incident energy, was determined experimentally. With the exception of scattering to the first one or two levels, inelastic scattering was derived from the knowledge of the total and fission cross-sections which are known to a great degree of accuracy in this energy range. The experimental uncertainty of the data was 8-10%. The total (n,n') reaction cross-section, taken from reference [21], and the cross-section for scattering to the first levels, taken from the BNAB-MIKRO data file [18], are plotted in Fig. 2. As can be seen from this figure, the evaluated total inelastic neutron scattering cross-section given

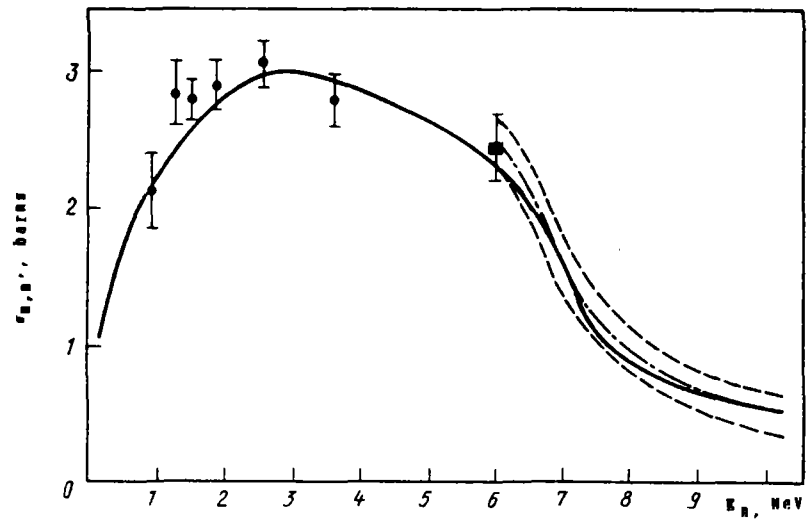

Fig. 2. Total inelastic scattering cross-section. Experimental data: ● [21], ■ [12]; —— evaluated data [18]; • — • — and — — — reference [12] data and their uncertainty respectively.

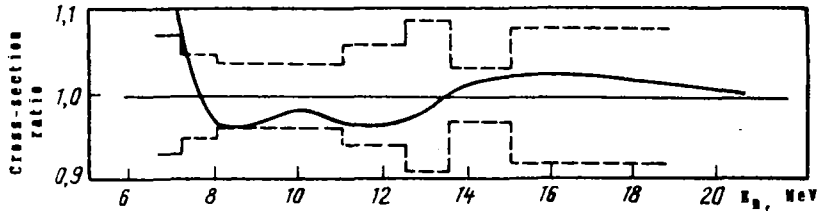

Fig. 3. Ratio of the (n,2n) cross-section taken from the BNAB-MIKRO library to that published in reference [22]; — — — cross-section uncertainty as given in reference [22].

in reference [18] agrees with the latest experimental results to within 10%.

The (n,2n) reaction. The (n,2n) reaction cross-section has been analyzed thoroughly in reference [22]. This cross-section and its uncertainty has been evaluated on the basis of all of the existing evaluated data, and the conclusion was reached that the requirements for its accuracy had been satisfied. After the completion of this evaluation [22], newly re-assessed data were published [23] which turned out to be approximately 10% lower, for E_0<10 MeV, than those recommended in reference [22]. This resulted in an unresolved situation with regard to the published evaluated data [22], revealing systematic differences in the experimental data which were measured using the activation method and a large scintillation detector for the detection of multiple neutrons. The (n,2n) reaction cross-section, which has been measured for E_0<10 MeV in a number of laboratories using the

activation method, are in good agreement with each other as well as with the recommended data published in reference [22]; it is therefore reasonable not to undertake a re-evaluation of these data before obtaining additional data, and in the mean time, to increase the uncertainty of the recommended data by 10%. A comparison of the (n,2n) reaction cross-section given in the BNAB-MIKRO evaluated data file [18] with the data published in reference [22] is given in Fig. 3. Within the limits of the uncertainties (evaluated in reference [22]), this comparison shows a satisfactory agreement between these data over a broad energy range, from 7 to 19 MeV.

The following conclusions can be made on the basis of this analysis:

1. The neutron spectra from the (n,n') and (n,2n) reactions included in the BNAB-MIKRO and ENDF/B-V evaluated data libraries are not in conformity with the current knowledge of reaction mechanisms, and the separation of the spectral components according to the partial processes is not done correctly.

2. Should it be necessary to include the non-isotropic dependence of inelastically scattered neutrons in the evaluated files, the necessary calculations can be done on the basis of the systematics developed in reference [19].

3. The (n,n') reaction cross-section given in the BNAB-MIKRO data library is in agreement with the experimental data that have been measured in the course of the last few years to within 10%. A similar agreement is observed in the case of the (n,2n) reaction cross-section.

REFERENCES

[1] SALNIKOV, O.A., LOVCHIKOVA, G.N., KOTELNIKOVA, G.V., Problems of Atomic Science and Technology. Ser. Nuclear Constants 7 (1971) 102 and 134, Nuclear Constants 10 (1972) 18, and Nuclear Constants 15 (1974) (in Russian).

[2] HERMSDORF, D., MUSIOL, G. et al., Rep. ZfK-243, Zentralinstitut fuer Kernforschung, Rossendorf (1972) 25.

[3] SALNIKOV, O.A., SAPRYKIN, E.M., KOTELNIKOVA, G.V., Yad. Fizika 17 (1973) 1001 (in Russian).

[4] BIRYUKOV, N.S., ZHURAVLEV, B.V., KORNILOV, N.V., et al., Preprint FEI-457, Institute of Physics and Power Engineering, Obninsk (1973) (in Russian).

[5] BIRYUKOV, N.S., ZHURAVLEV, B.V., KORNILOV, N.V., et al., Yad.Fizika 19 (1974) 1190 (in Russian).

[6] SALNIKOV, O.A., LOVCHIKOVA, G.N., SIMAKOV, S.P., et al., Neytronnaya Fizika (Proc. of 5th All-Union Conf. on Neutron Physics, Kiev, 1980), Part 2, TsNIIatominform, Moscow (1980) 144 (in Russian).

[7] BARYBA, V.Ya., ZHURAVLEV, Eh.V., KORNILOV, N.V., et al., Preprint FEI-679, Institute of Physics and Power Engineering, Obninsk (1976) (in Russian).

[8] KORNILOV, N.V., BARYBA, V.Ya., SALNIKOV, O.A., Neytronnaya Fizika (Proc. of 5th All-Union Conf. on Neutron Physics. Kiev, 1980), Part 1, TsNIIatominform, Moscow (1980) 44 (in Russian).

[9] SALNIKOV, O.A., Inelastic Neutron Scattering in the Region of Overlapping Levels, Thesis, Leningrad (1975) (in Russian).

[10] ZHURAVLEV, B.V., Inelastic Scattering for Incident Energies of 9 MeV and Nuclear Level Densities, Thesis, Moscow (1974) (in Russian).

[11] PLYASKIN, V.I., Neutron Angular and Energy Distribution for Incident energies of 9 MeV, Thesis, Dmitrovgrad (1975) (in Russian).

[12] KORNILOV, N.V., Experimental Investigation of the Interaction of Medium Energy Neutrons with ^{238}U Nuclei, Thesis, Leningrad (1981) (in Russian).

[13] SIMAKOV, S.P., Neutron Inelastic Scattering on a Number of Stable Nuclei in the 5-8 MeV Energy Range, Thesis, Leningrad (1983) (in Russian).

[14] IGNATYUK, A.V., LUNEV, V.P., Izv.Akad.Nauk SSSR, Ser. Fiz. 39 (1975) 2144 (in Russian).

[15] IGNATYUK, A.V., Statistical Properties of Excited Atomic Nuclei, Ehnergoatomizdat, Moscow (1983) (in Russian).

[16] BIRYUKOV, N.S., ZHURAVLEV, B.V., KORNILOV, N.V., et al., Neytronnaya Fizika (Proc. of 4th All-Union Conf. on Neutron Physics, Kiev, 1977), Part 1, TsNIIatominform, Moscow (1977) 260 (in Russian).

[17] GRUZDEVICH, O.T., IGNATYUK, A.V., MASSLOV, V.M., PASHCHENKO, A.B., Neytronnaya Fizika (Proc. of 6th All-Union Conf. on Neutron Physics, Kiev, 1983) Part 2, TsNIIatominform, Moscow (1984) 318 (in Russian).

[18] ABAGYAN, L.P., BAZAZYANTS, N.O., NIKOLAEV, M.N., Multigroup Data for Reactor and Shielding Calculations, Ehnergoizdat, Moscow (1981) (in Russian).

[19] KALBACH, C., MANN, F.M., (Proc. Symp. on Neutron Cross-Sections from 10 to 50 MeV, Brookhaven, 1980), Brookhaven National Laboratory, Rep. BNL-NCS-51245 (1980) 689, and IAEA Rep. INDC(USA)-84 (1980).

[20] ZHURAVLEV, B.V., KORNILOV, N.V., Problems of Atomic Science and Technology. Ser. Nuclear Constants 5(44) (1981) 16 (in Russian).

[21] SMITH, A.B., GUENTHER, P.T., McKNIGHT, R.D., (Proc. Int. Conf. Nuclear Data for Science and Technology, Antwerp, 1982), D.Reidel Pub. Co., Boston (1983) 39.

[22] KORNILOV, N.V., VINOGRADOV, B.N., GAI, E.V., et al., Problems of Atomic Science and Technology. Ser. Nuclear Constants 1(45) (1982) 33 (in Russian).

[23] FREHAUT, J., BERTIN, A., BOIS, R., JAVY, J., (Proc. Symp. on Neutron Cross-Sections from 10 to 50 MeV, Brookhaven, 1980), Brookhaven National Laboratory, Rep. BNL-NCS-51245 (1980), and IAEA Rep. INDC(US)-84 (1980).

ANALYSIS OF FAST NEUTRON SCATTERING CROSS-SECTIONS OF EVEN NICKEL ISOTOPES

I.A. Korzh

Abstract

Experimental differential data and integrated elastic and inelastic scattering cross-section data for the ^{52,60,62,64}Ni nuclei are analyzed together with the total cross-section in the 0.5 to 9.0 MeV energy range using the spherical optical, statistical and coupled channel models. The elastic and inelastic scattering cross-section data are compared with current evaluations.

Nickel is an important component of stainless steels which are widely used in nuclear reactor technology. This has determined the importance of data on the interaction of neutrons with nickel nuclei over a wide energy range. In addition to the practical usefulness of experimental data on fast neutron scattering cross-sections on nickel isotopes in the design of nuclear reactors, this information is of value in the development of theoretical nuclear models, and in the investigation of the dynamics of the dependence of neutron scattering on energy.

The fast neutron nickel cross-section data which have a practical importance are those which are needed to define the cross-sections of structural materials. The object of this exercise consists in compiling a new body of highly accurate and reliable experimental information on the fast neutron scattering by nickel nuclei.

Participants in this experiment have measured the elastic and inelastic scattering cross-sections (with the excitation of any one of the first four levels) of the ^{58,60,62,64}Ni isotopes for the following neutron energies: 1.5, 2.0 ,2.5, 3.0, 5.0, 6.0, and 7.0 MeV. Incomplete sets of these scattering cross-sections have been published [1-9] in the past; in this analysis they are presented in a systematic manner. The experimental data of this

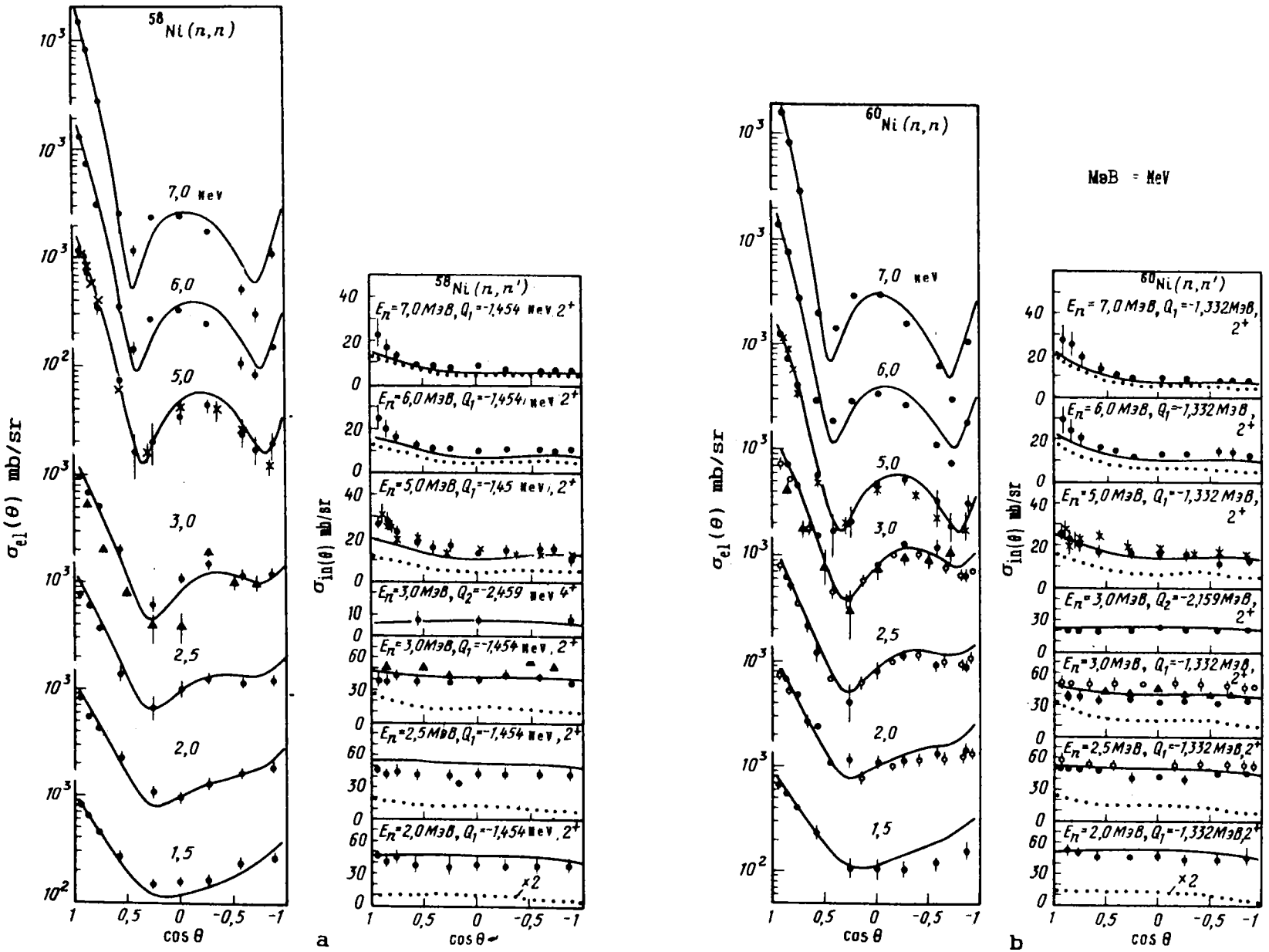

Fig. 1. Differential elastic and inelastic neutron scattering cross-sections at 1.5-7.0 MeV for: (a) ^{58}Ni, (b) ^{60}Ni, (c) ^{62}Ni and (d) ^{64}Ni. Experimental data: ● [1,2,4-9], x [12], ▲ [13], O [15]. Theoretical data: —— optical model (OM) and (HFM) statistical model calculations for elastic scattering and coupled channel (CC) and (HFM) statistical model calculations for inelastic scattering; ····· CC calculated cross-sections.

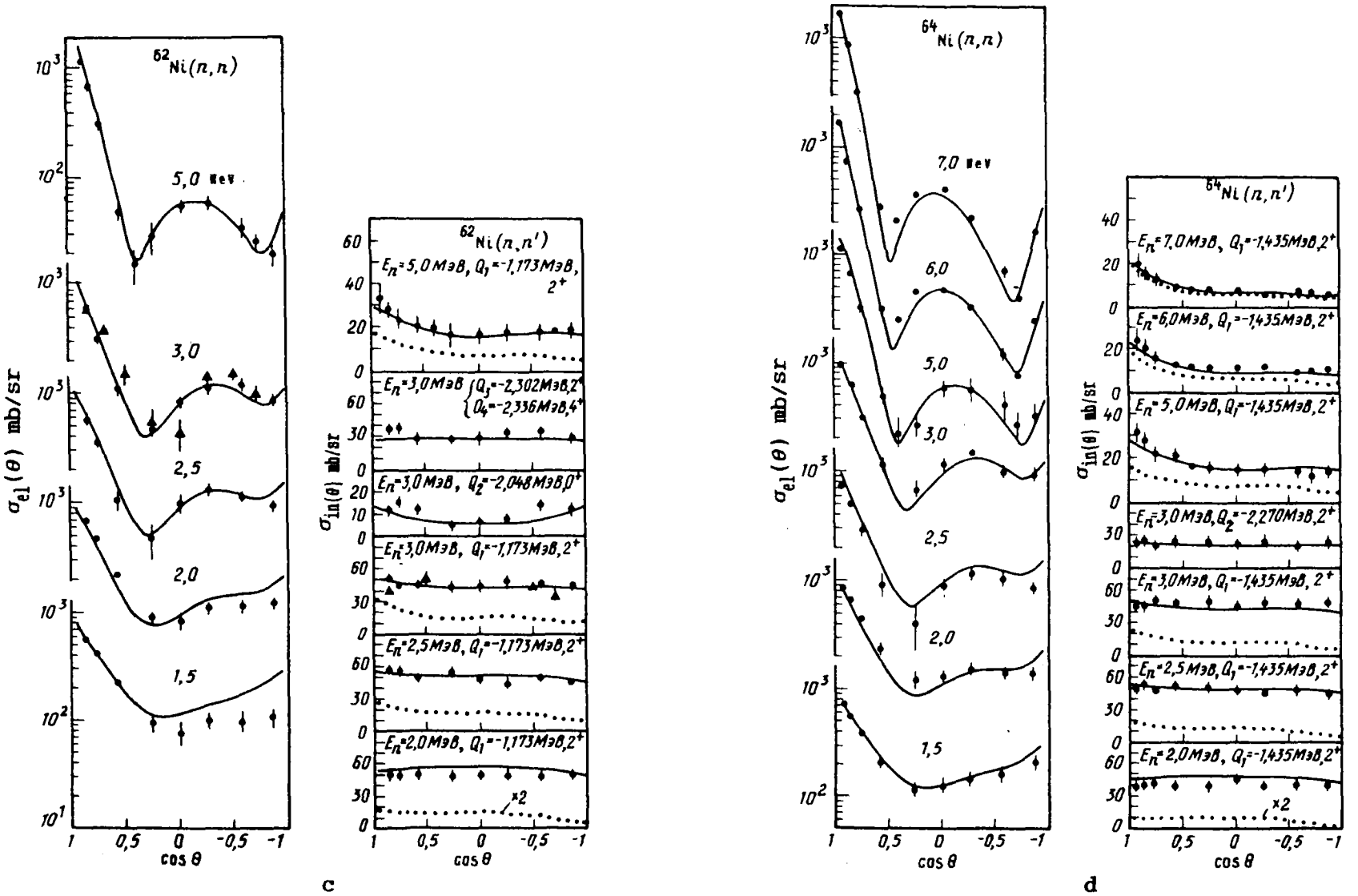

Fig. 1. (continued)

experiment, together with the data of other authors measured in the same energy range, have been analyzed in the framework of the spherical optical model, the statistical model and the coupled channel model. For the sake of completion this analysis also included the energy dependent total and integral neutron elastic and inelastic scattering cross-sections of the nickel isotopes under investigation, measured at energies ranging from 0.5 to 9.0 MeV, which had been published in the literature by other authors. The elastic and inelastic scattering cross-sections are compared with the results of current evaluations.

Experimental Results. The differential elastic and inelastic fast neutron cross-sections, with the excitation of one to four low-lying levels of (highly enriched, 95-98%) ^{58,60,62,64}Ni isotopes have been measured with a time-of-flight spectrometer [10,11]. The average energy spread was ±50 keV for 1.5-3.0 MeV neutrons, and 170-120 keV for 5.0-7.0 MeV neutrons. The elastic and inelastic differential cross-sections of the nickel isotopes were determined by integrating the scattered neutron spectrum measured over an angular span of 20-150°. The elastic scattering cross-sections were normalized to the neutron flux measured at 0°, and the inelastic scattering cross-section was normalized with respect to the well-known (n,p) scattering cross-section. The measurements were corrected for the anisotropy of the neutrons emitted from the target and for the attenuation of the neutron flux in the sample; in addition, the inelastic scattering cross-section was corrected for the angular resolution of the experiment and for multiple scattering in the sample. The measured values of the nickel isotope elastic and inelastic cross-sections at the energies of 1.5, 2.0, 2.5, 3.0, 5.0, 6.0, and 7.0 MeV are plotted in Fig. 1. The errors shown on the figures are the total errors, including the measurement, normalization and correction errors. In the 1.5 to 5.0 MeV energy range, the total error ranges from 10-20% for elastic scattering and 5-10% for inelastic scattering. At neutron energies of 6.0 and 7.0 MeV, the error is 3-10% (in the minima) for the elastic scattering cross-section, and 4-9% (with the exception of the three forward angles) for the inelastic scattering cross-section.

Most of the measurements were made for the first time. There are only four earlier experiments on the measurement of neutron scattering angular distributions of nickel isotopes [12-15]. The results of these experiment are also shown in Fig. 1 which shows that the reference [12] data are in good agreement with the data of this experiment; however, the angular distribution of the elastically scattered neutrons reported in reference [13], and the angular distribution of the inelastically scattered neutrons reported in reference [15] differ noticeably from the results of this experiment.

The data on differential inelastic scattering cross-sections at 2.0-3.0 MeV reported by these authors are comparable to results of inelastic scattering cross-section measurements of natural nickel reported in references [16] and [17]. The results of this experiment at 3.0 MeV agree with those reported in reference [16] with respect to both the shape of the angular distributions as well as to the value of the cross-section. The data for the first levels of the ^{58,60,62}Ni isotopes at the neutron energy of 2.02 MeV reported in reference [17] differ significantly (approximately by 50%) from the values obtained in this experiment for similar shapes of angular distributions. Except for the ^{62}Ni cross-section value at 2.65 Mev, the data agree with our results at neutron energies of 2.65 and 3.26 MeV.

On the basis of the results from our measurements of the fast neutron differential scattering cross-sections of even nickel isotopes, this experiment also yielded integral elastic and inelastic scattering cross-sections of the nickel isotopes at the neutron energies under investigation. The isotopic cross-section data were also used to derive the integral elastic neutron scattering cross-sections for elemental nickel. The energy dependence of the integral cross-sections are plotted in Figs. 2 and 3. The same figures also show the results from other authors in the energy range 0.5-9.0 MeV: for the elastic scattering cross-section [12,14,15,17-26], for the inelastic scattering cross-section [12,13,15-17,19,20,27-32], and for the total cross-sections of elemental nickel [33] and isotopes of nickel [12,15,18,34-36].

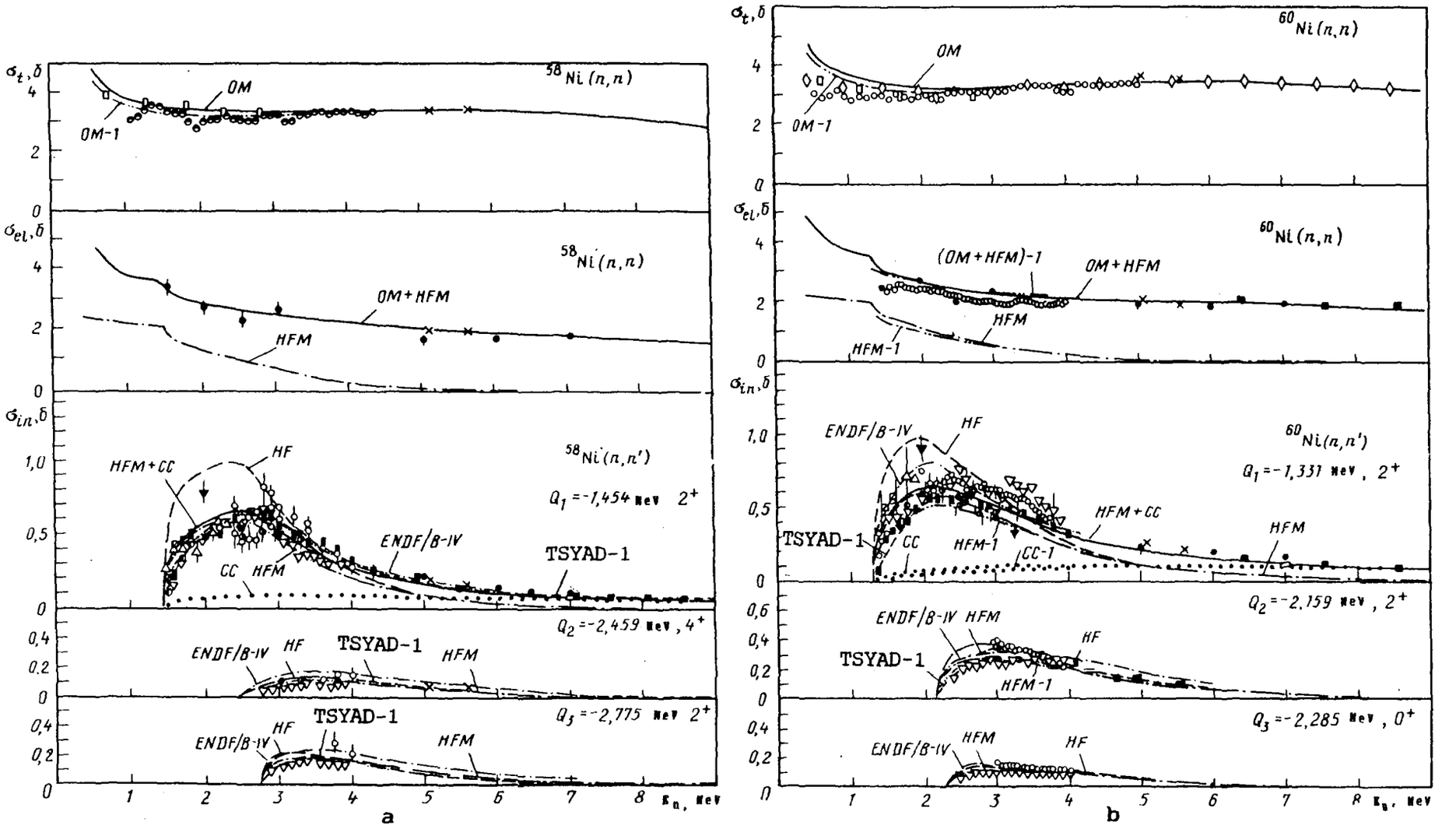

*Fig. 2. Energy dependence of the total cross-section and the elastic and inelastic neutron scattering cross-section for the excitation of three lowest levels of the ^{58}Ni (a), ^{60}Ni (b), ^{62}Ni (c) and ^{64}Ni (d) nuclei. Experimental data: ● [1,2,4-9], x [12], ▲ [13], ◑ [16], ▼ [17], + [18], ○ [15-19], ■ [14-20], ▌ [27], △ [28], ◐ [29], ▬ [30], ▨ [31], ▽ [32], ◇ [33], * [34], ▯ [35]. Curves: optical model calculations (OM, OM-1), coupled channel calculations (CC, CC-1), and statistical calculations, without level width fluctuations (HF) and with (HFM, HFM-1); as well as curves showing the TSYAD-1 and ENDF/B-IV evaluations.*

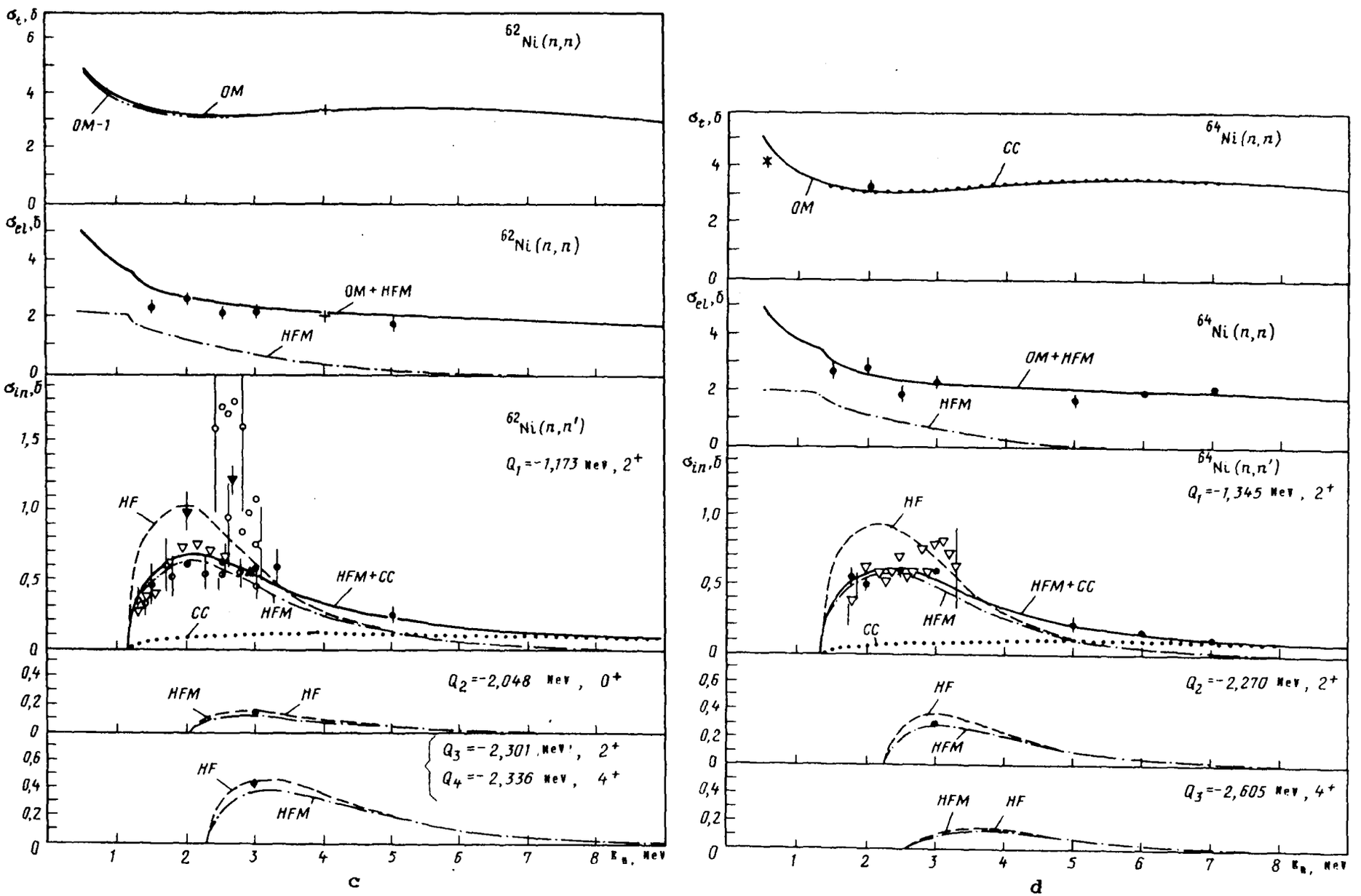

Fig. 2. (continued)

In the investigated energy region there is practically an absence of experimental information on total cross-sections for the ^{62,64}Ni isotopes. The available data on the total cross-sections of ^{58,60}Ni are not in disagreement with the total cross-section of elemental nickel. Fig. 2 shows that the data on the integral fast neutron elastic scattering cross-section for the even isotopes of nickel obtained in this experiment are in good agreement with published data. Fig. 3 shows that the integral neutron elastic scattering cross-section of elemental nickel in the neutron energy range of 1.5-7.0 MeV, is in good agreement with all experimental data, and except for a few individual points, the experimental data of different authors agree with each other.

Fig. 2 shows that for energies below 3.0 MeV, there is a considerable spread in the evaluated inelastic scattering cross-section data which often exceeds the experimental uncertainty of the data. This behavior is noticeable primarily for data that were obtained from measurements of gamma rays emitted in the neutron inelastic scattering process and for data obtained from the measurement of the neutron inelastic scattering on elemental nickel. The data obtained in his experiment are in good agreement with the overall energy dependence of the data; they contribute to the elimination of discrepancies between data of different authors, and helps in bridging gaps in the data at energies above 5 MeV.

Theoretical Analysis. The experimental data on the total cross-section, and the differential and integral elastic and inelastic scattering cross-sections obtained in this experiment and those published in the literature have been analyzed in the framework of existing theoretical models describing the interaction of neutrons with nuclei. The experimental data have been compared with data calculated using the following models: the spherical optical (OM) model, the coupled channel (CC) model, and the statistical Hauser-Feshbach (HF) and Hauser-Feshbach-Moldauer (HFM) models. The model calculations are described in detail in reference [37].

The parameters used in the optical model calculations consisted of averaged spherical optical potential parameters fitted to the

total and elastic scattering cross-sections of the average atomic mass nuclei in the 1.5-6.0 MeV neutron energy range [38]:

$$V_c = (48.7 - 0.033E)\ \text{MeV};\quad W_c = (7.2 + 0.66E)\ \text{Mev};$$
$$V_{so} = 7.5\ \text{MeV};\quad a_v = a_{so} = 0.65\ \text{fm};\qquad (1)$$
$$a_w = 0.98\ \text{fm};\quad r_c = 1.25\ \text{fm}.$$

In addition, the following set of optimal parameters for nickel fitted to the total cross-section in the 0.5-20 MeV neutron energy range [39] were used in the optical model calculations:

$$V_c = (51.33 - 0.331E)\ \text{MeV};\quad W_c = (8.068 + 0.112E)\ \text{MeV}$$
$$V_{so} = 7.0\ \text{MeV};\quad a_v = a_{so} = 0.541\ \text{fm};\qquad (2)$$
$$a_w = 0.40\ \text{fm};\quad r_v = r_{so} = 1.24\ \text{fm};\quad r_w = 1.4\ \text{fm};$$

The same spherical optical model parameters were used in the coupled channel method calculations, except that the value of W_c was reduced by 20% so as to maintain the same total cross-section values as in the spherical optical model. In the coupled channel calculations the first and second excited levels were assumed to be coupled because of their vibrational character. The coupled channel calculation were made by using a complex coupling potential and the following dynamic deformation parameter values: $\beta_2 = 0.20$ for the ^{58,64}Ni nuclei, and $\beta_2 = 0.22$the ^{60,62}Ni nuclei. A comparison of the total cross-sections of the investigated isotopes calculated using the optical and coupled channel method showed that their differences did not exceed 2% (see Fig. 2 d.).

The scattering cross-section was calculated using the compound nuclear theory according to the Hauser-Feshbach [42] and Hauser-Feshbach-Moldauer [43] statistical models. Statistical model calculations, below 3.0 -3.5 MeV, assumed that the discrete levels have known characteristics; contributions to the scattering cross-section from higher excitation levels were calculated from the compound nucleus as contributions from the continuum with a level density distribution determined by the Fermi gas model with a and Δ parameters taken from reference [44]. The statistical model calculations took only the neutron exit channels into account, the competing channels for the emission of protons and alpha particles for the ^{58,60}Ni nuclei were

calculated using the factor $(\sigma_c - \sigma_{np} - \sigma_{n\alpha})/\sigma_c$. Since statistical model calculations use transmission coefficients which are calculated with the optical model, when adding the direct cross-section contributions to the compound cross-sections, the latter were normalized using the factor $(\sigma_c^{OM} - \sigma_{2+}^{CC})/\sigma_c^{OM}$, where σ_c^{OM} is the cross-section for the formation of the compound nucleus calculated with the optical model, and σ_{2+}^{CC} is the cross-section for the direct excitation of the 2+ level calculated with the coupled channel model.

A comparison of the calculated and experimental differential elastic and inelastic neutron scattering cross-sections is shown in Fig. 1. It can be seen that the theoretical cross-sections, calculated with the use of a set of averaged optical potential parameters, are in good agreement with the experimental data. The theoretically calculated values of the total cross-sections and of the integral elastic and inelastic scattering cross-sections in the 0.5-9.0 MeV neutron energy range are plotted in Figs. 2 and 3. These curves show that the optical model calculation of the total cross-sections, using the parameters given in (1) and (2) above, do not differ much from each other, and are in agreement with the experimental data. However, the calculations using the second set of parameters (2) yield a lower direct (CC-1) and compound (HFM-1) contributions to the summed scattering cross-sections for the excitation of the first 2+ levels of the investigated nickel isotopes.

The data plotted in Figs 1 and 2 show that the theoretical cross-section, calculated in the framework of the optical-statistical model with the use of the first set of parameters (1), gives a good representation of the experimental data. These results can be used to make certain conclusions regarding the roles played by the direct and compound processes in the scattering of neutrons on nickel isotopes. In the energy range under consideration, the relative contributions to the scattering cross-section by the compound nucleus mechanism and by the direct process depends to a large extent on the energy of the incident neutrons. Thus, the cross-section for the direct process contribution to the total neutron scattering cross-section is approximately 50% for energies at the low end of the considered energy range, and at a

neutron energy of 7.0 MeV it becomes dominant. In the case of the inelastic scattering cross-section for the excitation of the first 2+ levels of the nickel isotopes, the direct process contribution to the total cross-section is less than 10% at the low energy end of the considered energy range, and reaches roughly 80% at neutron energies of 7.0 MeV. Such ratios between the compound and direct contributions to the scattering cross-section have also been observed for other even-even isotopes of medium mass nuclei (e.g., ^{50,52,54}Cr [45] and ^{92,94}Mo [37]).

Fig. 1 shows that the differential inelastic neutron scattering cross-sections for the excitation of the second and third levels of even nickel isotopes for neutron energies of 3.0 MeV are practically isotropic, and can be described rather well by the statistical HFM model using set (1) of optical model parameters. The energy dependence of the inelastic neutron scattering cross-section for the excitation of these levels up to energies of 4-5 MeV, also agrees with HFM statistical model calculations (see Fig. 2) which bears witness to the predominant role played by the compound nucleus mechanism in the excitation of these levels.

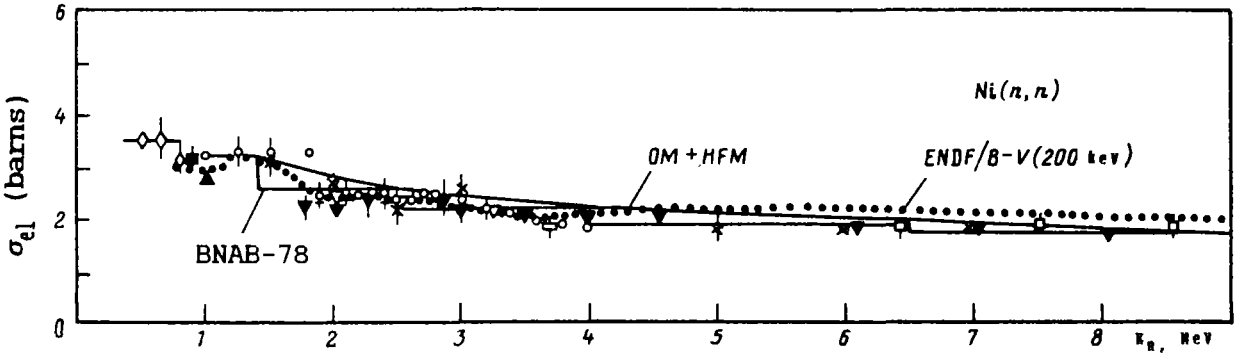

Fig. 3. Energy dependence of the integral fast neutron elastic scattering cross-sections for nickel. Experimental data: x [1-9], ▽ [17], ○ [19], □ [20], ◇ [21], ▼ [22], + [23], ■ [24], ▲ [25], ▭ [26]. —— statistical model HFM calculations with parameter set (1), •••• ENDF/B-IV data averaged over 200 keV intervals, BNAB-78 data given be continuous histogram.

Comparison of Current Evaluations with Experimental Data. In order to compare the experimental fast neutron integral elastic scattering cross-sections on nickel nuclei with evaluated data, the results of the ENDF/B-V [46] evaluation, averaged over 200 keV intervals, and the BNAB-78 [47] evaluated multigroup data are plotted together in Fig. 3. It can be seen that up to 4.0 MeV,

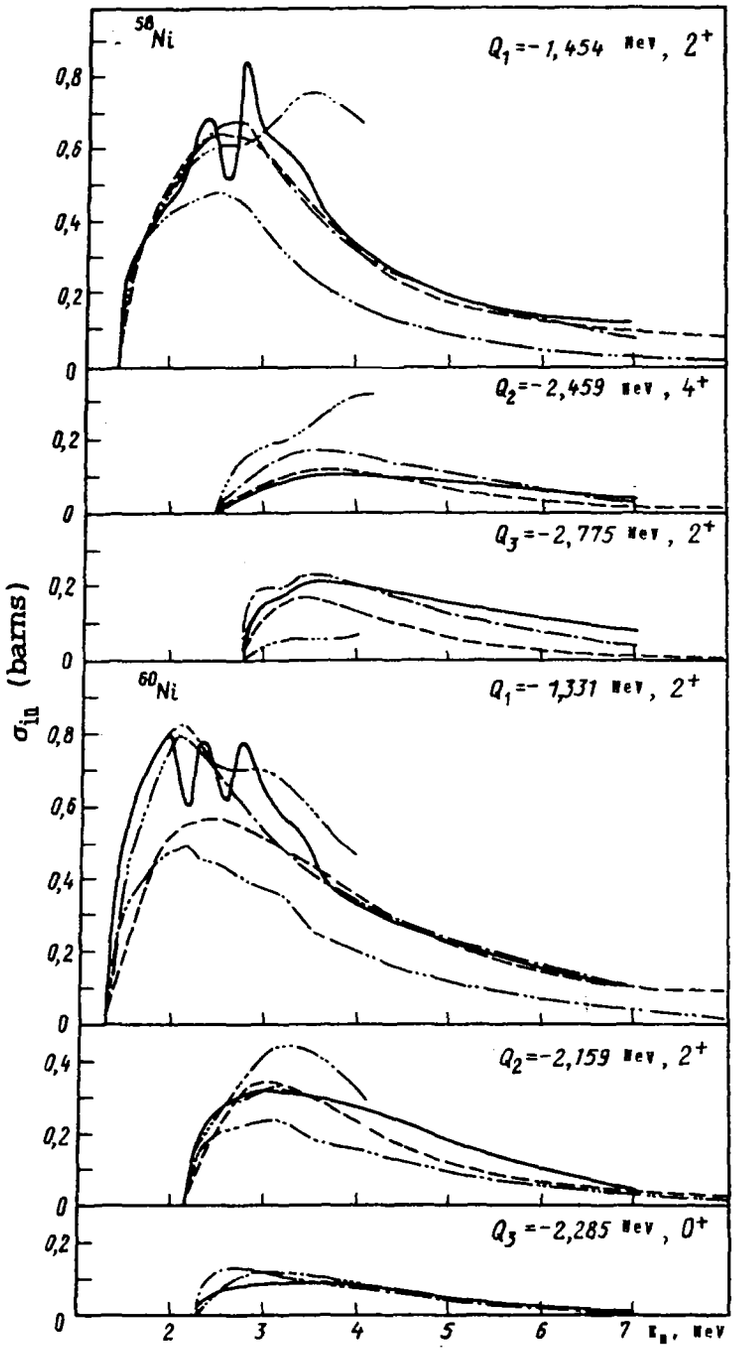

Fig. 4. Energy dependence of current evaluations of the neutron inelastic scattering cross-sections for the excitation of the three lowest levels of the ^{58,60}Ni nuclei: ENDF/B-V [46] (———), ENDF/B-IV [48] (—•—•—), TSYAD-1 [49] (— — —), KEDAK [50] (—•••—), and JENDL-1 [51] (—••—••—)

the ENDF/B-V data is in good agreement with the experimental data; for energies above 4.0 MeV, however, the experimental data are systematically higher by about 10%. It must be noted that the BNAB-78 multigroup data are in excellent agreement with the experimental data which had been measured before as well as after the publication of the BNAB-78 data library.

The experimental as well as the theoretically calculated inelastic neutron scattering cross-sections for the excitation of the first three levels of the ^{58,60}Ni nuclei are plotted together with the ENDF/B-IV [48] and the TSYAD-1 [49] evaluated data in Fig. 2a and 2b. This comparison shows that both of these evaluations are in poor agreement with the experimental data. The ENDF/B-IV evaluated data for the first ^{60}Ni level in the 1.33-2.5 MeV energy range lies along the upper boundary of the experimental data population spread, while the TSYAD-1 data curve in the same energy range lies along the lower boundary of the experimental data spread. At the neutron energy of 2.0 MeV, the evaluated data for the first ^{60}Ni energy level for these evaluations are 50% apart. The ENDF/B-V evaluation [46] did not improve the description of the experimental inelastic scattering cross-section data because it used only one set of measurements in the evaluation of these quantities. Even larger discrepancies exist between the KEDAK-3 [50] and JENDL-1 [51] evaluations and the experimental inelastic scattering cross-section of ^{58,60}Ni. This is illustrated in Fig. 4, which shows a comparison of the evaluated data for three levels of the ^{58,60}Ni nuclei from five different evaluated data libraries. The significant differences between the five inelastic scattering cross-section evaluations reflect not only the different approaches used in these evaluations but also the complexity of the evaluation process itself. A higher degree of confidence in evaluation results would be achieved if evaluations were based on the totality of the existing cross-section data.

In view of the considerable differences which exist between the various evaluations and between the evaluated and experimental data, there is a need for a new analysis of the elastic and inelastic scattering nickel cross-sections, which would take into account new experimental data and improvements in the theoretical methods describing the process of fast neutron scattering.

REFERENCES

[1] KORZH, I.A., MISHCHENKO, V.A., MOZHZHUKHIN, Eh.N., et al., Ukr.Fiz.Zh 22 (1977) 112 (in Russian).

[2] PRAVDIVYIJ, N.M., KORZH, I.A., MISHCHENKO, V.A., et al., Neytronnaya Fizika, (Proc of 4th All-Union Conf. on Neutron Physics, Kiev, 1977), Part 1, TSNIIatominform, Moscow (1977) 273 (in Russian).

[3] KORZH, I.A., MISHCHENKO, V.A., MOZHZHUKHIN, Eh.N., et al., Ukr.Fiz.Zh 22 (1977) 866 (in Russian); KORZH, I.A., MISHCHENKO, B.A., PRAVDIVYIJ, N.M., Akad.Nauk.Kaz.SSR, Ser.Fiz.-Mat. 6 (1978) 61 (in Russian).

[4] KORZH, I.A., MISHCHENKO, V.A., MOZHZHUKHIN, Eh.N., Yad.Fiz. 31 (1980) 13 (in Russian).

[5] KORZH, I.A., LUNEV, V.P., MISHCHENKO, V.A., et al., Neytronnaya Fizika, (Proc. of 5th All-Union Conf. on Neutron Physics, Kiev, 1980), Part 1, TSNIIatominform, Moscow (1980) 314 (in Russian).

[6] KORZH, I.A., LUNEV, V.P., MISHCHENKO, V.A., et al., At.Ehnerg. 50 (1981) 398 (in Russian).

[7] PASECHNIK, M.V., KORZH, I.A., MOZHZHUKHIN, Eh.N.,(Proc. Int. Conf. on Nuclear Cross-Sections for Technology, Knoxville, TE, 1979), US National Bureau of Standards Special Publication 594-AB7, US Government Printin Office Washington DC, (1980) 898.

[8] KORZH, I.A., MISHCHENKO, V.A., MOZHZHUKHIN, Eh.N., et al., Ibid. p. 893.

[9] KORZH, I.A., Neytronnaya Fizika, (Proc. of 6th All-Union Conf. on Neutron Physics, Kiev, 1983), Part 3, TSNIIatominform, Moscow (1984) 99 (in Russian).

[10] ZHUK, V.V., KOZAR, A.A., KORZH, I.A., et al., Neytronnaya Fizika, (Proc. of 2nd All-Union Cof. on Neutron Physics, Kiev, 1973) Part 4, Obninsk (1974) 203 (in Russian).

[11] KORZH, I.A., MISHCHENKO, V.A., SANZHUR, I.E., Ukr.Fiz.Zh. 25 (1980)109 (in Russian).

[12] BOSHUNG, P., LINDOW., J.T., SHRADER, E.F., Nucl.Phys. A161 (1971) 593.

[13] PASECHNIK, M.V., FEDOROV, M.B., YAKOVENKO, T.I., Neytronnaya Fizika, (Proc. of 1st All-Union Conf. on Neutron Physics, Kiev, 1971), Part 1, (1972) 277 (in Russian).

[14] PEREY, F.G., LE RIGOLEUR, C.O., KINNEY, W.E., Rep. ORNL-4523, Oak Ridge National Laboratory (1970).

[15] SMITH, A.B., GUENTHER, P., SMITH, D., WHALEN, J., Nucl.Sci.Eng. 72 (1979) 293.

[16] ETEMAD, M.A., Rep. AE-481, Studsvik AB, Nykoeping (1973).

[17] TSUKADA, K., TANAKA, S., TOMOTA, Y., MARUYAMA, M., Nucl.Phys. A125 (1969) 641.

[18] GORLOV, G.B., LEBEDEVA, N.S., MOROZOV, V.M., Yad.Fizika 6 (1967) 910 (in Russian).

[19] GUENTHER, P., SMITH, A.B., WHALEN, J., Nucl,Sci.Eng. 59 (1976) 106.

[20] KINNEY, W.E., PEREY, F.G., Rep. ORNL-4807, Oak Ridge National Laboratory (1974).

[21] KORZH, I.A., PASECHNIK, M.B., TOTSKIJ, I.A., At.Ehnerg. 20 (1966) 8 (in Russian).

[22] HOLMQVIST, B., WIEDLING, T., Rep. AE-366, Studsvik AB, Nykoeping (1969); HOLMQVIST, B., et al., Rep. AE-385, Studsvik AB, Nykoeping (1970).

[23] KAZAKOVA, L.Ya., KOLESSOV, V.G., POPOV, V.I., et al., (Proc. of Int. Mtg. on Nuclear Structure Study with Neutrons, Antwerp), (1966) 576.

[24] LOVCHIKOVA, G,N., At.Ehnerg. 13 (1962) 60 (in Russian).

[25] WALT, M., BARSHALL, H.H., Phys.Rev., 93 (1954) 1062.

[26] MACHWE, M.K., KENT, D.M.Jr., SNOWDON, S.C., Phys.Rev. 114 (1959) 1563.

[27] TOWLE, J.H., BATCHELOR, R., GILBOY, W.B., (Proc. Int. Conf. on Nuclear Data for Reactors, Paris, 1966), Vol.1, IAEA, Vienna (1967) 367.

[28] BRODER, D.L., KOLESSOV, V.E., LASHUK, A.I., et al., At.Ehnerg. 16 (1964) 103 (in Russian).

[29] ROGERS, V.C., BEGHIAN, L.E., CLIKEMAN, F.M., Nucl.Sci.Eng. 45 (1971) 297.

[30] TOWLE, J.H., OWENS, R.O., Nucl.Phys. A100 (1967) 257.

[31] KONOBEEVSKIJ, E.C., MUSSAELYAN, R.M., POPOV, V.I., SURKOVA, I.V., Fiz.Ehlem.Chastits.At.Yadra 13 (1982) 300 (in Russian).

[32] TRAIFOROS, S., MITTLER, A., SCHIER, W.A., et al., Nucl.Sci.Eng. 72 (1979) 191.

[33] GARBER, D.I., KINSEY, R.R., Neutron Cross-Sections, 3rd edn., Vol.2, Brookhaven National Laboratory, Rep. BNL-325 (1976).

[34] FARRELL, J.A., BILPUCH, E.G., NEWSON, H.W., Ann.Phys. 37 (1966) 367.

[35] FEDOROV, M.B., OVDIENKO, V.D., SMETANIN, G.A., YAKOVENKO, T.I., Neytronnaya Fizika, (Proc. of 5th All-Union Conf. on Neutron Physics, Kiev, 1979), Part 1, TSNIIatominform, Moscow (1980) 309 (in Russian).

[36] SMITH, A.B., et al., Rep. ANL/NDM-61, Argonne National Laboratory (1981).

[37] KORZH, I.A., LUNEV, V.P., MISHCHENKO, V.A., et al., Problems of Atomic Science and Technology, Ser. Nuclear Constants 1(5) (1983) 40 (in Russian).

[38] PASECHNIK, M.B., KORZH, I.A., KASHUBA, I.E., Neytronnaya Fizika, (Proc. of 1st All-Union Conf. on Neutron Physics, Kiev, 1971), Part 1, Kiev (1972) 277 (in Russian).

[39] KAWAI, M. "Determination of spherical optical model parameters for structural materials", in Proc. of NEANDC Mtg. Topical Discussion on Progress in Neutron Cross-Section Measurements and Evaluation, Concerning Structural Materials for Fast Reactors, Geel, 1979.

[40] IGNATYUK, A.B., LUNEV, V.P., SHORIN, V.C., Problems of Atomic Science and Technology, Ser. Nuclear Constants 13 (1974) 59 (in Russian).

[41] STELSON, P.H., GRODZINS, L., Nucl.Data A1 (1965) 21.

[42] HAUSER, W., FESHBACH, H., Phys.Rev. 87 (1952) 366.

[43] MOLDAUER, P., Phys.Rev. B135 (1964) 642; and Rev.Mod.Phys. 36 (1964) 1079.

[44] DILG, W.., SCHANTL, W., VONACH, H., UHL, M., Nucl.Phys. A217 (1973) 269.

[45] KORZH, I.A., MISHCHENKO, V.A., PASECHNIK, M.V., PRAVDAVYJ, N.M., At.Ehnerg. 57 (1984) 262 (in Russian).

[46] DIVADEENAM, M., Elemental Ni Neutron Induced Reaction Cross-Section Evaluation, Rep. BNL-NCS-51346, Brookaven National Laboratory (1979).

[47] ABAGYAN, A.P., BAZAZYANTS, N.O., NIKOLAEV, M.N., TSIBULYA, A.M., Multigroup Data for Reactor and Shielding Calculations, Ehnergoizdat, Moscow (1981).

[48] US NATIONAL NUCLEAR DATA CENTER, ENDF/B-IV Evaluated Nuclear Data Library, ^{28}Ni (MAT 1190), (M.R. Bhat, Eval.), Rep. BNL-17541, Brookhaven National Laboratory (1975).

[49] BYCHKOV, V.M., POPOV, V.I., Problems of Atomic Science and Technology, Ser. Nuclear Constants, 25 (1977) 55 (in Russian).

[50] GOEL, B., Graphical Representation of the German Nuclear Data Library KEDAK, Part 1: Non-Fissile Materials, Rep. KFK-2233, Kernforschungszentrum Karlsruhe (1975).

[51] ASAMI, T., TANAKA, S., Graphs of Neutron Cross-Section Data for Fusion Reactor Development, Rep. JAERI-M-8136, Japan Atomic Energy Research Establishment (1979).

PROPOSAL TO REPRESENT NEUTRON ABSORPTION BY FISSION PRODUCTS BY A SINGLE PSEUDO-FRAGMENT

A.M. Tsibulya, A.L. Kochetkov, I.V. Kravchenko and M.N. Nikolaev

Abstract

The concentration of fission products during reactor operation is analyzed. The dependence of a composite fission product capture cross-section as a function of time and on the nature of the A of the fissile nuclide are investigated, and the neutron radiative capture in fission products of a thermal reactor is evaluated. It is concluded that neutron absorption by fission products can be described by pseudo-fragments.

In fast neutron reactor calculations it is customary to represent the absorption of neutrons by fission products by replacing the effect of individual fission fragments by that of a few collective pseudo-fragments. Thus, in the BNAB [1] multigroup data library, the fission product group data for the fissile nuclides ^{233}U, ^{235}U and ^{239}Pu are obtained by averaging the cross-sections of stable or long-lived (for $T_{\frac{1}{2}}$ larger than 10-100 days) isotopes from each individual decay chain weighted by the fission yield of the corresponding chain. At energies below 160 keV, the contribution from the poisoning isotopes (i.e., isotopes which have a very large thermal neutron absorption cross-section, such as ^{113}Cd, ^{149}Sm, ^{151}Sm, ^{155}Gd and ^{157}Gd), whose concentrations depend on the irradiation history of the fuel, are not included in the pseudo-fragment cross-sections. In the calculation of thermal reactors, the cross-sections of the poisoning isotopes as well as those of the radioactive ^{135}Xe, whose concentrations are determined at the time of fission, must be added to the cross-sections of the nuclear ash in the BNAB data library.

In 1962, at the time when the BNAB data library was being developed, the composite fast neutron capture cross-sections for the fission products were known to approximately 20-30%. In view of such large uncertainties, it did not seem sensible to consider all individual fission products in fast reactor calculations, and each fission product, with the exception of the poisoning

isotopes, in the calculation of thermal reactors. Since then, the accuracy of fission product cross-sections has improved considerably: such that the uncertainty of the composite fission product fast neutron capture cross-sections barely exceed 10%. In view of this situation, the question arises whether it is sensible to describe the interaction of neutrons with fission products by means of a single pseudo-fragment. The drawbacks of such an approach are obvious. As a result of beta decay, the fission products, from the time of their formation, become gradually more neutron deficient, which causes their composite capture cross-section to increase with time. On the other hand, in a working reactor, those fission products that are high absorbers burn out faster, and are converted to weakly absorbing nuclides, with the result that the composite fission product absorption cross-section decreases with the gradual burnup of the fuel. As a result of these processes, the composite fission product cross-section in the reactor core changes with time, and depends on the reactor operation history. If the amplitude of such variations is smaller than the uncertainty of the composite cross-section (which is determined by the existing uncertainties in the knowledge of the neutron data), then the description of the interaction of neutrons with fission products by the characteristics of a single pseudo-fragment is feasible. If this is not the case, then it is then necessary to devise more differentiating means and consider the effects of the individual fission products.

Analysis of the evolution of the composite capture cross-section of fission products.

The value of the composite fission product capture cross-section as a function of time and degree of fuel burnup was investigated by studying this effect in the core of a 800 MW-electric fast reactor power station. The integral neutron spectrum in the core of the reactor was calculated using the 26-group BNAB-78 [2] cross-section library. The isotopic composition of the irradiated fuel material (including the fission products) was calculated using two independent computer programs: YIELD [3] and AFPA [4]. These two programs differ in the algorithm used to solve the isotope kinetics equation, in the number of isotopes

included in each isobaric chain, in the procedure used to construct the 26-group neutron cross-section sets for the nuclides being depleted and created in the fuel burnup process, and in the manner in which the various fission product yield and decay chain data compilations were used.

Both programs were used to calculate the time dependence of the average fission product cross-section during four reactor operating cycles without interruption for fuel loading. Each cycle consisted of an operating time of 110 days at a power level corresponding to a 190 kW/kg thermal load on the unirradiated fuel, and a 10 day reactor shutdown time. At the beginning of the first cycle, the reactor was loaded with unirradiated fuel. The isotopic composition of the fuel at the beginning of the first cycle, and at the end of each irradiation cycle is tabulated in Table I. In addition, the fuel composition at the beginning and at the end of each operating cycle during a continuous reactor operation with a regular fuel reloading of 1/4 of the fuel (that had been irradiated in the course of four cycles) with fresh fuel.

TABLE I. TIME HISTORY OF FUEL COMPOSITION DURING REACTOR OPERATION (in at%)

Nuclides	Unirradiated fuel	End of cycle				Continuous cycle	
		First	Second	Third	Fourth	Begin	End
U-235	0.32	0.27	0.23	0.19	0.16	0.25	0.21
U-238	80.88	78.97	77.11	75.30	73.54	78.06	76.23
Pu-238	0.10	0.09	0.08	0.08	0.07	0.09	0.08
Pu-239	11.28	11.10	10.91	10.71	10.50	11.00	10.80
Pu-240	4.60	4.73	4.84	4.93	5.00	4.78	4.88
Pu-241	2.05	1.74	1.51	1.34	1.22	1.66	1.45
Pu-242	0.77	0.79	0.80	0.80	0.80	0.79	0.80
Trans-Pu	-	0.08	0.14	0.20	0.25	0.10	0.17
Fission Products	-	2.23	4.38	6.45	8.46	3.27	5.38

Calculations performed with each of the two programs used various versions of the 26-group fission product cross-section sets: one used the data given in reference [5], another differed from the first by modifying the capture cross-sections of the most important fission products according to the data published in

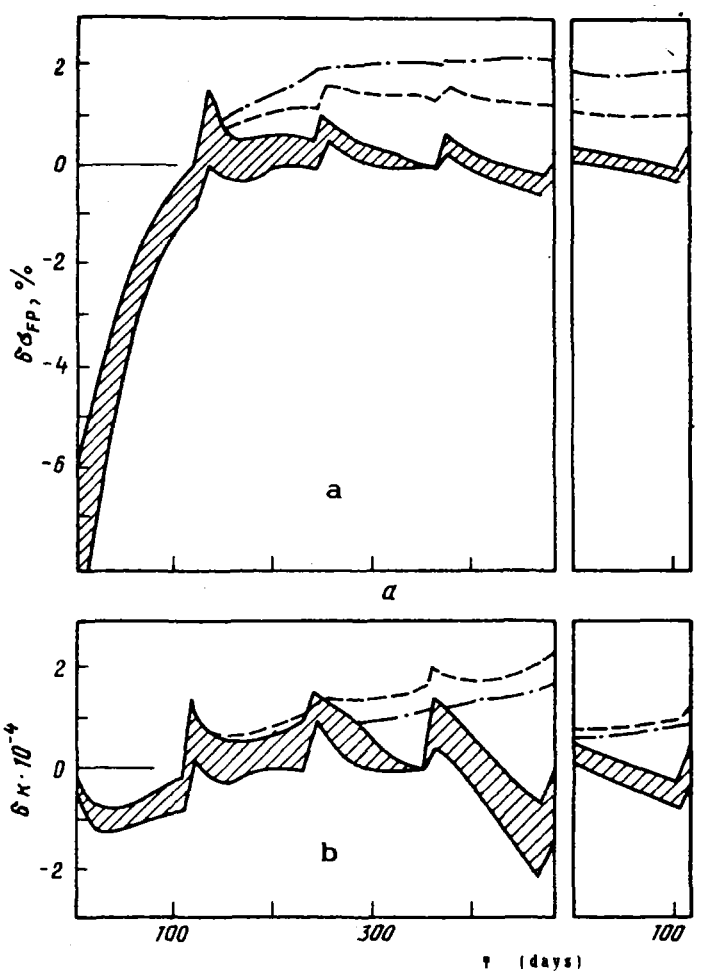

Fig. 1. Behavior of the evolution of (a) the composite fission product capture cross-section $\delta\sigma_{FP}$, and of (b) the uncertainty in the multiplication factor δK, as a function of reactor operating time.

1976 by L.P. Abagyan [4], the third was derived from ENDF/B-V [6], the fourth consisted of data taken from the reference JAERI-M-9715 [7], the fifth was a variation of the third in which the capture cross-sections for 30 fission products were replaced by data based on evaluations described in references [8-10] and in reference [11] for data in the region of resolved resonances. The last version of fission product group data evaluation, which was completed towards the end of 1983 at the Institute of Physics and Power Engineering (FEI) contains a more complete set of differential neutron data information than any of the earlier versions.

The BNAB-78 data were used in the ^{238}U, ^{239}Pu and ^{240}Pu burnup calculations, the data by Antsipov et al., [12] for the burnup of

^{241}Pu and ^{242}Pu, and the ENDF/B-V [6] data for the burnup of the trans-plutonium nuclides.

Fission product yield and decay scheme data were taken from the compilation made at the MIFI (institute) [4], the evaluation published in reference [13], and the Japanese compilation [7] based on the yield evaluation published in reference [14]. The calculations were made with yields for both thermal as well as fast neutrons. The isotopic compositions of the fuel and of the fission products, as well as the composite fission product capture cross-sections, were calculated with the various data set versions at a number of time points during each cycle. The results of these calculation, made with different data input, proved to be comparable. These results are included in the cross-hatched region shown in Fig. 1, which can be considered to be the uncertainty envelope of these data.

At the very beginning of the first irradiation cycle, when the concentration of the fission products is still very low, the fraction of relatively short-lived neutron rich nuclides is rather large. Therefore the composite fission product capture cross-section at this stage is lower by 7% than it is during the steady-state operation. As one approaches the middle of the irradiation cycle, the neutron rich nuclides which were formed in the beginning of the cycle, have already decayed to stable or long-lived nuclides which are characterized by high capture cross-sections. Neutron-rich nuclides which are continued to be generated by fission, against the background of the earlier fission products, represent by now a smaller fraction. As a result of these processes the composite capture cross-section tends to rise.

During reactor shutdown, because of the growth in the population of new fission products and the existing radiation capture capacity of the accumulated fission products, the enrichment of fission products by neutron-rich nuclei ceases; this results in a relatively fast increase in the value of the composite capture cross-section. The same process can be observed in the second and last operating cycles: the value of the composite fission product capture cross-section decreases gradually during

irradiation (primarily due to the conversion of strong fission product absorbers to weaker ones as a result of neutron radiative capture), and increases during shutdown.

The character of the time dependence of the composite fission product capture cross-section depends on the power level of the reactor and the degree of burnup corresponding to the end of the experiment. The continuous curve shown on Fig. 1, which represents conditions at the end of the fourth irradiation period of an operation at a thermal fuel load of 190 W/g, only 8.5% of the original heavy nuclides undergo fission. The dash-dot curve shows the same data for half the thermal fuel load, and the dotted curve for one fourth the thermal fuel load.

As seen from Fig. 1, the composite fission product capture cross-section does not vary much during the whole operation. In order to emphasize this behavior, the value of the composite cross-section is not given in barns, but in terms of percent deviation from a composite cross-section value represented as a function of (effective) time, given by $t_{eff}=(16/21)\ T$, after the start of a steady-state irradiation period. In the case of four fuel reloadings, the value of the composite fission product capture cross-section at a given t_{eff} time is equal to the cross-section averaged over the time period, and weighted by the fission product concentration and the (neutron) fluence (see below). Let us consider the case of a fission product concentration $x_n(t)$ in a TVS (fuel loading?) which has undergone (n-1) irradiation cycles in the reactor core, and was irradiated for a time t in the n-th cycle, and let $\sigma_n(t)$ be the composite capture cross-section for these fission products. If one assumes that each TVS is irradiated in the reactor core for N time periods (and 1/N part of the TVS is replaced with fresh fuel after each period), then the composite fission product capture cross-section at a time t after the start of irradiation in a given cycle, and in accordance with the specified fuel reloading schedule, can be represented by:

$$\sigma_c(t)=\sum_{n=1}^{N} x_n(t)\sigma_n(t)\Big/\sum_{n=1}^{N} x_n(t)$$

The time dependence of the composite fission product capture cross-section magnitude calculated with this equation for a steady-state operation for N=4 is shown on the right side of Fig. 1a. For N=1, the dependence will look more like the left-hand side of this figure (for a continuous irradiation period consisting of four time periods, the only difference would be the absence of the perturbation introduced by the reactor shutdowns). The results showed that during a steady state operation and four fuel reloadings, the deviation from a specified average composite cross-section does not exceed 1%, which is much smaller than the uncertainty (of approximately 10%) in the knowledge of the individual fission product capture cross-sections.

If all of the fuel is loaded in one operation and exchanged for a full load of fresh fuel at a given degree of burnup, the deviation is larger (as shown in the left-hand part of Fig 1. Even in this case, the maximum deviation from a value resulting from averaging over a steady-state operation with four separate reloadings (which is roughly 8%) is smaller than the uncertainty of 10% in the average cross-section. This condition is achieved only at the beginning of the whole operation, at times when the fission product concentration is low. It must be noted that the capture cross-section, averaged over the whole operation and weighted by the fission product concentration and the fluence for the case of N=1, differs from the case of N=4 only by 2%. It is therefore possible to describe the absorption of neutrons by fission products to an acceptable accuracy for any number of reloadings up to N=1 for the same thermal load and a maximum degree of burnup by a single pseudo-fragment, whose capture cross-sections are obtained by averaging over concentrations existing at a time (16/21)T after the start of irradiation during a steady-state operation cycle with N=4.

For low thermal loads but similar irradiation times, the composite fission product cross-section is larger. However, even under these condition it does not exceed 3%. Such uncertainties are considered to be acceptable because under these circumstances the concentration of fission products in the fuel would be correspondingly lower. If the same degree of burnup is achieved at such low thermal loads, then the deviation from the composite

cross-section, averaged over the increased irradiation period, will be considerably smaller.

Fig. 1b shows the time dependence of the reactor multiplication factor uncertainty as a result of representing the radiative capture in fission products by a single pseudo-fragment. It can be seen that these uncertainties are measured in 100ths of percents, and can therefore be neglected.

It can therefore be concluded that for the current knowledge of the accuracy of neutron cross-sections, it is possible and sensible to describe neutron radiative capture in terms of a single pseudo-fragment. The authors of reference [15] who investigated the effect of irradiation on the composite fission product capture cross-section for burnup values up to 150 MW-days/Kg, arrived at the same conclusion. They did not analyze the period of initial irradiation of fresh fuel when the values of the composite fission product cross-sections vary particularly fast as a result of the decay of neutron-rich nuclides. Consequently, their value for the variation of the fission product composite cross-section did not exceed ±2.5%

The authors of reference [16] have proposed to describe neutron radiative capture in fission products in terms of two pseudo-fragments instead of one: one to represent the strong-absorbing odd nuclides, and the other the weak-absorbing even-even nuclides. This gives the possibility to take into account the decrease in the composite capture cross-sections as a result of the burnup process. The authors of reference [16] succeeded in describing the evolution of the composite fission product capture cross-section to a fraction of a percent for burnup values of up to approximately 185 MW-days/Kg; however, the method which gave such good results in the calculation of the pseudo-fragment cross-section was not described. The authors of reference [15] have compared the results to calculate the capture of neutrons by fission products using one and two pseudo-fragments, and have found that the methodology used in reference [16] (at least to the extent that they understood it) gave less accurate results than with the use of a single pseudo-fragment.

It can be assumed that by using properly chosen cross-sections for two pseudo-fragments, it would be possible to reproduce the decrease in the value of the composite fission product capture cross-section. However, as noted above, there is no necessity for such an improvement (which would be achieved at the cost of a significant complication of the calculational method). The use of the two pseudo-fragment approach is also questionable because it is not possible to describe the effect of the increase of the composite capture cross-section due to the decay of the neutron-rich nuclides. Furthermore, this effect is not less important than the effect of fission product irradiation on the lowering of the composite capture cross-section.

Steady-state equilibrium concentration of fission products

Let us consider the operating reactor cycle in which fuel reloading is performed at regular intervals with a frequency N. During irradiation the concentration of fission product in the reactor core increases practically linearly:

$$C(t) = [(N-1)/N]\, C_{max} + (C_{max}/N)\ (t/T)$$

where C_{max} is the maximum fission product concentration reached after N irradiation cycles each of duration T. Assuming that the composite fission product capture cross-section also behaves linearly, then at a time t_e, the cross-section averaged over the whole operation is equal to [(9N-4)/(12N-6]T. The dependence of the quantity t_e on the reloading frequency is weak: for N=4 t_e=0.76 and for N=1: t_e=0.83. Denoting the concentration of the ith nuclide of the isobaric chain A by $C_{A,i}$, then at any time t_e, the average cross-section is equal to:

$$\bar{\sigma}_c = \sum_A \sum_i C_{A,i}\sigma_{c,A,i} \qquad (I)$$

where $\sigma_{c,A,i}$ is the capture cross-section of the nuclide (A,i). For most isobaric chains, the determining contribution to the summation over i is contributed by one (stable or very long-lived) nuclide. For the summation over the atomic masses A, the contributing input can be limited to the principal member of the chain and its concentration can be expressed by $C_A = \sum C_{A,i}$. If the precursor of a stable or very long-lived member of the chain has

a half-life on the order of months, then their concentrations are comparable. For these isobaric chains, it is advisable to include two members of the chain.

Let us furthermore limit the values of A in the peaks of the light and heavy fragment mass distribution to A_{min}=83 and A_{max}=110 for the light masses and A_{min}=127 and A_{max}=155 for the heavy masses. The light fragments comprise nuclides for which A<120. For the yields of isobaric chains for which $A < A_{min}$ and $A > A_{max}$, let us include the closest lying even A isotopes (namely ^{84}Kr, ^{110}Pd, ^{128}Te and ^{154}Sm), and the closest lying odd A isotopes (namely ^{83}Kr, ^{109}Ag, ^{127}I and ^{155}Eu). Let us denote the yields of the isobaric chains by Y_A. Since the degree of fission product burnup in a fast reactor is not large, the quantities C_A and Y_A are related linearly[1] by the expression $C_A = \alpha_A Y_A + \beta_A Y_{A-1}$ where α_A and β_A are the burnup coefficients and where $\beta_A = 1-\alpha_{A-1}$. The yields Y_A, and consequently the concentrations C_A, depend on the fissile nuclide which gave rise to the fission products. On the other hand, the coefficients α_A and β_A which are determined by the decay characteristics and the irradiation conditions, are independent of the nature of the fissile nuclide. As indicated above, the quantity σ_c=(t) (as well as σ_c) are weakly dependent on the irradiation conditions. Consequently, in the process of determining the capture cross-section of the pseudo-fragments, one can define standard irradiation conditions (as in the case of the calculation of group cross-sections where it is necessary to postulate a standard spectrum within the energy group) such as steady state irradiation condition with a partial fuel reloading at regular intervals with a frequency of N=4 and a degree of fuel burnup of approximately 9%. The coefficients α_A and β_A, determined for these operating conditions, can then be used to calculate the concentrations C_A, and subsequently the cross-section $\bar{\sigma}_c$ for any given fuel composition (it is assumed that the cumulative yields are known for each fissile nuclide).

A list of nuclides which were included in the modified summation equation (1), is given in Table II; burnup coefficients α,

---

[1]Isotopic transmutation related to the emission of delayed neutrons are not taken into account.

TABLE II. CHARACTERISTICS OF THE MAJOR FISSION PRODUCTS. (The contributions to the resonance integral and thermal cross-section are underlined)

Nuclide	Burnup Coeff. α	Steady-state concentration		Contribution to, %					
				σ absorp.		RI		σ capture	
		^{235}U	^{239}Pu	^{235}U	^{239}Pu	^{235}U	^{239}Pu	^{235}U	^{239}Pu
^{83}Kr	0,98	0,76	0,5I	I,0	0,5	0,6	0,3	3,4	I,8
^{84}Kr	I,0	I,5I	0,85	0,3	0,I	-	-	-	-
^{85}Rb	I,0	I,3I	0,57	0,8	0,3	-	-	-	-
^{86}Kr	I,0	I,97	0,76	-	-	-	-	-	-
^{87}Rb	I,0	2,58	I,00	0,I	-	-	-	-	-
^{88}Sr	I,0	3,68	I,38	-	-	-	-	-	-
^{89}Y	I,0	4,88	I,70	0,3	0,I	-	-	0,I	-
^{90}Sr	I,0	5,88	2,I0	0,2	0,7	-	-	0,I	-
^{91}Zr	I,0	5,94	2,5I	I,I	0,4	0,I	-	0,I	-
^{92}Zr	I,0	5,98	3,0I	I,9	0,7	-	-	-	-
^{93}Zr	I,0	6,40	3,89	2,2	I,0	0,8	0,3	0,2	0,I
^{94}Zr	I,0	6,44	4,4I	0,8	0,4	-	-	-	-
^{95}Mo	I,0	6,50	4,89	4,6	2,7	3,I	I,6	2,0	I,2
^{96}Zr	I,0	6,22	5,03	0,8	0,5	0,I	0,I	-	-
^{97}Mo	0,98	5,86	5,27	4,7	3,3	0,4	0,2	0,3	0,2
^{98}Mo	I,0	5,93	5,99	I,7	I,3	0,2	0,I	-	-
$\underline{^{99}Tc}$	0,97	5,93	5,98	8,8	6,8	7,2	5,I	2,6	2,I
^{100}Mo	I,00	6,38	7,00	I,2	I,0	0,I	0,I	-	-
^{101}Ru	0,94	4,78	5,60	8,2	7,4	2,I	I,7	0,3	0,3
^{102}Ru	I,0	5,53	6,39	2,I	I,9	0,I	0,I	0,I	0,I
^{103}Ru	0,95	0,58	I,32	0,6	I,I	0,I	0,2	0,I	0,2
$\underline{^{103}Rh}$	0,95	2,3I	5,28	3,8	6,7	9,7	I5,4	7,3	I3,3
^{104}Ru	I,0	I,98	6,32	0,8	I,9	0,3	0,I	-	-
^{105}Pd	0,95	0,92	5,II	2,0	8,6	0,3	I,3	0,4	I,8
^{106}Ru	I,0	0,45	4,58	0,I	0,8	-	-	-	-
^{107}Rd	0,94	0,I3	3,20	0,2	4,0	-	0,9	-	0,I
^{108}Rd	I,0	0,08	2,40	-	I,I	0,I	I,5	-	0,5
$\underline{^{109}Ag}$	0,93	0,09	2,06	0,I	2,3	0,5	8,5	0,2	3,2
^{110}Pd	I,0	0,08	0,89	-	0,3	-	-	-	-
^{127}I	0,97	0,I8	0,25	0,2	0,3	0,I	0,I	-	-
^{128}Tl	I,0	0,46	0,66	0,I	0,I	-	-	-	-
^{129}I	0,97	0,69	I,46	0,8	I,3	0,I	0,2	0,4	0,7
^{130}Tl	I,0	I,79	2,39	-	-	-	-	-	-
$\underline{^{131}Xe}$	0,97	2,80	3,75	2,8	2,9	$\underline{I0,2}$	$\underline{9,5}$	$\underline{5,3}$	$\underline{5,7}$
^{132}Xe	I,0	4,39	6,53	0,8	I,0	-	-	-	-
$\underline{^{133}Cs}$	I,0	6,70	7,03	7,8	6,3	$\underline{I0,7}$	$\underline{7,8}$	4,2	3,5
^{134}Xe	I,0	7,8I	7,66	0,8	0,6	-	-	-	-
^{135}Cs	I,0	6,55	7,42	4,6	4,0	I,6	I,3	I,3	I,2

TABLE II (continued)

Nuclide	Burnup Coeff.	Steady-state concentration*		Contribution to, %					
				σ absorp.		RI		σ capture	
	α	^{235}U	^{239}Pu	^{235}U	^{239}Pu	^{235}U	^{239}Pu	^{235}U	^{239}Pu
^{136}Xe	I,0	6,3I	6,66	0,2	0,2	-	-	-	-
^{137}Cs	I,0	6,2I	6,63	0,3	0,3	-	-	-	-
^{138}Ba	I,0	6,79	6,06	0,2	0,2	-	-	-	-
^{139}La	I,0	6,37	5,68	0,6	0,4	0,4	0,2	I,2	0,9
^{140}Cl	I;0	6,30	5,57	0,3	0,2	-		0,I	-
^{141}Pr	I,0	5,84	5,29	I,8	I,3	0,5	0,3	I,5	I,I
^{142}Cl	I,0	5,89	5,00	0,4	0,3	-	-	0,I	0,I
^{143}Nd	I,0	5,95	4,43	5,0	2,9	3,3	I,7	4I,8	24,9
^{144}Cl	I,0	5,48	3,74	0,8	0,4	-	-	0,I	0,I
^{145}Nd	0,97	3,80	2,90	5,0	2,9	4,2	2,2	II,7	7,I
^{146}Nd	I,0	3,09	2,55	0,8	0,5	-	-	0,I	0,I
^{147}Pm	0,92	2,05	I,89	5,8	4,I	I8,3	II,7	8,I	5,9
^{148}Nd	I,0	I,85	I,80	0,7	0,5	0,I	0,I	0,I	0,I
^{149}Sm	0,85	0,88	I,02	6,9	6,2	I3,5	I0,9	**	**
^{150}Nd	I,0	0,84	I,I8	0,3	0,4	-	-	-	-
^{151}Sm	0,85	0,36	0,65	2,2	3,2	5,2	6,5	**	**
^{152}Sm	I,0	0,33	0,7I	0,4	0,7	4,0	6,0	I,5	2,5
^{153}Eu	0,90	0,I4	0,33	I,0	I,8	0,9	I,4	I,4	2,6
^{154}Sm	I,0	0,II	0,50	-	0,2	-	-	-	-
^{155}Eu	I,0	0,04	0,26	0,3	I,5	0,5	2,4	3,5	I8,I

* In relative units, normalized to 200.
** Contribution from poisons is not taken into account

calculated for standard irradiation conditions are given for each considered fission product. Table II also lists the concentrations of ^{235}U and ^{239}Pu fission products recommended for the calculation of the pseudo-fragment cross-section. The concentrations were derived from the cumulative yields published in reference [14]. The yields are determined for thermal fission. Yields for fast neutrons correspond as a rule to neutrons generated by fission neutrons whose average energy of 2 MeV is considerably higher than the average neutron energy of 200 keV in a fast power reactor. Also shown in Table II are the fractional contributions from each listed fission product to the composite fission product capture cross-section for ^{235}U and ^{239}Pu fission in the integral spectrum of the reactor core of the

investigated model, as well as to the resonance integral and the thermal capture cross-section. The contributions of the ^{149}Sm and ^{151}Sm to the thermal cross-section were not included.

The data given in Table II are weakly dependent on the data set used; in these calculations, we used the 26-group fission product data set developed in 1983 at the Institute of Physics and Power Engineering (FEI).

Dependence of the composite fission product capture cross-section on the atomic number of the fissile nuclide.

As indicated above, it is possible with the aid of the data listed in Table II, to calculate the pseudo-fragment cross-section for each fissile nuclide as long as one knows the cumulative yield of each isobaric chain. That was indeed the method used in the development of the BNAB-64 [1] cross-section library which contained the fission product data for ^{233}U, ^{235}U and ^{239}Pu. In actual reactor calculations, the fission products of the principal fissile nuclide, such as ^{239}Pu which is used in fast breeder reactors, stand out among the other nuclides which make up the material of the reactor core. This approach has a certain disadvantage: the fissioning of ^{239}Pu in the core of a plutonium fueled breeder reactor, for instance, contributes less than half of the entire fission product population, the rest is produced by the fissioning of ^{238}U, ^{241}Pu and other fissile nuclides. One could, of course, calculate the cross-sections of the fission products produced by all fissionable materials; this would, however, lead to an unjustified increase in the volume of the group data library, and to an unreasonable increase in the number of nuclides which enter into the composition of the reactor. Such a situation would be undesirable because most computer programs, designed to process or utilize group data, have strong limitations with respect of the number of considered nuclides.

Actually, the dependence of the fission product cross-sections on the A of fissile nuclides is rather weak; one can therefore be assured that even a simple analytical description would guarantee an acceptable accuracy.

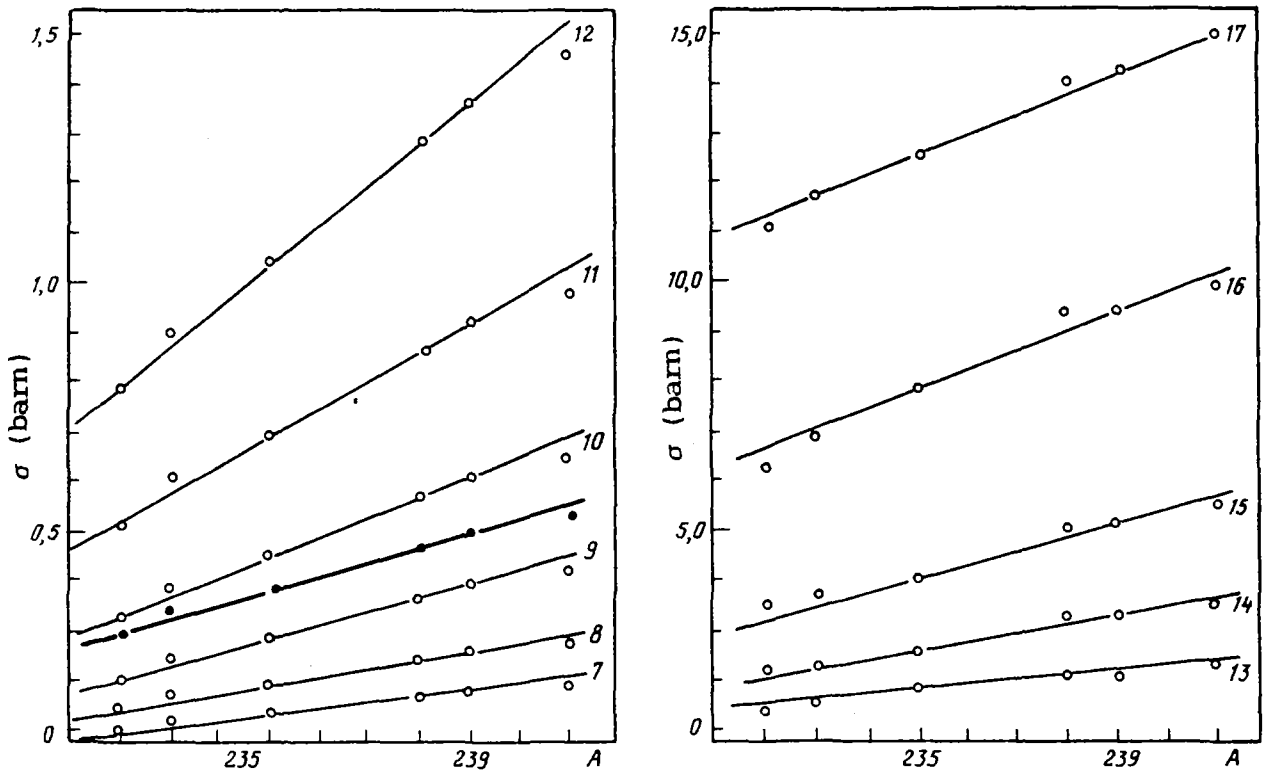

Fig. 2. Dependence of the composite fission product capture cross-section on the atomic number of fissile nuclide: — ∘ — group cross-sections (the group number is given in parentheses); — • — capture cross-section, averaged over a fast reactor spectrum.

The dependence of the group composite fission product capture cross-sections as a function of the atomic number of the fissile nuclide (from ^{232}Th to ^{241}Pu) is shown in Fig. 2. These cross-sections were calculated on the basis of the data listed in Table II, the cumulative yields given in reference [14], and the fission product group data developed at FEI. The calculated points are compared with the linearly dependent group capture cross-sections as a function of the atomic number of the fissile nuclide, normalized to the data of ^{235}U and ^{239}Pu. The data shown in this figure, refer to the energy grouping of the BNAB group data [1], and encompass the energy range 0.4 MeV to 46.5 eV, which is where most radiative capture events occur in a fast neutron reactor. The spectrum-averaged capture cross-section for the considered fast reactor core is also shown in this figure. It can be seen that the derived linear dependence of $\overline{\sigma_c}(t)$ can describe the calculated data to an accuracy of 5%. Such a systematical uncertainty is not any larger than the errors resulting from the inexact knowledge of the cumulative yields for

nuclides other than ^{235}U and ^{239}Pu (according to reference [17], this uncertainty can be as high as 8%).

It can therefore be concluded that such a linear approximation of $\bar{\sigma}_i(A)$ is quite acceptable. This now gives the possibility to prepare the fission product group data for applied calculations in the following manner. The group data library contains cross-section data for only two pseudo-fragments corresponding to the fission of ^{235}U and ^{239}Pu. In an actual calculation, the concentration of fission products and which of the two pseudo-fragment data sets to use, is determined by estimating which of the two atomic numbers (235 or 239) is closest to the average atomic number of the fuel mixture of the reactor core under investigation (for example, in the calculation of a reactor which contains ^{233}U and ^{232}Th in its core, it would sensible to choose the ^{235}U fission product set). The 26-group data set, prepared for the core composition under investigation, is used first of all for the preliminary approximation of the integral neutron spectrum in the reactor core. Normally this is done in the approximation of the material parameter. The evaluated neutron spectrum is used for the recalculation of the elastic slowing-down cross-sections and of the neutron fission spectrum [2]. The average atomic mass of the fuel mixture and the corresponding fission product population which accumulates in the reactor core can be estimated at the same stage of the calculation:

$$\bar{A}=\sum_i A_i C_i \sum_g \bar{\sigma}_{f,i}^g \varphi_i^g \Big/ \sum_i C_i \sum_g \bar{\sigma}_{f,i}^g \varphi_i^g$$

where i is the number of the nuclide, g the group number, and φ the neutron flux density.

The earlier determined group data for the predetermined fissile nuclide A_0, being either 235 or 239, can then be corrected by

$$\bar{\sigma}(\bar{A})=\bar{\sigma}(A_0)+\frac{\sigma(239)-\sigma(235)}{239-235}(\bar{A}-A_0), \qquad (2)$$

where σ is the cross-section for any one of the used group cross-sections. The effect of resonance self-shielding of the cross-sections can be introduced at this point in the calculation of $\bar{\sigma}(A_0)$. The quantities which enter in the evaluation of equation (2) can be stored in the program used in the refinement of the

fission product cross-section using that equation. It is not sound practice to recalculate the self-shielding factors (which are in any way close to unity) at the same time. The authors cannot recommend the use of the linear approximation for the dependencies of the transport and scattering cross-sections on A: scattering is responsible for less than 20% of the fission products activity [17], and the known accuracy of inelastic scattering data is lower than the known accuracy of the capture cross-sections.

It is also appropriate to mention here the considerations given to the migration of gaseous and volatile fission products from the reactor core into special cavities designed for that purpose in contemporary reactors. According to the authors of this analysis, and in agreement with the evaluation presented in reference [15], the contribution of gaseous and volatile fission products (e.g., isotopes of iodine and cesium) to the total fission product yield is approximately 21%. The equilibrium fraction of the products which remains in the reactor core depends on a number of factors: the nature of the core material, its temperature, the irradiation conditions, the degree of burnup, etc. It is normally estimated that the fuel material produces approximately 40% of gaseous and volatile fission products. This lowers the composite fission product capture cross-section by about 5%. As a result, if the escape of gaseous and volatile fission products from the reactor fuel is not taken into account, it leads to a systematic error which is actually smaller than the uncertainty due to the inexact knowledge of the neutron cross-sections (which is approximately 10%). If one knows the fraction of volatile products that escapes from the core, and denotes that fraction by δ, it would then be possible to account for the influence of this effect on the fission product neutron cross-sections by lowering the concentration of fission products by 12δ%. This may be an approximate evaluation, but the uncertainty of this approximation is lower than the uncertainty of the evaluation of δ.

Evaluation of the neutron radiative capture in fission products of a thermal reactor.

In contrast to fast neutron reactors, in which radiative capture occurs in a broad energy range (from hundreds of electronvolts to hundreds of kiloelectronvolts), in thermal reactors, the overwhelming majority of capture events take place in a relatively narrow energy range. Because of this difference, the individual properties of the fission product nuclei have a much more pronounced effect. The poison nuclides play a particularly important role when one considers that their thermal capture cross-sections exceed 5000 b. Among the fission products, there are five stable and long-lived poison nuclides and one short-lived poison ^{135}Xe. The cumulative yields of these poison nuclides, for the fission of ^{235}U and ^{239}Pu, as well as their thermal capture cross-sections are listed in Table III. In view of such high capture cross-sections, the concentrations of the poison nuclides quickly reach an equilibrium in thermal reactors. At this point, the absorption of neutrons is determined primarily by their fission yields, and do not depend on the cross-sections. The time needed to reach equilibrium is approximately $1/\sigma\varphi$, and ranges in power reactors from 1 day for ^{135}Xe to a few months for ^{155}Sm. In order to calculate the absorption of neutrons by the poison nuclides during the time that they are reaching equilibrium, it is necessary to know their capture cross-sections.

TABLE III. CHARACTERISTICS OF POISON NUCLIDES

Nuclides	Cumulative yield per 100 fissions		Thermal capture cross-section at 2200 m/s (b)
	^{235}U	^{239}Pu	
^{113}Cd	0.015	0.037	20000
^{149}Sm	1.08	1.24	41000
^{151}Sm ($T_{\frac{1}{2}}$=03 y)	0.42	0.78	15000
^{155}Gd	0.03	0.17	61000
^{157}Gd	0.006	0.075	254000
^{135}Xe ($T_{\frac{1}{2}}$=9.1 h)	6.54	7.42	265000

Of the remaining fission products only two (^{143}Nd and ^{155}Eu) have thermal neutron capture cross-sections whose values are comparable to (in the case of ^{143}Nd) or exceed (by a factor of six to seven in the case of ^{155}Eu) the fission cross-section of a fuel nuclide. The burnup of these and other high absorber poisons for fuel burnps of 5% leads to the lowering of the capture cross-section of poisons only by 1.5-2%. The effect due to the production of high absorbing nuclides as a result of neutron capture (as for example the production of ^{149}Sm from neutron absorption by ^{148}Nd) is extremely small. The equilibrium concentrations of individual fission products which contribute to the formation of nuclear ash, should be calculated in the same manner as it is done in the case of a fast reactor. Analyses of this effect have shown that possible variations of poison concentrations can bring about a change in the average value of the thermal neutron capture cross-section of not more than 5%.

Thus, if in the process of calculating pseudo-fragment cross-sections, which had been averaged for a fast reactor and weighted by steady-state fission product concentrations (see Table II), one were to omit the contribution of the poisons in the thermal region (see Table III), it would then be possible to utilize these data for the calculation of both fast and thermal reactors. In the latter case, it would be necessary to take the additional effect of thermal neutron absorption by the poison nuclides into account. It is not possible to neglect the absorption of thermal neutrons by the nuclear ash in the calculations of fast reactors. In the calculation of the dynamics of poison accumulation in thermal reactors one could question the possibility of their burnup due to the effect of slowing down neutrons. If it were possible to neglect the burnup, however, then the method described above, which takes the absorption of neutrons by the fission products into consideration, could be used in the calculations of thermal reactors.

A more correct procedure would be to separate and to analyze individually those fission products whose contribution to the resonance integral (or to the thermal cross-section of the ash) is particularly large. These consists of the following nuclides (see Table II): ^{99}Tc, ^{103}Rh, ^{109}Ag, ^{131}Xe, ^{133}Cs, ^{143}Nd, ^{145}Nd, ^{147}Pm,

^{151}Sm and ^{155}Eu. These ten fission products determine roughly 85% of the thermal cross-section and resonance integral of the nuclear ash. In their capacity as neutron absorbers, the rest of the fission products in a thermal reactor can be represented by one pseudo-fragment (which can then be collectively be referred to as ash). Inasmuch as the fraction of neutrons that are absorbed by this ash is not large, it is questionable whether there is any sense to take the dependence of this ash on the nature of the fissile nuclide into account; it is probably enough to have the data pertinent to the ash resulting from ^{235}U.

The methodology to calculate group data for fission products that has been described in this article has now been incorporated in the new version of the ARAMAKO nuclear data library [18], ARAMAKO-C1.

REFERENCES

[1] ABAGYAN, L.P., BAZAZYANTS, N.O., BONDARENKO, I.I., NIKOLAEV, M.N., Multigroup Data for Nuclear Reactor Calculations, Atomizdat, Moscow (1964) (in Russian).

[2] ABAGYAN, L.P., BAZAZYANTS, N.O., NIKOLAEV, M.N., TSIBULYA, A.M., Multigroup Data for Reactor and Shielding Calculations, Ehnergoizdat, Moscow (1981) (in Russian).

[3] KRAVCHENKO, I.V., KRIVTSOV, A.S., Study of the effect of evaluated nuclear data uncertainties on the accuracy of the calculation of the average cross-section of a fission product mixture, Problems of Atomic Science and Technology, Ser. Nuclear Constants 2(51) (1983) 31-36 (in Russian).

[4] KOLOBASHKIN, V.M., RUBTSOV, P.M., RUZHANSKIJ, P.A., et al., "Calculation of the radiation characteristics of a mixture of fission products in thermal and fast reactors", in Neytronnaya Fizika, (Proc. of the 4th All-Union Conf. on Neutron Physics, Kiev, 1977), Vol. 4, (1978) 117 (in Russian).

[5] BERTRAN, W.R., CLAYTON, E.A., COOR, J.L., et al., Australian Atomic Energy Commission Research Establ., Lucas Heights, Rep. AAEC/E214 (1971).

[6] SCHWERER, O., ENDF/B-V Fission Product Files - Summary Documentation, Rep. IAEA-NDS-25, IAEA, Vienna (1981).

[7] IHARA, H., MATUMOTO, Z., TASAKA, K., et al, Japan Nuclear Data Center Fission Product and Yield Data, Rep. JAERI-M-9715, Japan Atomic Energy Research Establishment, Tokai Mura (1981).

[8] BELANOVA, T.S., GORBACHEVA, L.V., GRUDZEVICH, L.V., Analytical Comparison of Neutron Radiative Capture Cross-Section Evaluations for Important Fission Products, At.Ehnerg. 57(4) (1984) 250 (in Russian).

[9] ZAKHAROVA, S.M., ABAGYAN, L.P., YUDKEVICH, M.S., MANTUROV, G.N., Multigroup Fission Product Cross-Section Library, Part 5, Isotopes ^{151}Sm and ^{153}Sm, Preprint FEI OB-174, Institute of Physics and Power Engineering, Obninsk (1983) (in Russian).

[10] ZAKHAROVA, S.M., ABAGYAN, L.P., KAPUSTINA, V.F., Multigroup Fission Product Cross-Section Library, Part 2, Isotopes of Prometheum, Preprint FEI OB-120, Institute of Physics and Power Engineering, Obninsk (1981) (in Russian).

[11] MUGHABGHAB, S.F., DIVADEENAN, M., HOLDEN, M.E., "Neutron resonance parameters and thermal cross-sections. Part A: Z=1-60", Neutron Cross-Sections, Vol.1, Academic Press, New York (1981).

[12] ANTSIPOV, G.V., KONSHIN, V.A., SUKHOVITSKIJ, E.Sh., Nuclear Data for Plutonium Isotopes, Nauka i Tekhnika, Minsk (1982) (in Russian).

[13] CROOCH, E.A.C., Fission product yields from neutron induced fission, At.Data and Nuc.Data Tables 19(5) (1977) 417-532.

[14] RIDER, B.F., MEEK, M.E., Compilation of Fission Product Yields. Rep. NEDO-12154-2(t), Vallecitos Nuclear Center, General Electric, San Jose (1978).

[15] LIAW, J.R., HENRYSON-II, Lumped fission product neutron cross-sections based on ENDF/B-V for fast reactor analysis, Nuc.Sci.and Eng. 84 (1983) 324.

[16] ATEFI, B., FISHER, G.J., DURSTON, C., Improved fission product model for fast reactor analysis, Trans.Amer.Nucl.Soc. 35 (1980) 527.

[17] PALMIOTTI, G, SALVATORES, M., NEACRP LMFBR Benchmark calculations for the intercomparison of fuel burnup, Rep. NEACRP-L-270, Nuclear Energy Agency Data Committee, Cadarache (1984).

[18] BAZAZYANTS, N.O., VYRSKIJ, M.Yu., GERMOGENOVA, T.A., et al., ARAMKO-2F - Neutron Data Library for the Calculation of Radiation Transport in Reactors and Shielding, AN SSSR IPM Publ., Moscow (1976) (in Russian).